


A routing protocol using trust management framework for wireless sensor networks (WSNS)

Ravula Jyothsna ; N. Prathyusha; Ganapavarapu Surekha



+ Author & Article Information

AIP Conf. Proc. 2548, 040005 (2023)

<https://doi.org/10.1063/5.0139358>

In this paper, a routing protocol using trust management framework for Wireless sensor Networks (WSNs) is implemented. These are used in the applications of military surveillance, discovery of forest fire and ultimate field. Multi hop routing is provided by the wireless sensor network. Because of this high security is provided to the network. Basically, in the applications of military and others, the trust plays very important role in sensor networks. So in this data security also plays very important role. Results give the comparative study in between proposed TMF routing protocol and existing routing protocols. Hence in this routing protocol using trust management framework (TMF) is introduced for high security and high accuracy.

Topics

[Sensors](#), [Data management](#), [Natural disasters](#)

REFERENCES

1. J. Polastre, W. Hong, G. Tolle, D. Culler, R. Szewczyk, K. Tu, N. Turner, T. Dawson, and S. Burgess, D. Gay, P. Buonadonna, "A macroscope in the redwoods," *3rd ACM SenSys*, New York, NY, USA, pp. 51–63, 2005.

[Google Scholar](#)



381–396, 2006.

Google Scholar

3. Y. Liu, M. Li “Underground coal mine monitoring with wireless sensor networks,”, *ACM Trans. Sen. Netw.*, vol. 5, pp. 10:1–10:29, 2009. <https://doi.org/10.1145/1614379.1614381>

Google Scholar Crossref

4. T. F. Abdelzaher, T. He, Q. Cao, P. Vicaire, G. Zhou, T. Yan, L. Luo, L. Gu, J. A. Stankovic, and R. Stoleru, “Achieving longterm surveillance in VigilNet,”, *ACM Trans. Sen. Netw.*, vol. 5, pp. 9:1–9:39, 2009.

Google Scholar

5. S. Rangwala, D. Estrin, N. Xu, D. Ganesan, K. K. Chintalapudi, R. Govindan, and A. Broad, “A WSN for structural monitoring,”, *2nd ACM SenSys*, New York, NY, USA, pp. 13–24, 2004.

Google Scholar

6. H. Ma, X. Zhang and L. Liu, “Optimal node selection for target localization in wireless camera sensor networks,”, *IEEE Trans. Veh Technol.*, vol. 59, no. 7, pp. 3562–3576, 2010. <https://doi.org/10.1109/TVT.2009.2031454>

Google Scholar Crossref

7. L. Xie, W. Xiao, and Y. Weng, “Sensor selection for parameterized random field estimation in WSN,”, *J. Control Theory Appl.*, vol. 9, pp. 44–50, 2011. <https://doi.org/10.1007/s11768-011-0240-y>

Google Scholar Crossref

8. Mehmood A. Abd, Sarab F. Al Rubeaai, Kemal E. Tepe, and Brajendra K. Singh, “3D Real-Time Routing Protocol with Tunable Parameters for WSN”, *IEEE Sensors Journal*, 2015.

Google Scholar

9. Abdul Waheed Khan, Kamalrulnizam Abu Bakar, Adnan Ahmed, Khalid Haseeb, and Muhammad Ibrahim Channa, “TERP: A Trust and Energy Aware Routing Protocol for WSN”, *IEEE*, 2015.

Google Scholar

10. Shalli Rani, Gurbinder Singh Brar, Rahul Malhotra, Vinay Chopra, Syed Hassan Ahmed, and Houbing Song, "Energy Efficient Direction Based PDORP Routing Protocol For WSN", *IEEE*, 2016.

[Google Scholar](#)

11. Jinfang Jiang, Mohsen Guizani, Guangjie Han, Liangtian Wan, and Na Bao, "Routing Protocols for Underwater Wireless Sensor Networks", *IEEE*, 2015.

[Google Scholar](#)

12. Mao-Yuan Zhang, Lein Harn, Ching-Fang Hsu, and Ou Ruan, "Novel Design of Secure End-to-End Routing Protocol in WSN", *IEEE SENSORS JOURNAL*, Vol. 16, No. 6, 2016.

[Google Scholar](#)

This content is only available via PDF.

©2023 Authors. Published by AIP Publishing.

You do not currently have access to this content.

Sign in

Don't already have an account? [Register](#)

Sign In

Username

Password

[Reset password](#)
[Register](#)

Sign in via your Institution

[Sign in via your Institution](#)

×

Pay-Per-View Access
\$40.00

 BUY THIS ARTICLE



Proceedings of 3rd International Conference on Recent Trends in Machine Learning, IoT, Smart Cities and Applications pp 647–656

[Home](#) > [Proceedings of 3rd International Conference on Recent Trends in Machine Learning, IoT, Smart Cities and Applications](#) > Conference paper

Performance Analysis of Classification Algorithms

[A. Prakash](#)  & [Vijender Kumar Solanki](#)

Conference paper | [First Online: 24 February 2023](#)

324 Accesses

Part of the [Lecture Notes in Networks and Systems](#) book series (LNNS, volume 540)

Abstract

Classification issues are crucial in machine learning and data mining. Classification difficulties are utilised in medical diagnostics, bank customer estimation, medicinal investigations and emotion analysis. Many categorisation methods have been created with many different parameter inputs. Using hyperparameter optimisation algorithms, this work aims to improve




International Conference on Communications and Cyber Physical Engineering, 2018

ICCCE 2023: **Advances in Cognitive Science and Communications** pp 1133–1139

[Home](#) > [Advances in Cognitive Science and Communications](#) > [Conference paper](#)

Automatic Alert and Triggering System to Detect Persons' Fall Off the Wheelchair

[Syed Musthak Ahmed](#) , [Sai Rushitha](#), [Shruthi](#), [Santhosh Kumar](#), [Srinath](#) & [Vinit Kumar Gunjan](#)

Conference paper | [First Online: 10 March 2023](#)

425 Accesses

Part of the [Cognitive Science and Technology](#) book series (CSAT)

Abstract

Sensor-based human activities need a lot of attention in the driving technologies of the Internet of Things (IoT) because it should set the human activities (make and perform personal assisting tasks) that should be performed well. Taking care of physically disabled




International Conference on Communications and Cyber Physical Engineering, 2018

ICCCE 2023: **Advances in Cognitive Science and Communications** pp 1141–1148

[Home](#) > [Advances in Cognitive Science and Communications](#) > [Conference paper](#)

Dietary Assessment by Food Image Logging Based on Food Calorie Estimation Implemented Using Deep Learning

[Syed Musthak Ahmed](#) , [Dayaala Joshitha](#), [Alla Swathika](#), [Sri Chandana](#), [Sahhas](#) & [Vinit Kumar Gunjan](#)

Conference paper | [First Online: 10 March 2023](#)

442 Accesses

Part of the [Cognitive Science and Technology](#) book series (CSAT)

Abstract

According to recent studies across the world, it is observed that a healthy diet is a key to have sound health and body. Nowadays people are more concerned with their diet than ever before. Obesity has become a significant health problem across the



Institutional Sign In

All



ADVANCED SEARCH

Conferences > 2023 7th International Confer... ?

Smart Device to Check Harmful Chemicals in Fruits and Vegetables

Publisher: IEEE

Cite This

PDF

Saranya R ; Antony Kumar K ; Rajendran P ; Nireesh Kumar S ; Keerthana P All Authors



44 Full Text Views

Alerts

Manage Content Alerts Add to Citation Alerts

Abstract



Download PDF

Document Sections

- I. Introduction
- II. Related Work
- III. Proposed Modelling
- IV. Module Description
- V. Experimental Setup

Show Full Outline

Authors

Figures

References

Keywords

Metrics

More Like This

Abstract:Fruits and vegetables square measure extraordinarily nutritive and kind as key food merchandise among the human consumption. They are extraordinarily destructible due to ... **View more**

Metadata

Abstract:

Fruits and vegetables square measure extraordinarily nutritive and kind as key food merchandise among the human consumption. They are extraordinarily destructible due to their low amount. Fruits and vegetables square measure the necessary provide of carbohydrates, proteins and minerals. These food commodities square measure reported to be contaminated with toxic and health unsafe chemicals. To overcome this problem, proposed model uses IOT to detect the chemical levels. In this method gas detector has placed and estimate the chemical level in fruits and vegetables. If any chemicals detected immediate alert is distributed through GSM to the owner. In most of the hostel mess and government schools, everybody is getting tormented by the food they consume. Milk and fruits like banana and alternative foods utilized in existence, as all of them don't provide quality since the existence of Fulani gases vary from time to time. To confirm food safety, it's tough to be monitored at every stage of the provision chain. Variation in hydrogen ions concentration is going to be fetch, style, flavor, shelf-life of farm product. These gases increase with time. The aim of this method is to note early food spoilage before signs square measure visible.

Published in: 2023 7th International Conference on Computing Methodologies and Communication (ICCMC)

Date of Conference: 23-25 February 2023

DOI: 10.1109/ICCMC56507.2023.10084204

Date Added to IEEE Xplore: 04 April 2023

Publisher: IEEE



Saranya R

Department of Computer Science & Engineering, Vel Tech Rangarajan Dr Sagunthala R&D Institute of Science and Technology, Chennai, Tamilnadu, India

Antony Kumar K

Department of Computer Science & Engineering, Vel Tech Rangarajan Dr Sagunthala R&D Institute of Science and Technology, Chennai, Tamilnadu, India

Rajendran P

Department of Computer Science & Engineering, CMR Institute of Technology, Hyderabad, India

Niresh Kumar S

Department of Computer Science & Engineering, Dhanalakshmi Srinivasan College of Engineering and Technology, Chennai, Tamilnadu, India

Keerthana P

Electronics and Communication Engineering, Selvam College Of Technology, Namakkal, Tamilnadu, India

☰ Contents

I. Introduction

Harmful chemical residues that are found on fruits and vegetables have grave effects on human health. The use of pesticides is requisite for the growth of fruits and vegetables. they are primarily used to nurture the yield of fruits and vegetables. However, being a safe brink of pesticide usage. Through hardware and code simulation optimization, there are numerous approaches to identify pesticides through Internet of Things (IoT).

Authors ▲

Saranya R

Department of Computer Science & Engineering, Vel Tech Rangarajan Dr Sagunthala R&D Institute of Science and Technology, Chennai, Tamilnadu, India

Antony Kumar K

Department of Computer Science & Engineering, Vel Tech Rangarajan Dr Sagunthala R&D Institute of Science and Technology, Chennai, Tamilnadu, India

Rajendran P

Department of Computer Science & Engineering, CMR Institute of Technology, Hyderabad, India

Niresh Kumar S

Department of Computer Science & Engineering, Dhanalakshmi Srinivasan College of Engineering and Technology, Chennai, Tamilnadu, India

Keerthana P

Electronics and Communication Engineering, Selvam College Of Technology, Namakkal, Tamilnadu, India

Figures ▼

References ▼

Keywords ▼



Machine Learning and Mechanics Based Soft Computing Applications pp
199–213

[Home](#) > [Machine Learning and Mechanics Based Soft Computing Applications](#) > Chapter

Complex Shear Imaging Based on Signal Processing and Machine Learning Algorithms

[Duc-Tan Tran](#)  & [Vijender Kumar Solanki](#)

Chapter | [First Online: 28 February 2023](#)

291 Accesses

Part of the [Studies in Computational Intelligence](#) book series
(SCI, volume 1068)

Abstract

The mechanical property of the tissue can be used for medical diagnosis. In a study about shear wave elastography.


This is a preview of subscription content, [log in via an institution](#).



Machine Learning and Mechanics Based Soft Computing Applications pp
151–162

[Home](#) > [Machine Learning and Mechanics Based Soft Computing Applications](#) > Chapter

Hybrid SARIMA—GRU Model Based on STL for Forecasting Water Level in Red River North Vietnam

[Pham Dinh Quan](#) , [Vu Hoang Anh](#), [Nguyen Quang Dat](#) & [Vijender Kumar Solanki](#)

Chapter | [First Online: 28 February 2023](#)

299 Accesses

Part of the [Studies in Computational Intelligence](#) book series (SCI, volume 1068)

Abstract

The Red River Delta is formed by the Red River System, which is the greatest river system in Vietnam's northern region. The primary river, the Red River, has neither an water storage dam nor a hydroelectric dam. Because of this disadvantage, water level forecasting is critical for regulating

agricultural water in Vietnam's second-largest rice-producing region. We present a model to anticipate the water level of Red River water level in Viet Tri, which is near Ha Noi, in this study. The new model is known as the SARIMA-GRU hybrid model, which can fully exploit seasonal patterns in the data. In comparison to the single models SARIMA and GRU, as well as the model ARIMA-RNN, published by Xu et al. in 2019, the new model has produced better results.

Keywords

SARIMA **GRU** **Hybrid** **Water level**

Forecasting

This is a preview of subscription content, [log in via an institution](#).

▼ Chapter

EUR 29.95

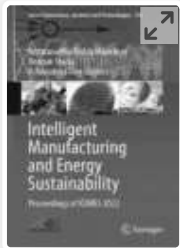
Price includes VAT (India)

- Available as PDF
- Read on any device
- Instant download
- Own it forever

Buy Chapter

> eBook

EUR 117.69



Intelligent Manufacturing and Energy Sustainability pp 625–633

[Home](#) > [Intelligent Manufacturing and Energy Sustainability](#) > Conference paper

Assessment on Multiple Aspects of Online Book Recommendation Systems

[Anusha Penugonda](#) & [Muralidhar Pantula](#) 

Conference paper | [First Online: 21 June 2023](#)

132 Accesses

Part of the [Smart Innovation, Systems and Technologies](#) book series (SIST, volume 334)

Abstract

The recommendation system plays a major role in the online platform that instructs consumers to buy the items they like. Most e-commerce websites, such as online library, online games, Netflix and amazon, recommend products that are preferred by consumers using the recommended system.

Consumers use the recommendation techniques to select the interested items and similar types of items

they are looking for. Recommended system that mostly uses techniques such as collaborative filtering, content-based filtering and hybrid approach. Book recommendation system (BRS) aids consumers in recommending the best books of their interest and the same type books they preferred earlier. Most research articles uses data set comprises book data, user data and rating data. This article compares well-known recommendation system techniques and the data set used to recommend books to consumers. We observed that hybrid technique named commenders is the best among the other research articles, but data sparsity is the complex problem among existing recommendation systems.

Keywords

Recommendation systems

Collaborative filtering **Content-based filtering**

K-nearest neighbour **Hybrid filtering**

This is a preview of subscription content, [log in via an institution](#).

▼ Chapter

EUR 29.95

Price includes VAT (India)

- Available as PDF
- Read on any device
- Instant download
- Own it forever



All



ADVANCED SEARCH

Conferences > 2023 International Conference... ?

Cloud Compliance Framework using Python

Publisher: IEEE

Cite This

PDF

Raja Rambabu Thumati ; L. Arokia Jesu Prabhu ; Vijender Kumar Solanki All Authors



47 Full Text Views

Alerts

Manage Content Alerts

Add to Citation Alerts

Abstract



Download PDF

Document Sections

- I. Introduction
- II. Literature Review
- III. Existing System
- IV. Proposed System
- V. Methodology

Show Full Outline

Authors

Figures

References

Keywords

Metrics

More Like This

Abstract:In today's Cloud environment there are number of issues related to cloud services such as data security, managing of resources. In this paper we are handling these issues... **View more**

Metadata

Abstract:

In today's Cloud environment there are number of issues related to cloud services such as data security, managing of resources. In this paper we are handling these issues by creating an eminent Framework using Python to audit all resources in the cloud platforms like AWS, Azure and GCP using AES and Diffie Hellman algorithm. There are works entitled on data security, which Handles, manages and mainly to store data using Triple DES, AES, RSA, BAT, HECC algorithms on specific cloud platforms. The proposed framework will imbibe AWS, Azure and GCP clouds and provide common platform to audit the resources before start using it and paying for it.

Published in: 2023 International Conference on Disruptive Technologies (ICDT)

Date of Conference: 11-12 May 2023

DOI: 10.1109/ICDT57929.2023.10150986

Date Added to IEEE Xplore: 19 June 2023

Publisher: IEEE

ISBN Information:

Conference Location: Greater Noida, India



I. Introduction

Cloud is a pool of resources, providing services like storage, servers, intelligence, analytics, networks and software via remotely or internet is known as the cloud. In other words, the cloud is referred to as such since the information retrieved is located in a remote or virtual location. The fundamental purpose of using any cloud is to achieve the following parameters prescribed below.

Sign in to Continue Reading

Authors	▼
Figures	▼
References	▼
Keywords	▼
Metrics	▼

More Like This

Towards Achieving Data Security with the Cloud Computing Adoption Framework
IEEE Transactions on Services Computing
Published: 2016

Big Data Security and Privacy Issues in Healthcare
2014 IEEE International Congress on Big Data
Published: 2014

Show More



All



ADVANCED SEARCH

Conferences > 2023 International Conference... ?

The Approach of Digital Marketing is Being Revolutionized by Machine Learning Possibilities

Publisher: IEEE

Cite This

PDF

K. Jagannayaki ; Mantha Srinivas ; K.Sharath Babu ; Naveen Kumar Butta ; Sayyad Saadiq Ali All Authors



64 Full Text Views

Alerts

Manage Content Alerts Add to Citation Alerts

Abstract



Download PDF

Document Sections

- 1. Introduction
- 1. MI: Concepts
- 3. MI'S Significance In Business
- 4. The Association Between Dm and MI
- 5. Conclusion

Abstract:As a result of changing customer behaviour, the proliferation of data, and the ongoing evolution of DM, marketers are sometimes forced to wade through massive amounts of ... **View more**

Metadata

Abstract:

As a result of changing customer behaviour, the proliferation of data, and the ongoing evolution of DM, marketers are sometimes forced to wade through massive amounts of data that might not even provide them with the overall picture they really ought to make impactful business choices. Eighty-four percent of marketing businesses are introducing or increasing their usage of ML in 2018 [1] following the transformation of ML algorithms in other real-world applications. It becomes simpler to accurately forecast and evaluate consumer behaviour. In our work, we first build a state of the art on the primary and most prevalent ML potentials in DM strategies, and we then demonstrate how ML technologies may be employed at a big scale for marketing by analysing extraordinarily huge data sets. They are able to better understand their target customers and maximise their contact with them because to the way that ML is incorporated into digital marketing methods.

Published in: 2023 International Conference on Computer Communication and Informatics (ICCCI)

Date of Conference: 23-25 January 2023

DOI: 10.1109/ICCCI56745.2023.10128490

Date Added to IEEE Xplore: 24 May 2023

Publisher: IEEE

Authors

Figures

References

Keywords

Metrics

More Like This



☰ Contents

I. Introduction

The marketing sector has been impacted by cutting-edge technologies recently. As a result of machine learning advancements and increases in data availability and quantity, more businesses are looking to incorporate the idea of machine learning into their marketing strategies in order to improve the efficiency and intelligence of their operations. QuanticMind reports disclosed that 97% of CEOs believe that how effectively digital marketers utilize ML will determine the direction of marketing in the future. [2]

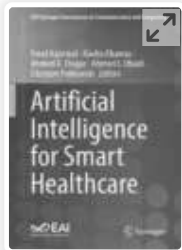
Authors	▼
Figures	▼
References	▼
Keywords	▼
Metrics	▼

More Like This

Financial Data Evaluation Simulation on Account of Machine Learning and Mobile Information Technology
2022 International Conference on Data Analytics, Computing and Artificial Intelligence (ICDACAI)
Published: 2022

Sentiment Analysis of Text Memes: A Comparison Among Supervised Machine Learning Methods
2022 9th International Conference on Electrical Engineering, Computer Science and Informatics (EECSI)
Published: 2022

Show More



Artificial Intelligence for Smart Healthcare pp 275–292

[Home](#) > [Artificial Intelligence for Smart Healthcare](#) > Chapter

ConvNet-Based Deep Brain Stimulation for Attack Patterns

[Angel Sajani Joseph](#), [Arokia Jesu Prabhu Lazar](#), [Dilip Kumar Sharma](#), [Anto Bennet Maria](#), [Nivedhitha Ganesan](#) & [Sudhakar Sengan](#)

Chapter | [First Online: 10 June 2023](#)

528 Accesses

Part of the [EAI/Springer Innovations in Communication and Computing](#) book series (EAI/ISCC)

Abstract

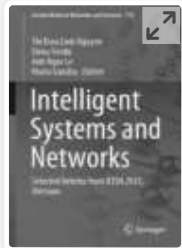
Symptoms of Parkinson's disease usually start slowly and steadily decline with age. People with Parkinson's disease may have problems walking and talking as the disease progresses. Additionally, they may discover psychological and cognitive changes, as well as sleep disturbances, depression, impaired memory,

and drowsiness. Parkinson's disease can affect both men and women. Deep brain stimulation (DBS) is a neurosurgical technique that utilises implantable cardiac electrodes and electrical stimulation to treat neurological dysfunction such as Parkinson's disease (PD), movement disorders, muscle spasms, and other neurodegenerative disorders. Authentication in those operating systems plays a critical role as it can significantly impact the human body's psychological, physical, and emotional states immediately. The present investigation helped develop and verify a deep learning (DL) algorithm that determines the individual diagnosis of patients with PDs focusing on a limited cross-sectional brain structural MRI scan. A type of RNN known as LSTM can learn order dependence in encoding prediction and classification. This is a demand in various problem domains, including computational linguistics, voice recognition, etc. Deep learning's LSTMs are a challenging subject. The work uses a short-term long memory (LSTM), a convolutional neural network (CNN), to anticipate the most trembling speed predicting fake and natural stimulation. The specific design efficiently detected various sorts of replicated attack patterns and informed the physician of potential threats.

Keywords

Deep brain stimulation Energy Symptoms

CNN AI ConvNet Patterns




[The International Conference on Intelligent Systems & Networks](#)

ICISN 2023: **Intelligent Systems and Networks** pp 610–619

[Home](#) > [Intelligent Systems and Networks](#) > Conference paper

A Conceptual Model of Digital Twin for Potential Applications in Healthcare

[Anh T. Tran](#), [Duc V. Nguyen](#), [Than Le](#), [Ho Quang Nguyen](#) ,
[Chi Hieu Le](#), [Nikolay Zlatov](#), [Georgi Hristov](#), [Plamen Zahariev](#)
& [Vijender Kumar Solanki](#)

Conference paper | [First Online: 20 August 2023](#)

192 Accesses

Part of the [Lecture Notes in Networks and Systems](#) book series (LNNS, volume 752)

Abstract

Digital Twin (DT) is one of the important enabling technologies for Smart Manufacturing and Industry 4.0, with a huge potential for many impactful applications in healthcare and industries. This paper presents a conceptual model of a DT system, with a proof-of-concept (POC) prototype of a robot for

demonstrations and further investigations of DT applications in telehealth and in-home healthcare. The successfully developed POC prototype were tested to evaluate time delay, and possible errors when operating and controlling the virtual and physical models of a robot. The proposed conceptual model of a DT system can be used for demonstrations about DT, with further developments for potential applications in healthcare and industries, especially when it is integrated with emerging technologies such as artificial intelligence, machine learning, big data analytics, smart sensors, augmented reality and virtual reality.

Keywords

Digital Twin Industry 4.0

Human-robot Interaction ROS Unity

This is a preview of subscription content, [log in via an institution](#).

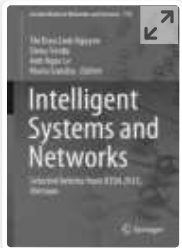
▼ Chapter

EUR 29.95

Price includes VAT (India)

- Available as PDF
- Read on any device
- Instant download
- Own it forever

Buy Chapter



[The International Conference on Intelligent Systems & Networks](#)

ICISN 2023: **Intelligent Systems and Networks** pp 263–270

[Home](#) > [Intelligent Systems and Networks](#) > Conference paper

A Novel Private Encryption Model in IoT Under Cloud Computing Domain

[Sucharitha Yadala](#), [Chandra Shaker Reddy Pundru](#)  & [Vijender Kumar Solanki](#)

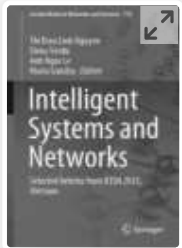
Conference paper | [First Online: 20 August 2023](#)

177 Accesses

Part of the [Lecture Notes in Networks and Systems](#) book series (LNNS, volume 752)

Abstract

The presence of the Internet of Things (IoT) works with the assortment and diffusion of metropolitan information data. In any case, it can release clients' very own security data in brilliant urban areas. Many works have been done and different security systems identifying with the precautions of distributed computing have been implemented from copious



[The International Conference on Intelligent Systems & Networks](#)

ICISN 2023: **Intelligent Systems and Networks** pp 263–270

[Home](#) > [Intelligent Systems and Networks](#) > Conference paper

A Novel Private Encryption Model in IoT Under Cloud Computing Domain

[Sucharitha Yadala](#), [Chandra Shaker Reddy Pundru](#)  & [Vijender Kumar Solanki](#)

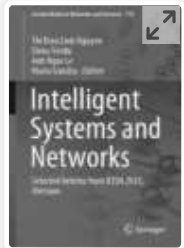
Conference paper | [First Online: 20 August 2023](#)

177 Accesses

Part of the [Lecture Notes in Networks and Systems](#) book series (LNNS, volume 752)

Abstract

The presence of the Internet of Things (IoT) works with the assortment and diffusion of metropolitan information data. In any case, it can release clients' very own security data in brilliant urban areas. Many works have been done and different security systems identifying with the precautions of distributed computing have been implemented from copious



[The International Conference on Intelligent Systems & Networks](#)

ICISN 2023: **Intelligent Systems and Networks** pp 240–246

[Home](#) > [Intelligent Systems and Networks](#) > Conference paper

Blockchain and Federated Learning Based Integrated Approach for Agricultural Internet of Things

[Vikram Puri](#) , [Vijender Kumar Solanki](#) & [Gloria Jeanette Rincón Aponte](#)

Conference paper | [First Online: 20 August 2023](#)

191 Accesses

Part of the [Lecture Notes in Networks and Systems](#) book series (LNNS, volume 752)

Abstract

The agriculture industry has undergone considerable changes in recent decades due to technological improvements and the introduction of new technologies such as the Internet of Things (IoT), artificial intelligence (AI), and secure communication protocols. Even in harsh weather, it is now possible to

Retraction

Retracted: Blockchain-Based Privacy Access Control Mechanism and Collaborative Analysis for Medical Images

Security and Communication Networks

Received 10 October 2023; Accepted 10 October 2023; Published 11 October 2023

Copyright © 2023 Security and Communication Networks. This is an open access article distributed under the Creative Commons Attribution License, which permits unrestricted use, distribution, and reproduction in any medium, provided the original work is properly cited.

This article has been retracted by Hindawi following an investigation undertaken by the publisher [1]. This investigation has uncovered evidence of one or more of the following indicators of systematic manipulation of the publication process:

- (1) Discrepancies in scope
- (2) Discrepancies in the description of the research reported
- (3) Discrepancies between the availability of data and the research described
- (4) Inappropriate citations
- (5) Incoherent, meaningless and/or irrelevant content included in the article
- (6) Peer-review manipulation

The presence of these indicators undermines our confidence in the integrity of the article's content and we cannot, therefore, vouch for its reliability. Please note that this notice is intended solely to alert readers that the content of this article is unreliable. We have not investigated whether authors were aware of or involved in the systematic manipulation of the publication process.

Wiley and Hindawi regrets that the usual quality checks did not identify these issues before publication and have since put additional measures in place to safeguard research integrity.

We wish to credit our own Research Integrity and Research Publishing teams and anonymous and named external researchers and research integrity experts for contributing to this investigation.

The corresponding author, as the representative of all authors, has been given the opportunity to register their agreement or disagreement to this retraction. We have kept a record of any response received.

References

- [1] P. S. Prasad, G. N. Beena Bethel, N. Singh, V. Kumar Gunjan, S. Basir, and S. Miah, "Blockchain-Based Privacy Access Control Mechanism and Collaborative Analysis for Medical Images," *Security and Communication Networks*, vol. 2022, Article ID 9579611, 7 pages, 2022.

Research Article

Blockchain-Based Privacy Access Control Mechanism and Collaborative Analysis for Medical Images

Puja Sahay Prasad ¹, G N Beena Bethel ², Ninni Singh ³, Vinit Kumar Gunjan ³, Samar Basir ³, and Shahajan Miah ⁴

¹Department of Computer Science and Engineering, Geethanjali College of Engineering and Technology, Hyderabad, India

²Department of Computer Science and Engineering, Gokaraju Rangaraju Institute of Engineering and Technology, Hyderabad, India

³Department of Computer Science and Engineering, CMR Institute of Technology, Hyderabad, India

⁴Department of EEE, Bangladesh University of Business and Technology (BUBT), Dhaka, Bangladesh

Correspondence should be addressed to Shahajan Miah; miahbubt@bubt.edu.bd

Received 9 February 2022; Revised 12 April 2022; Accepted 26 April 2022; Published 29 June 2022

Academic Editor: Mukesh Soni

Copyright © 2022 Puja Sahay Prasad et al. This is an open access article distributed under the Creative Commons Attribution License, which permits unrestricted use, distribution, and reproduction in any medium, provided the original work is properly cited.

Medical image analysis technology based on deep learning has played an important role in computer-aided disease diagnosis and treatment. Classification accuracy has always been the primary goal pursued by researchers. However, the image transmission process also faces the problems of limited wireless ad-hoc network (WAN) bandwidth and increased security risks. Moreover, when user data are exposed to unauthorized users, platforms can easily leak personal privacy. Aiming at the abovementioned problems, a system model and an access control scheme for the collaborative analysis of the diagnosis of diabetic retinopathy (DR) are constructed in this paper. The system model includes two stages of data cleaning and lesion classification. In the data cleaning phase, the private cloud writes the model obtained after training into the blockchain, and other private clouds use the best-performing model on the chain to identify the image quality when cleaning data and pass the high-quality image to the lesion classification model for use. In the lesion classification stage, each private cloud trains the classification model separately; uploads its own model parameters to the public cloud for aggregation to obtain a global model; and then sends the global model to each private cloud to achieve collaborative learning, reduce the amount of data transmission, and protect personal privacy. Access control schemes include improved role-based access control (RAC) used within the private cloud and blockchain-based access control used during the interaction between the private cloud and the public cloud program (BAC). RAC grants both functional rights and data access rights to roles and takes into account object attributes for fine-grained level control. Based on certificateless public-key encryption technology and blockchain technology, BAC can realize the identity authentication and authority identification of the private cloud while requesting the transmission of model parameters from the private cloud to the public cloud and protect the security of the identity, authority, and model parameters of the private cloud to achieve the effect of lightweight access control. In the experimental part, two retinal datasets are used for DR classification analysis. The results show that data cleaning can effectively remove low-quality images and improve the accuracy of early lesion classification for doctors, with an accuracy rate of 90.2%.

1. Introduction

With the development of digital medicine and machine learning, more and more e-health systems are favored by academia and industries. Due to the digital nature, much

medical data need to be stored electronically and shared through cloud platforms for higher quality and broader applications. The medical image analysis process is usually based on the identification of doctors or experts. Still, it is easy to cause visual fatigue, which leads to a decrease in

identification accuracy. Deep learning algorithms, especially convolution neural networks, can automatically learn more specific features to improve classification accuracy. Therefore, it has quickly become a research hotspot for analyzing medical images [1]. However, the amount of image data will affect the model training accuracy and it is not easy to gather all the photos of all hospitals together in reality. Scholars have proposed deep collaborative learning to improve the classification accuracy and applied it in medical image analysis [2]. However, in these medical image data processing systems with independent private clouds, user data are easily exposed to illegal users [3]. Access control set of access rules can ensure that authorized users can access resources and unauthorized users cannot access them to solve the problems of data security and privacy leakage [4].

In the past, people have used deep learning or collaborative deep learning algorithms to analyze medical images. A feature transfer network and local background suppression-based method for microaneurysm detection, for example, is proposed in literature [5]. A deconvolutional neural network, on the other hand, is proposed in literature [6]. Using morphological opening and closing operations, reference [7] can get rid of isolated noise points. To make training and test sets, for example, a method of comparing the size of each picture is used. As an example, the literature [8] came up with a collaborative deep learning model to help people figure out which lung nodules are malignant and which are not, even though they have limited chest CT data. This model is based on multiview knowledge [9] based on two collaborative convolutional neural network models; this section proposes an automatic segmentation algorithm for shoulder joint images that can accurately segment the glenoid and humeral head in shoulder collective images [10]. This section proposes a segmentation learning method for deep learning of healthcare collaboration. However, the existing deep learning and collaborative deep learning algorithms only think about how to make models. So, it does not take into account how data cleaning and classification work together, which will lead to low data quality. There are also issues with personal privacy and data security.

2. Related Work

Scholars have come up with a variety of ways to keep medical data safe and private. For example, in literature [11], there is a way to control access to medical images by using a two-layer system. S. M. Islam and others came up with a risk-based access control model that changes as people get more or less access. Role-based access control (RBAC), attribute-based access control (ABAC), and blockchain-based access control are some of the most common access control models (blockchain-based access control, BBAC). RBAC uses the user's role to set a security policy and the procedure is usually linked to the user's job. This is common in a hospital information system (HIS) that is used in the real world. Literature [11] came up with a way to control access to a cloud infrastructure-as-a-service based on roles. N. Weng and his team came up with a way to get reasonable fine-grained access control. They came up with the attribute-

based controlled collaborative access control (ABCCCC) model. The data owner chooses a group of people to collaborate with. In [12], attribute-based fine-grained access control encryption is designed to mark ciphertexts with attribute sets so that only certain people can read them. Because of the blockchain's decentralization and immutability, it is a good idea to use it to solve problems with electronic medical records' interoperability and security [13]. Blockchain-based access control methods have been used in some medical information systems before. In [14], a design that is both scalable and robust is shown. It uses blockchain technology for access control. It uses a discrete wavelet transform method to make it more secure. Blockchain was used by O. Oktay et al. to keep patient health records safe and private, which solved the problem of losing control when encrypting data [15]. Some works do not pay attention to how fine-grained access is at the attribute level. For BBAC, many pieces do not pay attention to the fact that they are lightweight. So, the performance and scalability of their scheme are limited by complicated consensus mechanisms that take a lot of time.

Two access control schemes are proposed in this paper to keep people from getting their hands on medical data without permission. One is an improved role-based access control (RAC) scheme and the other is a blockchain-based access control (BAC) scheme. RAC is based on how important a role is, with attribute-level constraints that keep people who are not supposed to be able to access the HIS from doing so. BAC uses blockchain technology to keep third-party trusted third-party authorities out of the distributed network architecture, which does not need them. Access control policies use a lightweight certificateless public-key encryption algorithm to protect medical data's security, as well as to cut down on the amount of data that needs to be sent. So that other systems used are more secure and have enough bandwidth, because most of the HIS's functions are done on the local network. For example, when using the system functions on a LAN, the role-based access control scheme is used. The lightweight access control scheme based on blockchain, however, is used when using system functions for WAN.

3. Deep Learning for Classification

The quality of clinical medical images is uneven and low-quality color fundus images mainly have problems such as low contrast, overexposure, and noise in the picture. These low-quality images significantly increase the difficulty of diagnosis for ophthalmologists and even cannot distinguish the types of lesions in the early stage of DR, such as bleeding spots and hard exudates. At the same time, when using computer technology to detect DR lesions automatically, low-quality color fundus images will significantly interfere with the training process of the detection model, so that a model for accurate detection of lesions cannot be trained. Therefore, culling these low-quality images in the data cleaning stage can significantly improve model detection. In this paper, the CNN model is used to detect low-quality

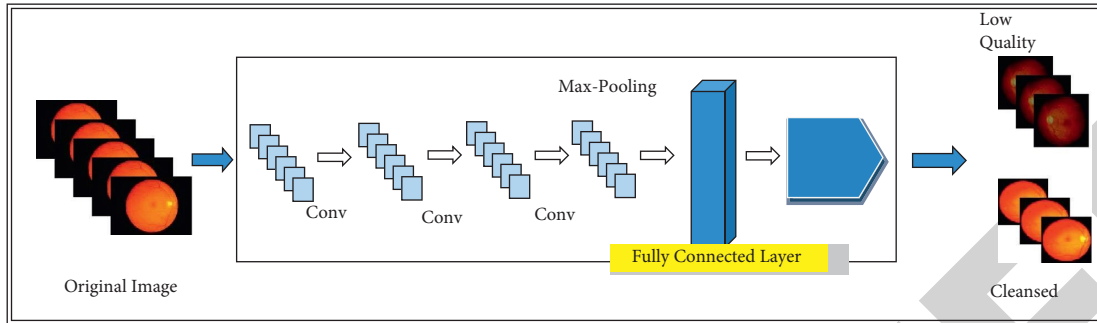


FIGURE 1: Data cleaning model.

TABLE 1: Data cleaning model parameters.

Floor	Type	Feature map size	Filter size	Step size	Number of parameters
0	Input	$88 \times 88 \times 3$	—	—	—
1	Convolution layer	$88 \times 88 \times 24$	$5 \times 5 \times 24$	1	624
2	Convolution layer	$80 \times 80 \times 16$	$3 \times 3 \times 16$	1	160
3	Convolution layer	$78 \times 78 \times 8$	$3 \times 3 \times 8$	1	80
4	Max-pooling	$39 \times 39 \times 8$	2×2	2	—
5	Fully connected layer	64	—	—	778688
6	Fully connected layer	2	—	—	126

TABLE 2: Comparison of role-based access control.

Model	RBAC (proposed)	ABCCC [17]	E-RBAC [18]	SAT-RBAC [19]	ABAC-IaaS [20]
Support attribute	Support	Support	Not support	Not support	Support
Flexibility	High	Low	High	Low	Generally
Dynamism	High	Low	Low	Low	High
Extensibility	High	Low	Low	Low	High
Multilevel security control	Support	Support	Not support	Not support	Not support
Model safety	High	High	Low	Generally	Low

photos. The model structure is shown in Figure 1, and the model parameters are shown in Table 1. In this paper, the model in [16] is used to detect bleeding points and hard exudates in fundus images, and the detection effect is better than most of the existing methods.

4. Experiments and Result Analysis

4.1. Comparison of RBAC Schemes. Table 2 lists some role-based access control models and compares them with the RAC model in this paper in terms of attribute-based, flexibility, and dynamism. The RAC model proposed in this paper can be flexibly configured when controlling data domain access. Different levels of roles can realize data access in different scopes. Functional operations can be increased or decreased according to business needs. It has the characteristics of flexibility, dynamism, and scalability. It has been applied in practical projects and proved available and convenient. In addition, RAC enables fine-grained access control based on attributes. As shown from Table 2, RAC is superior to ABCCC, E-RBAC/SAT-RBAC, and ABAC-IaaS in terms of whether to support attribute-level power, flexibility, dynamism, scalability, multilevel security control, and model security.

4.2. Comparison of Running Time in BAC. The runtime comparison tests were done on a computer with the Windows 10 operating system that had a 2.9 GHz Intel(R) Core(TM) i7-7500U, 8 Gb RAM, 128 Gb SSD, and 1 Tb HDD. IDEA 2018.3.1 Ultimate Edition was used to write the code. Encryption and decryption, as well as signing and verifying, are based on ECIES and ECDSA. In Secp160r1, we use the parameters in Secp160r1 (SEC2) as a guide for the security strength of ECC with 160 bit keys. The algorithm for symmetric keys in Encrypt is 128 bit AES. If you want to figure out how much time it takes to do arithmetic operations like hashing and symmetric cryptography, you usually look at the number of scalar multiplications and the running time of each one (a scalar multiplication running time the average is about 0.81 ms).

In the BAC scheme, PE is encrypted/decrypted, signed, and authenticated with BL-CL-PKC. Compared to the literature, it encrypts L-CL-PKS and PKE with the literature [21–23] and PKS with the literature [16, 24–26], [27–29]. Figure 2(a) shows how long it takes the algorithm to do encryption and decryption on PE. The figure shows that the algorithm L-CL-PKE is better than the comparison algorithm when it comes to how long it takes to encrypt and decrypt a piece of data. As you can see in Figure 2(b), the

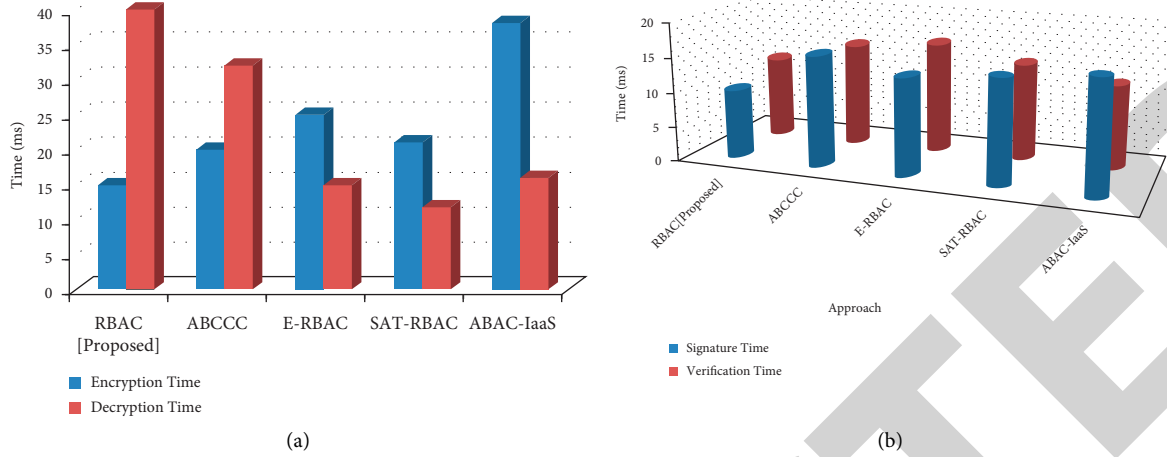


FIGURE 2: Time consumption comparison. (a) Encryption and decryption. (b) Signature and authentication.

algorithm's running time for PE signature and authentication operations is shown. L-CL-PKS is a better algorithm than the comparison algorithm when it comes to the time it takes to sign and authenticate a PE file, as shown in the figure. Due to the bilinear pairings used in CL-PKE, the running time is longer. Because the cost is more than scalar multiplication, the other algorithms have more scalar multiplication than this one [30]. On the other hand, the design of L-CL-PKE in this paper does not use identity-based encryption. Instead, it tries to make ECC work with ID instead. Still, it has the same features of identity-based public-key encryption. So, the proposed BAC scheme is very light. Table 3 shows the comparison between encryption and decryption time. Also, the comparison between signature and verification time is shown in Table 4.

4.3. Lesion Classification Results. DR early lesion detection is done on the fundus images in the DIARETDB1 (DB1) dataset in this paper. In this paper, data cleaning experiments are done on the DIARETDB0 (DB0) dataset. 130 color fundus images are in the DB0 dataset and 89 color fundus images are in the DB1 dataset. The size of the fundus images in both datasets is 1500 * 1152. Images in DB0 are broken down into low-quality and high-quality ones. The DB0 dataset is used to train the model that cleans data. To see how well the model works, this paper uses the DB1 dataset to test the model that was trained. The results of the experiments show that the model chosen in this paper can filter out low-quality fundus images and its accuracy can be increased to 74.4%. It also has ground truth maps of bleeding spots and hard exudates, which are used to check the model's lesion classification. At the same time, this paper uses the 10-fold cross-validation method to both train and test the model and it does both. The sensitivity and accuracy of the detection results are two of the measurement standards. It is the percentage of correct positive samples to all correct positive samples. It is used to see how well the model can predict which positive samples will be correct. It is the ratio of the number of positive and negative examples correctly classified to the sum of all positive and negative examples. It is

TABLE 3: Comparative encryption and decryption time.

Approach	Time (MS)	
	Encryption time	Decryption time
RBAC (proposed)	15	40
ABCCC	20	32
E-RBAC	25	15
SAT-RBAC	21	12
ABAC-IaaS	38	16

TABLE 4: Signature and verification time.

Approach	Time (milliseconds)	
	Signature time	Verification time
RBAC (proposed)	10	12
ABCCC	16	15
E-RBAC	14	16
SAT-RBAC	15	14
ABAC-IaaS	16	12

used to figure out how well the whole model classification did. The following are the ways to do:

$$\text{Sensitivity} = \frac{TP}{TP + FN}, \quad (1)$$

$$\text{Accuracy} = \frac{TP + TN}{TP + FN + TN + FP},$$

where TP is the correctly predicted positive sample, TN is the correctly predicted negative sample, FP is the incorrectly predicted positive sample, and FN is the incorrectly predicted negative sample. In this experiment, the detection accuracy of the positive and negative models reached 90.2%. Sensitivity is the detection effect of one of the color fundus images. Figure 3 shows classification results of bleeding spots and hard exudates on the DB1 dataset.

In addition to sensitivity and accuracy, this paper also uses the ROC curve to measure the detection effect of different lesions, which depicts the relationship between sensitivity and the average number of false detections per

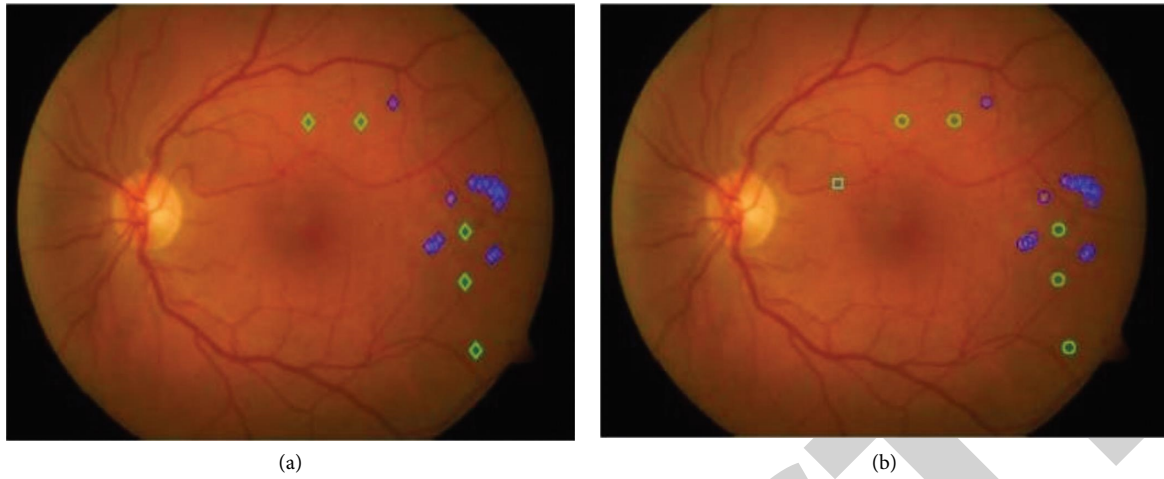


FIGURE 3: Classification results of bleeding spots and hard exudates on the DB1 dataset. (a) Raw retinal image. (b) Classification results.

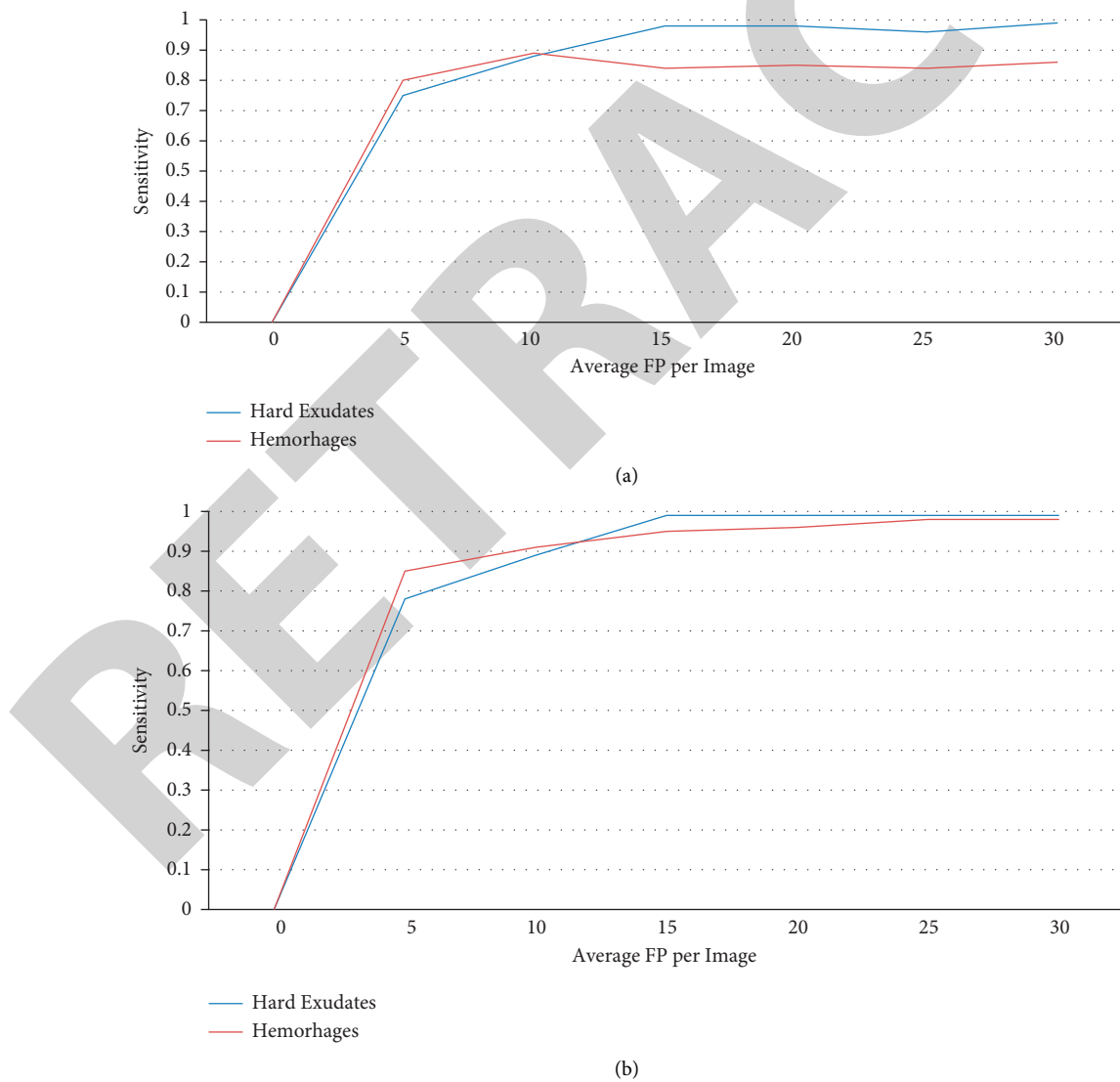


FIGURE 4: ROC curves for DR lesion classification. (a) ROC curve without data cleaning. (b) ROC curve using data cleaning.

TABLE 5: Sensitivity without data cleaning.

FP/Image	Hard exudates	Hemorhages
0	0	0
5	0.75	0.8
10	0.88	0.89
15	0.98	0.84
20	0.98	0.85
25	0.96	0.84
30	0.99	0.86

TABLE 6: Sensitivity with data cleaning.

FP/Image	Hard exudates	Hemorhages
0	0	0
5	0.78	0.85
10	0.89	0.91
15	0.99	0.95
20	0.99	0.96
25	0.99	0.98
30	0.99	0.98

TABLE 7: Detection sensitivity of DR lesions (1000 iteration).

Approach	Hemorhages	Hard exudates
No data cleaning	0.8564	0.9623
RBAC (proposed)	0.9125	0.9845
ABCCC	0.6265	0.8766
E-RBAC	0.5264	0.8304
SAT-RBAC	0.5856	0.8205
ABAC-IaaS	0.840	0.8045

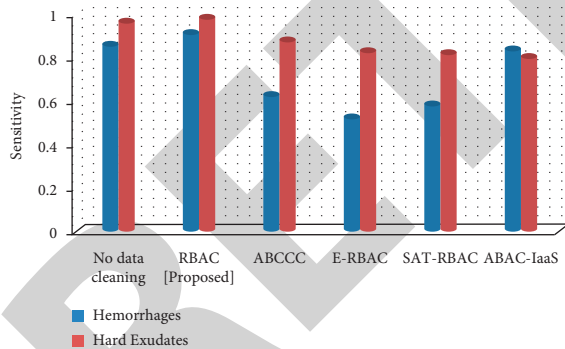


FIGURE 5: Detection sensitivity of DR lesions (1000 iteration).

image. Figures 4(a) and 4(b) depict the ROC curves before and after data cleaning. It can be seen from the angles that the detection sensitivity of different lesions is improved after cleaning. Tables 5 and 6 show the sensitivity without and with data cleaning, respectively.

Sensitivity for each lesion is listed in Table 7, with increased sensitivity for bleeding spots and hard exudates after data cleaning. This has been shown graphically in Figure 5. To more objectively verify the detection performance of this model, this paper also compares the detection of fundus images by different existing methods, as shown in Table 5. It can be seen from the table that the bleeding points are hard

exudates after data cleaning. The sensitivity of this model has been improved and the detection performance of this model is better than other existing methods, which shows the effectiveness of this method for fundus target detection.

5. Conclusion

This paper designs a medical image collaborative analysis system model based on deep learning, which can protect the security of medical data and model parameters, reduce the amount of data transmission, save bandwidth, and achieve more accurate lesion classification. The first stage in the system model is data cleaning, that is, the doctor collects images, uploads them to the private cloud for data cleaning, and transfers the cleaned high-quality images to the classification model; the second stage is classification, that is, the private cloud uses high-quality images to perform model training, upload the model parameters to the public cloud for aggregation, and then the public cloud will transfer the newly obtained global model to the private cloud. This paper designs two access control schemes in these two stages, RAC and BAC. RAC can implement fine-grained, flexible, and dynamic access control based on roles and attributes. BAC is a blockchain-based solution that eliminates trusted third parties to prevent single-point-of-failure authentication or man-in-the-middle attacks. Based on certificates, the public-key encryption technology enables light data transmission over WAN. In addition, when the private cloud requests to upload model parameters from the public cloud, it does not need to perform identity authentication and authority identification separately but encapsulates the identity and authority information together with the model parameters to reduce the separate identity identification operation. Both schemes prevent unauthorized users from accessing medical data. Data cleaning can remove low-quality images to diagnose early DR lesions and effectively improve accuracy. The experimental results and security analysis prove that the scheme can effectively protect the system's security to classify medical data, and the classification accuracy can reach 90.2%.

Data Availability

The data will be made available on request from corresponding author.

Conflicts of Interest

The authors declare that they have no conflicts of interest.

References

- [1] X. Guo, P. Zhang, C. Wang, B. Sun, and S. Sun, "A novel deep learning model for palmprint/palmvein recognition," *IEEE Access*, vol. 9, Article ID 122847, 2021.
- [2] Q. Yan, J. Huang, C. Xiong, Z. Yang, and Z. Yang, "Data-driven human-robot coordination based walking state monitoring with cane-type robot," *IEEE Access*, vol. 6, pp. 8896–8908, 2018.

- [3] B. T. Baker, R. F. Silva, V. D. Calhoun, A. D. Sarwate, and S. M. Plis, "Large scale collaboration with autonomy: decentralized data ICA," in *Proceedings of the IEEE 25th International Workshop on Machine Learning for Signal Processing (MLSP)*, pp. 1–6, Boston, MA, USA, September 2015.
- [4] Ieee, "IEE colloquium on 'medical imaging: image processing and analysis' (digest No.051)," in *Proceedings of the IEE Colloquium on Medical Imaging: Image Processing and Analysis*, London, UK, March 1992.
- [5] F. Ritter, "Medical image analysis," *IEEE Pulse*, vol. 2, no. 6, pp. 60–70, 2011.
- [6] S. K. Sen, M. Foskey, J. S. Marron, and M. A. Styner, "Support vector machine for data on manifolds: an application to image analysis," in *Proceedings of the 5th IEEE International Symposium on Biomedical Imaging*, pp. 1195–1198, Paris, France, May, 2008.
- [7] W. J. Niessen, B. M. T. H. Romeny, and M. A. Viergever, "Geodesic deformable models for medical image analysis," *IEEE Transactions on Medical Imaging*, vol. 17, no. 4, pp. 634–641, 1998.
- [8] W. Yuan, M. Hamit, A. Kutluk, and C. Yan, "Feature extraction and analysis on Xinjiang uygur medicine image by using color histogram," in *Proceedings of the IEEE International Conference on Medical Imaging Physics and Engineering*, pp. 259–264, Shenyang, China, October, 2013.
- [9] D. Tellez, G. Litjens, J. van der Laak, and F. Ciompi, "Neural image compression for gigapixel histopathology image analysis," *IEEE Transactions on Pattern Analysis and Machine Intelligence*, vol. 43, no. 2, pp. 567–578, 2021.
- [10] R. A. Brown, H. Zhu, and J. R. Mitchell, "Distributed vector Processing of a new local MultiScale Fourier transform for medical imaging applications," *IEEE Transactions on Medical Imaging*, vol. 24, no. 5, pp. 689–691, 2005.
- [11] S. M. Islam and H. S. Mondal, "Image enhancement based medical image analysis," in *Proceedings of the 10th International Conference on Computing, Communication and Networking Technologies (ICCCNT)*, pp. 1–5, Kanpur, India, July, 2019.
- [12] O. Oktay, W. Bai, R. Guerrero, and M. Rajchl, "Stratified decision forests for accurate anatomical landmark localization in cardiac images," *IEEE Transactions on Medical Imaging*, vol. 36, no. 1, pp. 332–342, 2017.
- [13] A. V. Nikolaev, L. D. Jong, G. Weijers, and V. Groenhuis, "Quantitative evaluation of an automated cone-based breast ultrasound scanner for MRI–3D US image fusion," *IEEE Transactions on Medical Imaging*, vol. 40, no. 4, pp. 1229–1239, 2021.
- [14] H. Bogunović, F. Venhuizen, and S. Klimescha, "RETOUCH: the retinal OCT fluid detection and segmentation benchmark and challenge," *IEEE Transactions on Medical Imaging*, vol. 38, no. 8, pp. 1858–1874, 2019.
- [15] O. Oktay, E. Ferrante, K. Kamnitsas, and M. Heinrich, "Anatomically constrained neural networks (ACNNs): application to cardiac image enhancement and segmentation," *IEEE Transactions on Medical Imaging*, vol. 37, no. 2, pp. 384–395, 2018.
- [16] W. Xianghong, Y. Shi-e, and X. Xincheng, "An effective method to colour medical image enhancement," in *Proceedings of the IEEE/ICME International Conference on Complex Medical Engineering*, pp. 874–877, Beijing, China, May, 2007.
- [17] N. Weng, Y. Yang, and R. Pierson, "Three-dimensional surface reconstruction using optical flow for medical imaging," *IEEE Transactions on Medical Imaging*, vol. 16, no. 5, pp. 630–641, 1997.
- [18] M. J. J. P. van Grinsven, B. van Ginneken, C. B. Hoyng, T. Theelen, and C. I. Sánchez, "Fast convolutional neural network training using selective data sampling: application to hemorrhage detection in color fundus images," *IEEE Transactions on Medical Imaging*, vol. 35, no. 5, pp. 1273–1284, 2016.
- [19] G. V. Pendse, R. Baumgartner, A. J. Schwarz, A. Coimbra, D. Borsook, and L. Becerra, "A statistical framework for optimal design matrix generation with application to fMRI," *IEEE Transactions on Medical Imaging*, vol. 29, no. 9, pp. 1573–1611, 2010.
- [20] S. Kostopoulos, D. Cavouras, A. Daskalakis, and P. Bougioukos, "Colour-Texture based image analysis method for assessing the Hormone Receptors status in Breast tissue sections," in *Proceedings of the 29th Annual International Conference of the IEEE Engineering in Medicine and Biology Society*, pp. 4985–4988, Lyon, France, August 2007.
- [21] C. H. Li and P. C. Yuen, "Regularized color clustering in medical image database," *IEEE Transactions on Medical Imaging*, vol. 19, no. 11, pp. 1150–1155, Nov, 2000.
- [22] A. S. Panayides, A. Amini, N. D. Filipovic, and A. Sharma, "AI in medical imaging informatics: current challenges and future directions," *IEEE Journal of Biomedical and Health Informatics*, vol. 24, no. 7, pp. 1837–1857, 2020.
- [23] M. Geng, X. Meng, J. Yu, L. Zhu, and L. Jin, "Content-noise complementary learning for medical image denoising," *IEEE Transactions on Medical Imaging*.
- [24] S. M. Pizer, "The medical image display and analysis group at the university of North Carolina: reminiscences and philosophy," *IEEE Transactions on Medical Imaging*, vol. 22, no. 1, pp. 2–10, 2003.
- [25] C. Vertan and G. Voicea, "A comparison of decolorization methods performance for medical color images," in *Proceedings of the E-Health and Bioengineering Conference (EHB)*, pp. 1–4, November, 2015.
- [26] J. Kim, W. Cai, D. Feng, and H. Wu, "A new way for multidimensional medical data management: volume of interest (VOI)-Based retrieval of medical images with visual and functional features," *IEEE Transactions on Information Technology in Biomedicine*, vol. 10, no. 3, pp. 598–607, 2006.
- [27] H. Xu, C. Li, M. M. Rahaman, Y. Yao, and Z. Li, "An enhanced framework of generative adversarial networks (EF-GANs) for environmental microorganism image augmentation with limited rotation-invariant training data," *IEEE Access*, vol. 8, Article ID 187455, 2020.
- [28] W. Yang and J.-R. Liu, "Research and development of medical image fusion," in *Proceedings of the IEEE International Conference on Medical Imaging Physics and Engineering*, pp. 307–309, Shenyang, China, October 2013.
- [29] Y. Chen, Z. Li, L. Wang, N. Wang, and B. Hong, "High-capacity reversible watermarking algorithm based on the region of interest of medical images," in *Proceedings of the 14th IEEE International Conference on Signal Processing (ICSP)*, pp. 1158–1162, Beijing, China, August 2018.
- [30] K. Gong, K. Kim, D. Wu, M. K. Kalra, and Q. Li, "Low-dose dual energy CT image reconstruction using non-local deep image prior," in *Proceedings of the IEEE Nuclear Science Symposium and Medical Imaging Conference (NSS/MIC)*, pp. 1–2, Manchester, UK, October 2019.

Retraction

Retracted: Machine Learning and Cloud-Based Knowledge Graphs to Recognize Suicidal Mental Tendencies

Computational Intelligence and Neuroscience

Received 3 October 2023; Accepted 3 October 2023; Published 4 October 2023

Copyright © 2023 Computational Intelligence and Neuroscience. This is an open access article distributed under the Creative Commons Attribution License, which permits unrestricted use, distribution, and reproduction in any medium, provided the original work is properly cited.

This article has been retracted by Hindawi following an investigation undertaken by the publisher [1]. This investigation has uncovered evidence of one or more of the following indicators of systematic manipulation of the publication process:

- (1) Discrepancies in scope
- (2) Discrepancies in the description of the research reported
- (3) Discrepancies between the availability of data and the research described
- (4) Inappropriate citations
- (5) Incoherent, meaningless and/or irrelevant content included in the article
- (6) Peer-review manipulation

The presence of these indicators undermines our confidence in the integrity of the article's content and we cannot, therefore, vouch for its reliability. Please note that this notice is intended solely to alert readers that the content of this article is unreliable. We have not investigated whether authors were aware of or involved in the systematic manipulation of the publication process.

Wiley and Hindawi regrets that the usual quality checks did not identify these issues before publication and have since put additional measures in place to safeguard research integrity.

We wish to credit our own Research Integrity and Research Publishing teams and anonymous and named external researchers and research integrity experts for contributing to this investigation.

The corresponding author, as the representative of all authors, has been given the opportunity to register their agreement or disagreement to this retraction. We have kept a record of any response received.

References

- [1] V. K. Gunjan, Y. Vijayalata, S. Valli, S. Kumar, M. O. Mohamed, and V. Saravanan, "Machine Learning and Cloud-Based Knowledge Graphs to Recognize Suicidal Mental Tendencies," *Computational Intelligence and Neuroscience*, vol. 2022, Article ID 3604113, 10 pages, 2022.

Research Article

Machine Learning and Cloud-Based Knowledge Graphs to Recognize Suicidal Mental Tendencies

Vinit Kumar Gunjan ¹, Y. Vijayalata ², Susmitha Valli ², Sumit Kumar ³,
M. O. Mohamed ⁴ and V. Saravanan ⁵

¹Department of Computer Science and Engineering, CMR Institute of Technology, Hyderabad, India

²Department of CSE, GRIET, Telangana, India

³Indian Institute of Management, Kozhikode, India

⁴Mathematics Department, Zagazig University, Faculty of Science, Egypt

⁵Department of Computer Science, College of Engineering and Technology, Dambi Dollo University, Dambi Dollo, Oromia Region, Ethiopia

Correspondence should be addressed to Vinit Kumar Gunjan; vinitkumargunjan@gmail.com and V. Saravanan; saravanan@dadu.edu.et

Received 31 January 2022; Revised 11 February 2022; Accepted 19 February 2022; Published 17 March 2022

Academic Editor: Deepika Koundal

Copyright © 2022 Vinit Kumar Gunjan et al. This is an open access article distributed under the Creative Commons Attribution License, which permits unrestricted use, distribution, and reproduction in any medium, provided the original work is properly cited.

To improve the quality of knowledge service selection in a cloud manufacturing environment, this paper proposes a cloud manufacturing knowledge service optimization decision method based on users' psychological behavior. Based on the characteristic analysis of cloud manufacturing knowledge service, establish the optimal evaluation index system of cloud manufacturing knowledge service, use the rough set theory to assign initial weights to each evaluation index, and adjust the initial weights according to the user's multiattribute preference to ensure that the consequences are allocated correctly. The system can help counselors acquire psychological knowledge in time and identify counselors with suicidal tendencies to prevent danger. This paper collected some psychological information data and built a knowledge graph by creating a dictionary and generating entities and relationships. The Han language processing word segmentation tool generates keywords, and CHI (Chi-square) feature selection is used to classify the problem. This feature selection is a statistical premise test that is acceptable when the chi-square test results are distributed with the null hypothesis. It includes the Pearson chi-square test and its variations. The Chi-square test has several benefits, including its distributed processing resilience, ease of computation, broad information gained from the test, usage in research when statistical assumptions are not satisfied, and adaptability in organizing information from multiple or many more group investigations. For improving question and answer efficiency, compared with other models, the BiLSTM (bidirectional long short-term memory) model is preferred to build suicidal tendencies. The Han language processing is a method that is used for word segmentation, and the advantage of this method is that it plays a key role in the word segmentation tool and generates keywords, and CHI (Chi-square) feature selection is used to classify the problem. Text classifier detects dangerous user utterances, question template matching, and answer generation by computing similarity scores. Finally, the system accuracy test is carried out, proving that the system can effectively answer the questions related to psychological counseling. The extensive experiments reveal that the method in this paper's accuracy rate, recall rate, and F1 value is much superior to other standard models in detecting psychological issues.

1. Introduction

Cloud manufacturing (CMfg) is a new service-oriented and knowledge-based networked and agile manufacturing model [1] that integrates advanced technologies, such as existing

information technology, cloud computing [2], and the Internet of Things [3]. It centrally stores the optimized and integrated manufacturing resources in the cloud pool of the manufacturing system and provides users with various high-quality and fast manufacturing services on demand through

the network. As a result, cloud manufacturing knowledge is a dynamic resource that is infiltrating all cloud manufacturing service life cycles [4]. At the same time, cloud manufacturing knowledge service (CMKS) is a knowledge transfer and sharing service that can effectively support cloud manufacturing. As a result, all manufacturing activities in the manufacturing environment are carried out efficiently, stably, and accurately.

The addition of knowledge services significantly improves cloud manufacturing systems' operational efficiency and problem-solving capabilities [5]. The organic combination of CMfg and knowledge services promotes the extension of "manufacturing as a service" to "knowledge as a service," enabling enterprises to quickly obtain the required manufacturing knowledge and services with the support of the cloud platform, effectively solving the problems in the production and operation process of enterprises. Technical bottleneck problem improves its comprehensive competitiveness. It is a statistical premise test that is acceptable when the chi-square test results are distributed with the null hypothesis. It includes the Pearson chi-square test and its variations. The Chi-square test has several benefits, including its distributed processing resilience, ease of computation, broad information gained from the test, usage in research when statistical assumptions are not satisfied, and adaptability in organizing information from multiple or much more group investigations. At present, scholars at home and abroad have explored the relevant theories and technologies of knowledge services in the cloud manufacturing environment. For example, author [6] proposed a personalized knowledge service technology based on user perception of the cloud manufacturing environment. The platform user task requirements and information actively push knowledge resources related to user manufacturing tasks. To a certain extent, it has promoted the evolution of cloud service platforms from "useable" to "easy to use." Author [4] proposed a cloud manufacturing knowledge service method based on uncertain rule reasoning, which realizes the knowledge service from quantitative to qualitative and then from quantitative to qualitative. The conversion to quantitative provides a new idea for the accurate distribution of cloud manufacturing knowledge services. Reference [7] builds a knowledge service realization model for the machining process of blade parts in complex curved parts in a cloud manufacturing environment, which shortens the time to a certain extent. In this research, we have inferred that LSTM-based models are quite higher than ML algorithms because the LSTM framework for organizations was used to improve the knowledge graph, and a heuristics candidate answer ordering approach was employed to verify the system's performance.

The generation time of the tool path in the processing of blade parts is improved, and the processing efficiency and quality of the blade are improved. The literature [8] proposes an optimization method for matching the knowledge service demander and the provider and uses a fuzzy axiomatic design. The theoretical measurement of matching satisfaction provides a specific theoretical basis for matching the supply and demand of knowledge services. To realize the

acquisition, storage, and sharing of different types of knowledge, literature [9] designs a cloud computing industry alliance based on the behavioral characteristics of knowledge interaction. To a certain extent, the knowledge resource sharing efficiency of the cloud computing industry alliance and the level of knowledge service have been improved. In this research, we have used the graph knowledge method. The limitation of this method is as follows: its evaluation measures concerning the model fit or factor levels cannot be done using graphic approaches since they do not provide certainty ranges for the variables (levels supplied by a correlation tool for all of this type of data are wrong). The above research has promoted the development of CMKS to a certain extent. The correctness and trustworthiness of the knowledge service offered cannot be ensured, resulting in low knowledge service performance. To that purpose, this study uses the user's mental behavioral traits as a judgment element, combining the benefits of the rough set theory in dealing with ambiguity and uncertainty. The CMKS is a knowledge-sharing and sharing service that can help cloud manufacturers succeed. As a consequence, all manufacturing operations in the manufacturing environment run smoothly, consistently, and precisely. Still, the research on the optimal decision-making method of knowledge service is relatively lacking. The accuracy and credibility of the provided knowledge service cannot be guaranteed, resulting in the low efficiency of knowledge service. To this end, this paper takes the user's psychological behavior characteristics as a decision-making factor and combines the advantages of the rough set theory in dealing with uncertainty and ambiguity. The optimal selection of services provides a reference idea and method.

2. Characteristics Analysis of Cloud Manufacturing Knowledge Service

CMKS is a kind of service guided by users' knowledge needs on the cloud manufacturing service platform, aiming at knowledge innovation, solving the manufacturing problems faced by users, and proactively providing users with personalized and specialized knowledge resources [10, 11]. The cloud manufacturing knowledge service (CMKS) is an information-sharing and sharing service that can help cloud manufacturers succeed. As a consequence, all manufacturing processes in the manufacturing environment run smoothly, consistently, and precisely. The integration of knowledge services enhances the operating effectiveness and problem-solving capacities of cloud manufacturing systems dramatically.

Compared with other services, knowledge services in the cloud manufacturing environment have the following salient features:

- (a) Knowledge transformation is complex: there are many types of knowledge resources in the cloud manufacturing environment, including explicit knowledge, such as standards, patents, and documents, and tacit knowledge, such as experience and capabilities. Most of these highly personalized and

challenging to standardize implicit knowledge resources come from different enterprises. Because of the inconsistency of knowledge resource management and processing methods, other users can benefit from the same knowledge resources. Therefore, converting cloud manufacturing knowledge service resources into their proper value is more challenging.

- (b) Dynamic changes in value: in the cloud manufacturing environment, the value of complex manufacturing resources will decrease with aging and wear and tear, while the value of knowledge resources changes in different directions. For example, with the growth of age and the continuous accumulation of knowledge, the value of employee experience will become higher and higher. With the advancement of technology and users' higher requirements for product quality, the value of a specific method or patent will become higher. Cloud platforms need to monitor these knowledge resources and continuously update their value status to provide appropriate services to users at the right time.
- (c) Highly integrated and shared: as an intellectual resource on the cloud manufacturing service platform, knowledge can provide oral, written, electronic, and other means and is minimally affected by geographical location. Therefore, compared with the complex manufacturing resources on the cloud manufacturing platform, the integration and sharing of resources are better.
- (d) Heterogeneity and isomerism coexist: Because of the differences in thinking habits and problem-solving methods, the manifestations of knowledge condensed by people are also complex and diverse. The utility of the same type of knowledge services is also different. Therefore, knowledge services in the cloud manufacturing environment are heterogeneous.

3. Mental Illness

The pace of life in the current society is getting faster and faster, and people are facing more pressure from work and study, which makes them susceptible to mental illness. The new corona epidemic has brought psychological stress, panic, and anxiety to people and increased mental illnesses' prevalence. Mental diseases have become a significant global public health problem [12]. Mental illness requires timely treatment. Otherwise, the long-term accumulation of negative emotions it brings will cause incalculable consequences [13]. For example, Cui Yongyuan, the famous host of CCTV, suffered from depression because of his work troubles, and suicides of college and middle school students are also familiar [14].

On the one hand, this phenomenon is because of people's lack of basic knowledge of mental illness, lack of a clear understanding of the dangers of mental illness, and lack of advanced means to popularize the understanding of the mental illness. However, on the other hand, psychological

counselors are in short supply, and counselors cannot get timely and effective help [15], lacking a scientific theoretical system to solve psychological problems intelligently. Therefore, an intelligent platform is needed to store the relevant psychological counseling knowledge. Then, when the user needs to obtain psychological understanding, the platforms can quickly get feedback from the immense ability to help and guide the mentally ill patients in time. The knowledge graph is a better method for intelligently storing information at present. This method was proposed by Google in 2012 and was quickly used for intelligent semantic search [16]. At present, artificial intelligence technology is gradually becoming mature and has penetrated all aspects of society, especially the development of natural language processing technology. The knowledge graph has more application prospects. The influence of social media on mental health is that it may have an effect on psychological health and behavioral activities that might have potential medical care concerns, and social networking holds an ever expanding route for both our everyday lives and globally. As a result, there is a pressing need to develop a better understanding of the long-term effects of social media on people's health. As an essential application direction of the knowledge graph, the question answering system based on knowledge graph can quickly find the correct answer from the knowledge graph through the input natural language question and present it to the user in the form of natural language, and this question answering system is efficient in response and feedback. To solve the above problems, this study, firstly, constructs a knowledge map of psychological counseling, promotes the knowledge of the mental illness, and provides quick psychological counseling services by establishing an immediate semantic psychological question answering system. The system uses the BiLSTM algorithm to detect suicidal tendencies, identify people who commit suicide, self-mutilation, and harm others in time, help users identify diseases, and help consultants understand relevant knowledge through knowledge quizzes. The BiLSTM method is used to predict the next piece of information based on the previous piece of information, making it ideal for having dealt with contextually related text data like sentences. As there might be delays of undetermined time across critical occurrences in a time series, LSTM methods are well-suited to categorizing, processing, and generating forecasts time series analysis. This research allows counselors to relieve their troubles, make up for the shortage of psychological counseling resources, and improve the work efficiency of psychological counseling.

4. Related Work

Knowledge graphs can be divided into general knowledge graphs and domain knowledge graphs. Typically available knowledge graph representatives include Freebase [8], DBpedia, Yago, Baidu, Google, etc., and they are mainly based on triple fact-based knowledge and have a certain tolerance for the quality of knowledge extraction. Typical domain knowledge graphs include e-commerce, finance, medical care, etc. In the field of e-commerce, take Alibaba

as an example. Its knowledge graph has reached tens of billions, widely supporting commodity search, commodity shopping guides, intelligent question and answer, etc. Knowledge graphs allow investors and financiers to understand investment behaviors more quickly and grasp market conditions in the financial field. Aiming at the lack of financial charts, the author constructed a small financial knowledge graph using the crawled structured data, such as financial stocks and corporate information. At present, knowledge graphs are used primarily for clinical treatment decision support, medical intelligent semantic search, and medical question-answering systems in medicine. Clinical treatment decision support is to automatically generate a treatment plan for each patient according to the patient's situation, combine it with extensive data analysis in the medical field, and provide it to doctors for reference. Medical intelligent semantic search is to combine related entities from the medical knowledge graph. It can be used to query information such as the relationships and attributes to optimize the search results of medical information. Medical question and answer is another form of medical information retrieval. Its returned answers are in the form of natural language.

In terms of question answering system based on the knowledge graph, Tan Gang et al. used the LSTM model for entities/assertions to enhance the knowledge graph, used a heuristic candidate answer ranking method, and finally verified that the system has good performance through experiments. The author proposed a multi-round question answering system based on the knowledge graph of road regulations, which can better identify user intentions; the author with knowledge graph as database support, designed a question-and-answer system, which is based on the e-commerce field and realizes functions, such as question answering and reasoning. The authors are the parts of preprocessing, question classification, question template matching, and answer generation in a question answering system are implemented. The question answering procedures established above have been well-implemented in their respective fields, and the characteristics of the domain are integrated into the question answering system process. However, no scholars have studied question-answering systems in psychological counseling, and few texts have been classified as applied to question answering systems.

5. Question Answering System Framework

Compared with traditional search engines, the question answering system is more targeted, accurate, and more accessible for users to accept. The knowledge graph of psychological counseling realizes the association and integration of various kinds of knowledge in psychological counseling. It expresses understanding semantically in a professional and structured way, which can conveniently manage and query knowledge. The BiLSTM technique is used to predict suicidal inclinations, identify persons who commit suicide, self-mutilation, or damage others in a timely manner, assist users in identifying

illnesses, and assist consultants in understanding necessary knowledge via knowledge assessments. The question-and-answer system constructed in this paper is biased toward acquiring professional knowledge of psychological counseling to help people with psychological problems find the correct answer and incorporate suicidal tendency detection to identify dangerous speeches promptly. The framework of the psychological counseling question answering system based on knowledge graph mainly includes four parts: data acquisition, graph construction, problem understanding, and user interface (Figure 1).

The data acquisition module of this system obtains relevant data of web pages through crawler technology. It combines the open data of Chat opera, organizes it into structured data through data processing, and uses Neo4j's python to drive py2neo to construct a knowledge graph. The question-understanding module uses the HanLP tool for word segmentation, part-of-speech tagging, etc. It then uses the CHI feature selection, uses the established BiLSTM model classifier to classify the question and judge whether it has suicidal tendencies, and finally uses the BERT (bidirectional encoder representation from transformers) model to convert queries into queries word vectors for semantic similarity calculation to match question templates and generate answers. The user interface module is the user's question input, and the system answers feedback and involves the mutual conversion of speech and text.

6. Question Answering System Implementation

6.1. Data Acquisition. The data sources for constructing knowledge graphs and classifying texts are web text data and Chat opera datasets, containing questions and label information. Web text data uses web crawler technology to crawl questions about suicide, self-injury, and injury tendencies and structured data about mental illnesses from Weibo Shudong, Baidu Know, 525 Psychology, Yixin, and Simple Psychology. Chat opera cooperated with some professionals to complete a corpus, which is the first open knowledge question-and-answer corpus in the field of psychological counseling, including 20,000 pieces of psychological counseling data. The dataset includes the annotation information of suicidal tendency, and the annotation information and question information are extracted from this dataset. Question information consists of three columns, cat-id, cat, and question, category (Table 1).

6.2. Knowledge Graph Construction. The knowledge graph is used as the database support of the question answering system. Hence, it is necessary to build the knowledge graph first. The primary purpose of constructing a knowledge map of psychological counseling, referring to the psychological counseling ontology database created by author [16] and consulting relevant scholars, is to analyze and summarize the psychological counseling process and the psychological knowledge involved. The psychological counseling

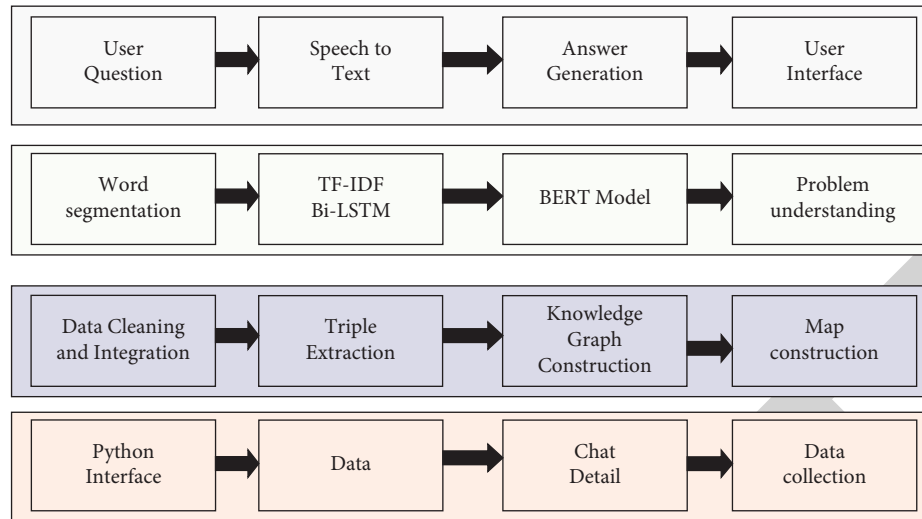


FIGURE 1: The representative framework for psychological question answering system.

TABLE 1: Examples of marked suicidal tendencies and normal questions.

Cat-id	Cat	Question
1	Tendency to self-harm	How to relieve the unreal feeling of depersonalization? In junior high school, my mood fluctuated a lot, and I cut myself with a knife because of some things and even suffered from severe depression
2	Normal	Ever since I reconciled with my boyfriend, he has always been hot and cold, and he does not want to admit that we are together. What does he mean?
3	Tendency to harm	Am I mentally ill? Ever since I was a child, I have had the idea of killing people and killing people around me.
0	Suicidal tendencies	I want to jump off a building, but I am afraid of heights

information is divided into six categories: patients, symptoms, diagnostic criteria, causes of disease, diagnostic results, and treatment methods. Among them, disease causes are divided into biological causes, psychological causes, social causes, and defense mechanisms. There is a causal relationship between the cause of the disease and the diagnosis result. The diagnosis result is divided into the severity of the disease and the name of the mental illness. Diagnosis results and treatment methods are decisive, and treatment methods are divided into psychological treatment, drug treatment, and food treatment. The treatment method has an executive relationship with the patient. The patient needs to adopt the treatment method. The patient mainly includes the patient's identity information, such as age, height, occupation, gender, etc., and the patient's past medical history, which will affect the treatment of the consultant. There is a relationship between patients and symptoms, and symptoms mainly include severity and symptoms. Symptoms and diagnostic criteria are subordinate, and the diagnostic criteria include disease course criteria, severity criteria, and exclusion criteria. It shows that these elements involve various aspects of mental illness, and a question and answer usually involves parts of multiple aspects of mental illness. There are often causal relationships and dependencies between these elements. The protégé tool is used to build an entity-relationship diagram in the field of psychological counseling (Figure 2).

6.3. Instance Layer Construction. The crawled data is organized into structured data and is divided into 12 fields, which correspond to the entity-relationship of psychological counseling designed above, and they are divided into diseases and disease-related entities and attributes. The entities are diseases, aliases, symptoms, complications, drugs, and foods, and the details are susceptible populations, examination methods, treatment methods, cure periods, costs, and causes of disease.

The instance layer construction is divided into entity extraction, relation extraction, attribute extraction, triple construction, and knowledge storage. Here, the python-driven py2neo tool of the Neo4j tool is used to create the knowledge graph. Entity extraction is to extract entities according to the concept of the schema layer and save the entity field information in the structured data after sorting into a dictionary. Relation extraction finds the relationship between entities and saves the relationship between diseases and other entities and attributes as a dictionary. Attribute extraction is to extract the attribute information of some entities, i.e., to save the attribute field information in the sorted, structured data into a dictionary. The construction of triples is to organize the data into the form of (entity, relationship, entity), create nodes without attribute fields and disease nodes with attributes, and then use disease nodes as start-nodes and attribute nodes as end-nodes, with query = "match(p:%s), (q:%s), where p.name = "%s" and

q.name = "%s" create(p)-[rel:%s{name: "%s"}]->(q)" % (start_node, end_node, p, q, rel_type, rel_name) command, and create a triple by creating a node relationship edge through the previously established relationship dictionary. Knowledge storage uses the platform to store the constructed knowledge graph. Here, the Neo4j platform stores the constructed small knowledge graph of psychological counseling Figure 3.

6.4. Word Segmentation Processing. Firstly, several mainstream word segmentation tools, such as Jieba, HanLP, and Chinese Academy of Sciences word segmentation NLPiR, are tested. The question-and-answer sentences of the psychological counseling QA corpus are selected as the data source. Before the test, psychology professionals were required to choose 100 data records and manually annotate them to achieve word segmentation and part-of-speech tagging as the actual value of the experiment. During the test, the 100 data records were processed with three-word segmentation tools, respectively, and the processing results were compared with the annotation results of professionals. The three-word segmentation tools obtained evaluation indicators, such as the accuracy rate, recall rate, F1 value, and word segmentation time (Table 2). Through the evaluation of the three-word segmentation tools, it can be concluded that NLPiR has the fastest word segmentation efficiency, however, HanLP has the highest accuracy. Combined with the evaluation results and psychological counseling needs, this study selected the HanLP tool for text segmentation. It imported the dictionary of disease information constructed above into HanLP's custom dictionary to make word segmentation more accurate.

6.5. Question Category. This paper combines the obtained psychological counseling question-and-answer data and consults professional psychological counselors to divide the frequently asked questions into five categories: disease identification, factual questions, method questions, list questions, and other questions. Disease identification questions mainly answer "what disease," real questions mainly answer "what," method questions mainly answer "how to do," list questions mainly answer "what are," and suicidal tendency questions are input by the user.

Since the principle of question classification is the same as that of suicidal tendency detection, the detailed process of suicidal tendency text classification is an example to illustrate. This article divides suicidal tendencies into four categories: suicidal tendencies, self-harm tendencies, harming others, and standard classes. Firstly, select 1500, 1200, 1000, and 9000 items from each dataset type as training data and then select another 150, 120, 100, and 900 items as test data. Then, using the HanLP word segmentation tool combined with stop words to perform word segmentation and afterword segmentation, the characteristic terms of suicidal tendency, self-harm tendency, injury tendency, and normal tendency were obtained, and the word cloud map of each category was drawn.

$$\text{chi} = \frac{n(ad - bc)^2}{(a + c)(b + d)(a + b)(c + d)} \quad (1)$$

Equation (1) is used to calculate the CHI value of all words after HanLP segmentation, which is used as the basis for feature selection of problem classification and suicidal tendency classification.

In the formula, N is the total number of labelled questions, A is the total number of documents used to record the word t in a specific category, B represents the documents that do not belong to a particular category but also contain the word t , and C represents a category that does not have the word t . In t documents, D represents documents that do not belong to a specific category and do not contain t . The CHI value denotes the degree of distinction between the two categories. The larger the CHI value, the more the word can represent a specific category.

Sort all the words according to the CHI value from large to small. Then, by selecting the 150 words with the most oversized CHI in each category, the selected 1000-dimensional feature list is obtained, and the feature vector weight of each question sentence is calculated, i.e., the word is in the question. If it appears in the sentence, it is assigned a value of 1. Otherwise, it is 0, and the final output is a feature vector that the classifier can recognize.

6.6. Problem Classification Model Selection. In text classification, five models of Naive Bayes, decision tree, SVM, XGBoost, and BiLSTM were used. Each model's training effects were compared, and the classification model with the best result was selected for the system. When testing each model, the precision rate, recall rate, and F1 value of each type of question will be obtained first, and then the precision rate, recall rate, and F1 value of all kinds of questions will be averaged. In the information extraction system, the BiLSTM model is tuned for suicidal propensity identification. The BiLSTM method is used to diagnose suicidal inclinations, identify those who commit suicide, self-mutilation, or damage others in a timely manner, assist users in identifying illnesses, and assist consultants in comprehending necessary facts through knowledge quizzes. Counselors can use this study to ease their stress, compensate for a lack of psychological treatment resources, and improve the efficiency of their job. In the information extraction system, the BiLSTM model is tuned for suicidal propensity identification. These values represent different models—the classification accuracy of (Table 3). From the test results in Table 3, it can be seen that the BiLSTM model is more accurate in the classification effect.

The BiLSTM model can predict the subsequent information using the previous information, which is suitable for dealing with contextually related text data, such as sentences. Taking the classification process of the BiLSTM model for suicidal tendency problems as an example, the HanLP word segmentation tool is selected for word segmentation, and the loss function and accuracy function image are obtained after the classification is completed (Figures 2–4).

TABLE 2: Evaluation results of three-word segmentation tools.

Word segmentation tool	Accuracy	Recall	F1 value	Word segmentation time (s)
Jieba	0.90	0.89	0.89	12.480
HanLP	0.91	0.90	0.90	04.478
Academy of Sciences word segmentation NLPiR	0.81	0.75	0.78	30.0598

TABLE 3: Classification performance of model.

Model	Accuracy	F1-score	Precision
Naïve Bayes	79.65	80.56	69.56
Decision tree	74.52	81.26	65.25
SVM	75.62	76.85	70.62
XGBoost	80.54	82.54	72.56
BiLSTM	85.63	89.85	75.65

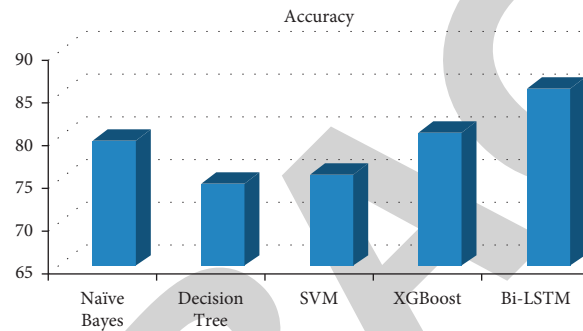


FIGURE 2: represents the accuracy of tendency classification model.

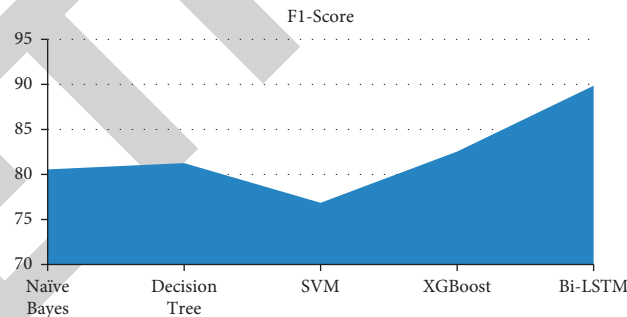


FIGURE 3: The F1-Score of tendency classification model.

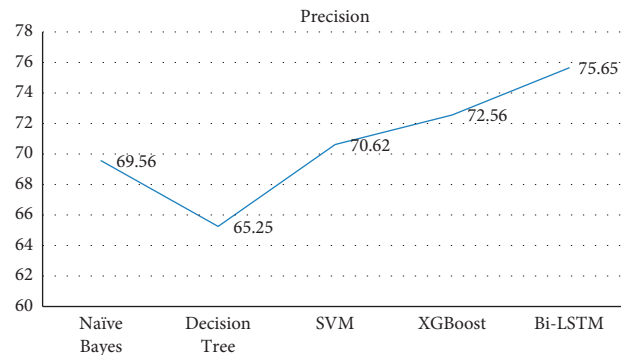


FIGURE 4: Representation of the precision of the tendency classification model.

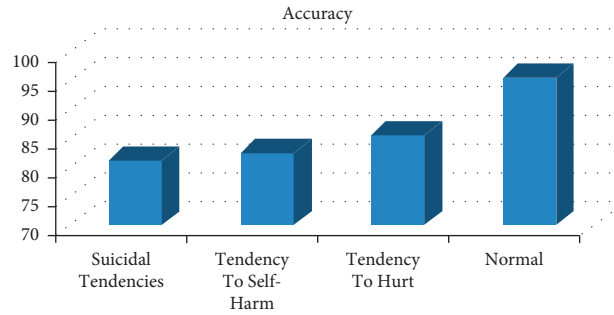


FIGURE 5: The accuracy of suicidal tendency classification by BiLSTM model.

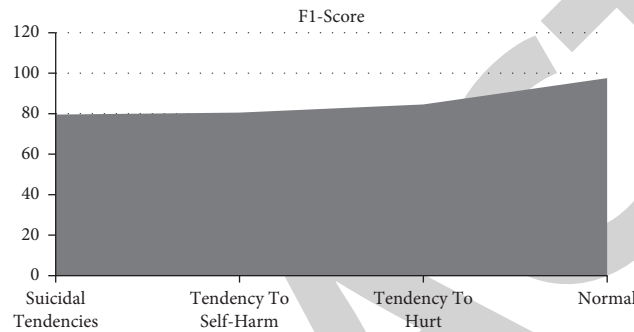


FIGURE 6: The F1-Score of suicidal tendency classification by BiLSTM model.

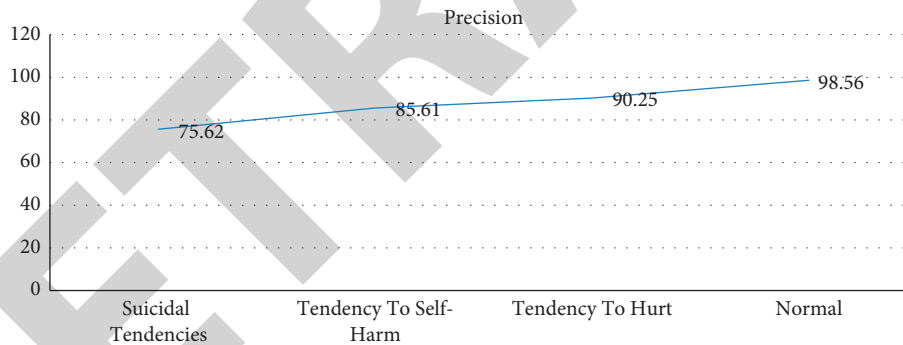


FIGURE 7: Representation of the F1-Score of suicidal tendency classification by BiLSTM model.

In Figures 5–7, the train represents the training set. The test means the test set. The horizontal axis of the function is the number of training iterations, and the vertical axis represents the loss value and the accuracy value, respectively. When the number of iterations becomes more extensive, the loss rate gradually decreases and starts to level off when the number of iterations is 14. The training set tends to be between 0.1 and 0.2, and the test set tends to be between 0.2 and 0.3. The accuracy gradually increases and starts to level off when the number of iterations is 14. The training set tends to be 0.975, and the test set tends to be between 0.925 and 0.950.

By testing the precision rate, recall rate, and F1 value of each type of question to evaluate the model (Table 4), it can be concluded that the BiLSTM model has a better classification effect than the previous four models.

TABLE 4: Suicidal Tendency classification by BiLSTM Model.

Question	Accuracy	F1-score	Precision
Suicidal tendencies	81.26	79.56	75.62
Tendency to self-harm	82.62	80.54	85.61
Tendency to Hurt	85.68	84.56	90.25
Normal	95.62	97.56	98.56

Comparing the questions answered correctly by the system with the questions answered incorrectly by the system, it can be seen that most of the questions answered correctly have similar characteristics to the question template, and some questions have the same entity and semantics as the question template. However, the expression methods are different, proving that the question answering

system has a high semantic understanding ability. For questions that are not answered correctly, it has two characteristics: the system can recognize the entities in these questions but cannot recognize the semantic information that does not appear in the template, such as “What is the general age of onset of bipolar disorder?,” “Can bipolar disorder be cured?,” etc. Another feature is that the entity attribute information involved is not comprehensive enough, for example, what side effects of drugs exist and other attribute information should be added to the knowledge graph.

7. Conclusion

Today’s society is facing the problem of knowledge explosion, especially the intermixing of knowledge in various fields, which affects people’s acquisition and understanding of knowledge. This study is geared on gaining the professional understanding of psychological counseling to assist people with psychological issues in determining the proper answer, as well as including suicidal inclination detection to quickly identify risky remarks. The advantage of this research is that this study uses the user’s psychological behavior traits as a decision-making element, combining the benefits of rough set theory in responding with uncertainty. A comparable notion and approach are provided by the best service choice. The vertical domain knowledge graph stores professional knowledge in a particular area, which significantly facilitates users to understand the knowledge in this field and use this knowledge to reduce losses or create a more excellent value. The psychological counseling knowledge graph and question answering system constructed in this paper has the following characteristics: (1) It provides a platform to store the knowledge of mental illness, which is more semantic than traditional databases. (2) The built question answering system realizes a complete set of word segmentation, question classification, question template matching, and answer generation, which can help users’ judgmental illnesses and help users query relevant knowledge about mental illnesses research significance and value. (3) The BiLSTM model is optimized for suicidal tendency detection in the question answering system. The experimental results show that the accuracy rate, recall rate, and F1 value of the model in this paper are significantly better than other traditional models in the detection of suicidal tendency.

Data Availability

The data shall be made available on request.

Conflicts of Interest

The authors declare that they have no conflicts of interest.

References

- [1] W.-C. Chiang, P.-H. Cheng, M.-J. Su, H.-S. Chen, S.-W. Wu, and J.-K. Lin, “Socio-health with personal mental health records: suicidal-tendency observation system on Facebook for Taiwanese adolescents and young adults,” in *Proceedings of the 2011 IEEE 13th International Conference on e-Health Networking, Applications and Services*, pp. 46–51, Columbia, MI, USA, June 2011.
- [2] S. B. Hassan, S. B. Hassan, and U. Zakia, “Recognizing suicidal intent in depressed population using NLP: a pilot study,” in *Proceedings of the 2020 11th IEEE Annual Information Technology, Electronics and Mobile Communication Conference (IEMCON)*, pp. 0121–0128, Faridabad, India, November 2020.
- [3] P. Gupta and B. Kaushik, “Suicidal tendency on social media: a case study,” in *Proceedings of the 2019 International Conference on Machine Learning, Big Data, Cloud and Parallel Computing (COMITCon)*, pp. 273–276, February 2019.
- [4] C. Wu, P. Lu, F. Xu, J. Duan, X. Hua, and M. Shabaz, “The prediction models of anaphylactic disease,” *Informatics in Medicine Unlocked*, vol. 24, no. 100535, Article ID 100535, 2021.
- [5] G. Manimala, V. Kavitha, P. Pranav, and G. Vishnu Prasad, “Monitoring mental Heal TH using physiological signals,” in *Proceedings of the 2020 International Conference on Power, Energy, Control and Transmission Systems (ICPECTS)*, pp. 1–9, IEEE, Chennai, India, December 2020.
- [6] J. Yuan, X. Lu, Y. Liu, D. Shi, T. Pan, and Y. Li, “Depressive tendency recognition using the gated recurrent unit from speech and text features,” in *Proceedings of the 2021 International Conference on Asian Language Processing (IALP)*, pp. 42–46, Yantai, China, October 2021.
- [7] A. Tiwari, V. Dhiman, M. A. M. Iesa, H. Alsarhan, A. Mehbodniya, and M. Shabaz, “Patient behavioral analysis with smart healthcare and IoT,” *Behavioural Neurology*, vol. 2021, Article ID 4028761, 9 pages, 2021.
- [8] L. Chang, A. Cassinelli, and C. Sandor, “Augmented reality narratives for post-traumatic stress disorder treatment,” in *Proceedings of the 2020 IEEE International Symposium on Mixed and Augmented Reality Adjunct (ISMAR-Adjunct)*, pp. 306–309, Recife, Brazil, November 2020.
- [9] A. Dev, N. Roy, M. K. Islam et al., “Exploration of EEG-based depression biomarkers identification techniques and their applications: A systematic review,” *IEEE Access*, vol. 10, pp. 16756–16781, 2022.
- [10] N. Q. Anayan and V. L. Penuela, “Coping mechanism of students below poverty line towards continuous education amidst COVID 19 pandemic,” in *Proceedings of the 2021 IEEE International Conference on Educational Technology (ICET)*, pp. 226–229, Beijing Shi, China, June 2021.
- [11] H. D. Calderon-Vilca, W. I. Wun-Rafael, and R. Miranda-Loarte, “Simulation of suicide tendency by using machine learning,” in *Proceedings of the 2017 36th International Conference of the Chilean Computer Science Society (SCCC)*, pp. 1–6, Arica, Chile, December 2017.
- [12] S. Liu, J. Shu, and Y. Liao, “Depression tendency detection for microblog users based on SVM,” in *Proceedings of the 2021 IEEE International Conference on Artificial Intelligence and Computer Applications (ICAICA)*, pp. 802–806, Dalian, China, June 2021.
- [13] A. B. Rahmat and K. Iramina, “Classification of multiclass EEG signal related to mental task using Higuchi fractal dimension and 10-Statistic Parameters - support Vector Machine,” in *Proceedings of the TENCON 2015 - 2015 IEEE Region 10 Conference*, pp. 1–6, November 2015.
- [14] S. Saleque, G. A. Z. Spriha, R. Ishraq Kamal, R. Tabassum Khan, A. Chakrabarty, and M. Z. Parvez, “Detection of major depressive disorder using signal processing and machine learning approaches,” in *Proceedings of the 2020 15th IEEE Conference on Industrial Electronics and Applications (ICIEA)*, pp. 1032–1037, Kristiansand, Norway, November 2020.

- [15] G. Roland, S. Kumaraperumal, S. Kumar, A. D. Gupta, S. Afzal, and M. Suryakumar, "PCA (principal component analysis) approach towards identifying the factors determining the medication behavior of Indian patients: an empirical study," *Tobacco Regulatory Science*, vol. 7, no. 6, pp. 7391–7401, 2021.
- [16] M. Deshpande and V. Rao, "Depression detection using emotion artificial intelligence," in *Proceedings of the 2017 International Conference on Intelligent Sustainable Systems (ICISS)*, pp. 858–862, Palladam, India, December 2017.

RETRACTED

Document details - Short-term forecasting electricity load by long short-term memory and reinforcement learning for optimization of hyper-parameters

1 of 1
Export Download More... >

Evolutionary Intelligence
Volume 16, Issue 5, October 2023, Pages 1729-1746

Short-term forecasting electricity load by long short-term memory and reinforcement learning for optimization of hyper-parameters(Article)

Nguyen, N.A., Dang, T.D., Verdú, E., Kumar Solanki, V.

^aSchool of Applied Mathematics and Informatics, Hanoi University of Science and Technology, Hanoi, Viet Nam

^bSchool of Engineering and Technology, Universidad Internacional de La Rioja, Logroño, Spain

^cDepartment of Computer Science and Engineering, CMR Institute of Technology, Hyderabad, India

Abstract

Electricity load forecasting is an essential operation of the power system. Deep learning is used to improve accurate electricity load forecasting. In this study, combining Long short-term memory and reinforcement learning are proposed to encourage the advantage of a single approach for forecasting. Importance input features, including the mutual feature of electricity load, are used to increase accuracy. First, multi-time series input can handle by Long short-term memory and the addition of features supports to the load feature will make the model better efficient. Because the LSTM model is quite complex, choosing a good set of hyperparameters is difficult. Therefore, the purpose of using reinforcement learning is to optimize hyper-parameters of the Long short-term memory model. The proposed model is the combination of Long-short term memory and

Cited by 0 documents

Inform me when this document is cited in Scopus:
Set citation alert > Set citation feed >

Related documents
Find more related documents in Scopus based on:
Authors > Keywords >

Document details - Gaussian Differential Privacy Integrated Machine Learning Model for Industrial Internet of Things

1 of 1

Export Download More... >

SN Computer Science

Volume 4, Issue 5, September 2023, Article number 454

Gaussian Differential Privacy Integrated Machine Learning Model for Industrial Internet of Things(Article)

Lazar, A.J.P., Soundararaj, S., Sonthi, V.K., Palanisamy, V.R., Subramaniyan, V., Sengan, S. 

^aDepartment of Computer Science and Engineering AI & ML, CMR Institute of Technology, Telangana, Hyderabad, 501401, India

^bDepartment of Software Systems, School of Computer Science and Engineering, Vellore Institute of Technology, Tamil Nadu, Vellore, 632014, India

^cDepartment of Computer Science and Engineering, Koneru Lakshmaiah Education Foundation, Andhra Pradesh, Vaddeswaram, 522502, India

[View additional affiliations](#) 

Abstract

Agriculture, energy, mining, healthcare, and transportation are a few of the top industries transformed by the industrial internet of things (IIoT). Industry 4.0 mainly relies on machine learning (ML) to use the vast interconnectedness and large amounts of IIoT data that IIoT primarily drives. ML approaches are trained on confidential data generated by the IIoT environment often exposes privacy to adversarial assaults. Blockchain-based ML is established in the proposed secured IIoT research work to safeguard and enhance privacy. This research proposes a Gaussian differential privacy-integrated machine learning model (GDPIMLM) created for a scalable and controlled IIoT system. fully connected (FC) layer implemented

Cited by 0 documents

Inform me when this document is cited in Scopus:

[Set citation alert](#) >

[Set citation feed](#) >

Related documents

Find more related documents in Scopus based on:

[Authors](#) >

[Keywords](#) >

Document details - Electrocardiogram signal classification in an IoT environment using an adaptive deep neural networks


1 of 1

Export Download More... >

Neural Computing and Applications

Volume 35, Issue 21, July 2023, Pages 15333-15342

Electrocardiogram signal classification in an IoT environment using an adaptive deep neural networks(Article)

Mary, G.A.A., Sathyasri, B., Murali, K., Prabhu, L.A.J., Bharatha Devi, N. 

^aDepartment of ECE, VelTech Rangarajan Dr. Sagunthala R&D Institute of Science and Technology, Avadi, Chennai, India

^bDepartment of ECE, Vijaya Institute of Technology for Women, Vijayawada, India

^cDepartment of CSE, CMR Institute of Technology, Hyderabad, India

[View additional affiliations](#) 

Abstract

IoT is an emerging technology that is rapidly gaining traction throughout the world. With the incredible power and capacity of IoT, anyone may connect to any network or service at any time, from anywhere. IoT-enabled gadgets have transformed the medical industry by granting unprecedented powers such as remote patient monitoring and self-monitoring. Accurate electrocardiogram (ECG) interpretation is critical in the clinical ECG process since it is most often connected with a condition that might create serious difficulties in the body. Cardiologists and medical

Cited by 1 document

Faezipour, M. , Faezipour, M. , Pourreza, S.

Resiliency and Risk Assessment of Smart Vision-Based Skin Screening Applications with Dynamics Modeling

(2023) *Sustainability (Switzerland)*

[View details of this citation](#)

Inform me when this document is cited in Scopus:

[Set citation alert >](#)

[Set citation feed >](#)

Related documents

Find more related documents in Scopus based on:

Document details - A New Multimedia Web-Data Mining Approach based on Equivalence Class Evaluation Pipelined to Feature Maps onto Planar Projection

1 of 1

Export Download More... >

Informatica (Slovenia)

Volume 47, Issue 7, June 2023, Pages 81-90

A New Multimedia Web-Data Mining Approach based on Equivalence Class Evaluation Pipelined to Feature Maps onto Planar Projection(Article)(Open Access)

Ravi, M., Ekambaram Naidu, M., Narsimha, G.

^aCMR Institute of Technology, Telangana, Hyderabad, 501401, India

^bSRK Institute of Technology, Vijayawada, 521108, India

^cJawaharlal Nehru Tech University, Hyderabad, 500085, India

Abstract

Multimedia information are semi-organized or unstructured information elements whose essential substance is separately or by and large utilized for correspondence. Sight and sound information mining recognizes, arranges, and recovers important highlights from an assortment of media to recognize enlightening examples furthermore, connections for information acquisition. Computer Vision (CV)-based systems have been increasingly popular in recent years, owing to the growing number and complexity of datasets. In CV, finding meaningful photos in a huge dataset is a difficult task to solve. Traditional search engines retrieve photos based on text such as captions and metadata, but this strategy can result in a lot of irrelevant output, not to speak the time, effort, and money required to tag this textual data. In this paper, we proposed a pipelined deep learning oriented

Cited by 0 documents

Inform me when this document is cited in Scopus:

Set citation alert > Set citation feed >

Related documents

Find more related documents in Scopus based on:

Authors > Keywords >

Document details - Deep Graph Neural Network with Fish-Inspired Task Allocation Algorithm for Heart Disease Diagnosis

1 of 1
Export Download More... >

Journal of Current Science and Technology
Volume 13, Issue 2, May - August 2023, Pages 392-411

Deep Graph Neural Network with Fish-Inspired Task Allocation Algorithm for Heart Disease Diagnosis(Article)(Open Access)

Gopu, K.L.K., Kannan, S.

^aDepartment of Computer Science and Engineering, CMR Institute of Technology, Telangana, Hyderabad, 501401, India
^bDepartment of Information Technology, Kalasalingam Academy of Research and Education, Krishnankoil, Tamil Nadu, Srivilliputhur, 626126, India

Abstract

Heart disease is a very hazardous disease and many people suffered from this disease globally. The major aim is "to diagnose the heart disease with higher accuracy through decreasing error rate including computational complexity". The existing techniques did not proffer adequate accuracy and also increased the error rate. Therefore, a Deep Graph Neural Network with Fish-Inspired Task Allocation Algorithm is proposed in this manuscript for categorizing heart disease diagnosis (DGNN-FITA-HDD). Synthetic Minority Oversampling and standard scalar strategies are utilized for pre-processing process. The pre-processed output is given to feature selection process. Two- Stage Feature Selection method selects the most important features from pre-processing output. Extracted features are transferred to Deep Graph Neural Network (DGNN) for categorizing presence and absence of heart disease. DGNN does not require any definition of optimization strategies for calculating the optimum parameters to secure accurate

Cited by 0 documents

Inform me when this document is cited in Scopus:
Set citation alert > Set citation feed >

Related documents
Find more related documents in Scopus based on:
Authors > Keywords >

PSO Optimized CNN-SVM Architecture for Covid - 19 Classification

P.V. Naresh¹, R. Visalakshi², B.Satyanarayana³

¹Research Scholar, Annamalai University, Department of Computer Science and Engineering, Tamilnadu, India
Email id : naresh.groups@gmail.com

²Assistant Professor. Annamalai University, Department of Information Technology, Tamilnadu, India
Email id : visalakshi_au@yahoo.in

³Principal, CMR Institute of Technology, Telangana, India
Email id : bsat777@gmail.com

*Corresponding Author ORCID ID : 0000-0003-1067-1038

Abstract— This paper presents a hybrid model that utilizes PSO particle swarm optimization, Convolution Neural Networks (CNN) and (SVM) Support Vector Machine architecture for recognition of Covid19. The planned model extracts optimized structures with particle swarm optimization then passes to Convolution Neural Network for automatic feature extraction, while the SVM serves as a Multi classifier. The dataset comprises Covid 19, Pneumonia and Normal Chest X-Ray pictures used to hone and evaluate the suggested algorithm. The most distinct traits are automatically extracted by the algorithm from these photographs. Experimental results show that the suggested framework is effective, with an average recognition accuracy of 97.42%. The most successful SVM Kernel was RBF.

Keywords- CNN, SVM, PSO, deep learning, Covid, Chest X-Ray)

I. INTRODUCTION

The primary purpose of this investigation is to optimize the features of images using particle swarm optimization and passing these features to CNN for automatic extraction of features and the SVM classifier is regarded known to be among machine learning's most reliable classifiers. This study employs the PSO CNN algorithm in combination with the SVM classifier to classify the disease. Most conventional approaches use different methods for feature extraction and classification, making them unsuitable for real-time applications due to high computational time. The CNN algorithm is dissimilar from traditional machine learning algorithms because it does not require a separate feature extraction operation.

At current, deep learning techniques like Convolution Neural Networks (CNNs) are fast and reliable for image recognition and classification[1-2]. Yet, some photographs with a little more noise in them may cause a neural network to classify them wrongly. This is due to CNN's extensive usage of enhanced training data, which enables the use of changed input images. We tried to address this problem by implement our model using PSO – CNN-SVM model. The remainder of the essay is explained as follows. Section 2 details the suggested approach. Experimental design and findings are covered in Section 3, performance comparison is covered in Section 4, and the conclusion is covered in Section 5.

II. PROPOSED METHODOLOGY

The proposed planning of PSO-CNN-SVM Model is shown in **Fig 3**; it consists of particle swarm optimization technique which optimizes the features with base classifier as random forest. Then the optimized features are passed and given input to the convolution neural network (CNN) for automatic feature extraction. In the approach 3x3 the most recognizable features are extracted from the raw input photos using a kernel or filter. An nxn input neuron from the input layer is convolved with a mxm filter in the convolution layer, producing an output with the dimensions (n-m+1) x (n-m+1). Each layer's output serves as the following layer's input. Effective sub-regions are calculated from the image using CNN's receptive field feature. The extracted features are then approved for classification to SVM.

Support Vector Machine (SVM) is highly efficient in minimizing generalization error on unseen data; however, it may not perform well on noisy data. Moreover, SVM finds it challenging to learn complex features because of its shallow construction. In this paper, a hybrid CNN-SVM model is presented to address these constraints. The better classification accuracy may be due to the SVM classifier's mapping of the input features to a higher dimensional space. Here, SVM is employed as a Multi class classification and replaces the softmax layer of CNN

III. DATASET COLLECTION

The dataset used in this work is an open source compiled and taken from various sources like kaggle and github. The images are divided into Covid, Normal, Pneumonia and the splits of the dataset are given in the table 1. The dataset is further categorized into training and testing with 80% for training and 20% for testing purpose.

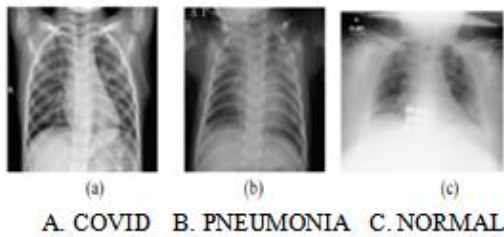


Fig.1 Sample of the labeled X-Rays

Table 1
Dataset

	Training	Testing	Total
Covid-19	796	212	1008
Pneumonia	846	210	1056
Normal	845	200	1045
Total	2487	622	3109

II.II PSO-OPTIMIZATION IN THE PROPOSED ARCHITECTURE

Dr. Kennedy first presented the PSO optimization technique in 1995[3]. A swarm of particles is randomly scattered over the search space at the beginning of the PSO algorithm. Each particle stands for a possible answer to the optimization issue. Each particle's position indicates a potential solution, and its velocity describes its travel in the search space in terms of both its direction and its speed. At respectively iteration, the particles move towards the best position they or their neighbors have visited so far, called the personal best (Pbest) and global best (Gbest), respectively. The movement of each particle is determined by the velocity update equation:

$$v_i(t + 1) = w * v_i(t) + c_1 * r_1 * (Pbest_i - x_i(t)) + c_2 * r_2 * (Gbest - x_i(t)) \quad (1)$$

where $v_i(t)$ is the velocity of particle i at time t , $x_i(t)$ is the position of particle i at time t , $Pbest_i$ is the personal best position of particle i , $Gbest$ is the global best position among all particles, w is the inertia weight that controls the impact of the previous velocity, c_1 and c_2 are the acceleration coefficients that control the influence of $Pbest$ and $Gbest$, respectively, and r_1 and r_2 are random numbers uniformly distributed between 0 and 1. The velocity update equation is used to compute the new position of each particle

$$x_i(t + 1) = x_i(t) + v_i(t + 1) \quad (2)$$

After updating the positions of all particles, the fitness function is evaluated for respectively particle, and the personal and global best positions are efficient if necessary. Unless a stopping requirement is satisfied, such as a maximum number of iterations or a suitable fitness value, the procedure is repeated.

PSO algorithm reads the images from the specified directory, resizes them to 32x32 pixels, converts them to numpy arrays, and appends them to the X array. It also assigns labels to the images based on their directories. Then, it shuffles the X array and normalizes its values. PSO algorithm, including the number of particles, dimensions, and options. It creates an instance of the PSO optimizer object and applies it to the cost function, f , which is defined as $f_per_particle$. The PSO algorithm is run for 2 iterations to optimize the features. Finally, it selects the optimized features with a value of 1 from the PSO and saves them as $X_selected_features$. It also saves the labels as Y . The code displays some information about the dataset, including the total number of images, the total number of features before and after applying PSO, and the classes in the dataset in Fig 2

```
Total images found in dataset: 3109
Total features found in image before applying PSO: 1024
Total features found in image after applying PSO: 576
Classes found in dataset: ['Covid19', 'Normal', 'Pneumonia']
```

Fig.2. PSO Optimized features

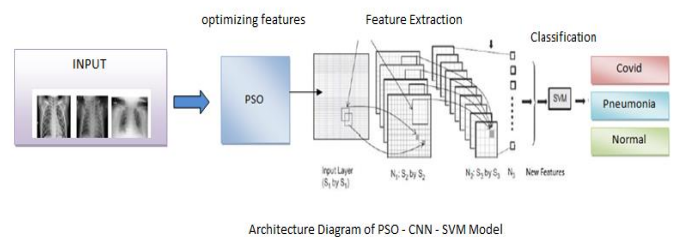


Fig 3. Architecture of the PSO-CNN- SVM Model

Algorithm 1. PSO Algorithm

- 1 Initialization
 - 1.1 For each particle I in a swarm population size p :
 - 1.1.1 Initialize X_i randomly
 - 1.1.2 Initialize V_i randomly
 - 1.1.3 Evaluate the fitness $f(X_i)$
 - 1.1.4 Initialize $pbest_i$ with a copy of X_i
 - 1.2 Initialize $gbest$ with a copy of X_i with the best fitness
- 2 Repeat until a stopping criterion is satisfied:
 - 2.1 For each particle in i :
 - 2.1.1 Update V_i^t and X_i^t accordingly to Eq (1) ,(2)

- 2.1.2 Evaluate the fitness $f(X_i^t)$
- 2.1.3 $Pbest_i X_i^t \leftarrow$ if $f(pbest_i) < f(X_i^t)$
- 2.1.4 $gbest_i X_i^t \leftarrow$ if $f(gbest_i) < f(X_i^t)$

II.III CONVOLUTION NEURAL NETWORK IN THE PROPOSED ARCHITECTURE

An input layer, convolution and pooling layers, and a fully connected classification layer make up the CNN architecture. The most crucial component of the CNN architecture is the convolution layer. This layer is made up of kernels or filters that cover the entire input. Each unit in this layer receives input from the layer above it., the last layer is dense with no of classes. The developed CNN for feature extraction has total 141,667 parameters.

```

Model: "sequential_1"
Layer (type)                Output Shape                Param #
-----
conv2d_1 (Conv2D)           (None, 22, 22, 32)         320
max_pooling2d_1 (MaxPooling2 (None, 11, 11, 32)         0
conv2d_2 (Conv2D)           (None, 9, 9, 32)           9248
max_pooling2d_2 (MaxPooling2 (None, 4, 4, 32)           0
flatten_1 (Flatten)         (None, 512)                 0
dense_1 (Dense)             (None, 256)                 131328
dense_2 (Dense)             (None, 3)                   771
-----
Total params: 141,667
Trainable params: 141,667
Non-trainable params: 0
    
```

Fig: 4 Model Summary of PSO CNN

II.IV SUPPORT VECTOR MACHINE IN THE PROPOSED ARCHITECTURE

After feature extraction and pre-processing, an SVM classifier is used to categorise the images. Using feature vectors that are stored as matrices, the SVM classifier's training procedure is carried out. Using the learned SVM classifier, testing of the images is then done. In contrast, the extracted features are given to the SVM module in the PSO CNN-SVM model for the dataset's training and testing. Both the training and testing data are used, and the results are recorded, to assess the accuracy of the SVM classifier and the PSO-CNN-SVM model. The hybrid model uses an RBF kernel function, and the SVM parameters, including degree and gamma of the kernel function and the shape of the decision function, are carefully determined because they have a big impact on SVM classification. [4]

III. EXPERIMENTAL SETUP AND RESULTS

For experiments, Google Colaboratory is used. For up to 8 hours, Colab offers 12GB of RAM with an NVIDIA Tesla K80 GPU. We have used the pyswarms ,swarmpackagepy, sklearn, matplotlib, libraries to implement the proposed model. The proposed model uses the Adam optimizer with loss as

definite cross entropy metrics = correctness. The extracted features from CNN are passed to SVM classifier for classification; we have achieved promising results with an overall correctness of 97.42

III.I PERFORMANCE EVALUATION

The performance of PSO-CNN-SVM Model has been assessed by means of confusion matrix, classification report and correctness vs. loss graphs.

III.II CONFUSION MATRIX

Confusion Matrix generally has a 2×2 matrix to every cell representing the model detection rate as True Positive (TP), True Negative (TN), False Positive (FP), and False Negative (FN).

1. **True Positive (TP):** If the individual is essentially Covid positive and forecast also Covid then it is Called True Positive
2. **True Negative (TN):** If the subject is normal and the outcome is as expected, this is known as a true negative.
3. **False Positive (FP):** When a normal person is identified as having covid, it is referred to as a false positive and it reflects an inaccurate detection.
4. **False Negative (FN):** False Negative is a term used to describe an inaccurate detection when a Covid positive person predicts Normal.

$$\text{Accuracy: } \frac{\text{True Positive} + \text{True Negative}}{\text{True Positive} + \text{False Positive} + \text{True Negative} + \text{False Negative}} \quad (3)$$

$$\text{Precision: } \frac{\text{True Positive}}{\text{True Positive} + \text{False Positive}} \quad (4)$$

$$\text{Recall: } \frac{\text{True Positive}}{\text{True Positive} + \text{False Negative}} \quad (5)$$

$$\text{F1 Score: } 2x \frac{\text{PRECISION} * \text{RECALL}}{\text{Precision} + \text{Recall}} \quad (6)$$

SVM Accuracy on CNN Extracted Features: 97.42765273311898
 SVM Precision on CNN Extracted Features: 97.42705200649127
 SVM FSCORE on CNN Extracted Features: 97.44573046913771
 SVM Recall on CNN Extracted Features: 97.47002546475998

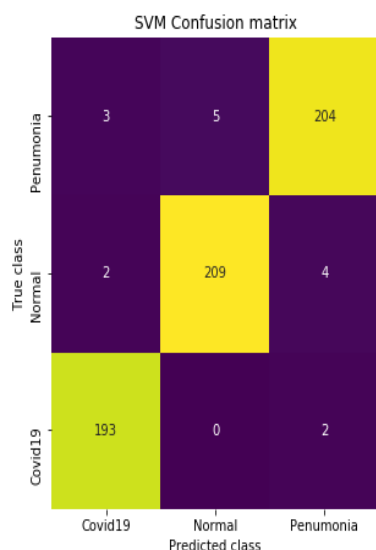


Fig 5. Confusion matrix with Classification Report

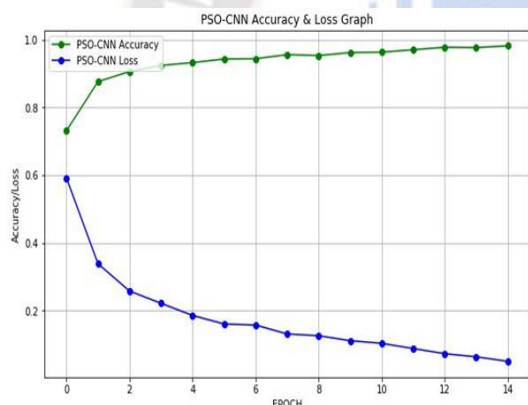


Fig 6. Accuracy vs Epoch Graph

IV. PERFORMANCE EVALUATION

This section compares the accuracy with some best models developed previously in multi classification with X-Rays. Though we found many articles on Covid-19. We have chosen only ten articles on 3 class classification with X-Rays. However from the below table we see our model performing better than previously developed models. We also found the scope of improving our model further using tuning the hyper parameters and increasing the dataset

Table 2: Comparison of Deep Learning Models

AUTHOR	MODEL	DATASET	CLASS	ACC
Arman Haghanifar et al [5]	COVID-CXNe	X-RAY	3	87.88
M.k. Pandit et al [6]	VGG-16	X-RAY	3	92.50%
Sarki R et al [7]	CNN	X-RAY	3	93.75%
Emtiaz Hussain et al[8]	CoroDet	X-RAY	3	94.20%
Ahmed s Elkorany[9]	Covidetecti on- Net	X-RAY	3	94.44%
Mahmoud Ragab [10]	CAPSNET	X-RAY	3	95.00%
Tianbowu et al [11]	ULNet	X-RAY	3	95.35%
Anubhav Sharma et al [12]	COVDC-NET	X-RAY	3	96.48 %
Abhijit Bhattacharya et al[13]	VGG-19	X-RAY	3	96.60%
Gaurav Srivastava et al[14]	CoviXNet	X-RAY	3	96.61%
Our proposed Model	PSO-CNN-SVM	X-RAY	3	97.42 %

V. CONCLUSION

The paper presents the hybrid model developed with combination of particle swarm optimization, CNN and SVM (PSO-CNN-SVM) model to optimize the features. The model produced good results of 97.42%. This method can be further improved and achieve better accuracy with larger datasets.

REFERENCES

- [1] V. Venugopal, J. Joseph, M. Vipin Das, M. Kumar Nath, An EfficientNet-based modified sigmoid transform for enhancing dermatological macro-images of melanoma and nevi skin lesions, *Comput. Methods Programs Biomed.* 222 (2022) 106935 doi <https://doi.org/10.1016/j.cmpb.2022.106935>
- [2] E. Benmalek, J. Elmhamdi, A. Jilbab, Comparing CT scan and chest X-ray imaging for COVID-19 diagnosis, *Biomed. Eng. Adv.* 1 (2021) 100003, <https://doi.org/10.1016/j.bea.2021.100003>
- [3] J. Kennedy, R. Eberhart, Particle swarm optimization, in: *Proceedings of ICNN'95- international Conference on Neural Networks*, vol. 4, IEEE, 1995, pp. 1942–1948.
- [4] dugganikeerthana, vipinvenugopal, Malaya kumarnath, madhusudhanmishra, “Hybrid Convolutional neural networks with SVM classifier for classification of skin cancer, *Biomedical Engineering Advances* 5 (2023) 100069 doi : <https://doi.org/10.1016/j.bea.2022.100069>
- [5] Arman Haghanifar, Mahdiyar Molahasani Majdabadi · Younhee Choi, S. Deivalakshmi · Seokbum Ko, COVID-CXNet: Detecting COVID-19 in frontal chest X-ray images using deep learning, *Multimedia Tools and Applications* (2022) 81:30615–30645, <https://doi.org/10.1007/s11042-022-12156-z>

- [6] M.K. Pandit, S.A. Bandy, R. Naaz, M.A. Chisti, "Automatic detection of Covid-19 from chest radiography using deep learning. Radiography 27 (2021), 483-489. Doi: <https://doi.org/10.1016/j.radi.2020.10.018>
- [7] Sarki R, Ahmed K, Wang H, Zhang Y, Wang K (2022) Automated detection of COVID-19 through convolutional neural network using chest x-ray images. PLoS ONE 17(1): e0262052. <https://doi.org/10.1371/journal.pone.0262052>
- [8] Emtiaz Hussain, Mahmudul Hasan, Md Anisur Rahman, Ickjai Lee, Tasmii Tamanna, Mohammad Zavid Parvez, "CoroDet: A deep learning based classification for COVID-19 detection using chest X-ray images", Chaos, Solitons and Fractals 142 (2021) 110495 doi: <https://doi.org/10.1016/j.chaos.2020.110495>
- [9] Ahmed S. Elkorany, Zeinab F Elsharkawy, "COVID Detection-Net: A tailored COVID-19 detection from chest radiography images using deep learning", Optik - International Journal for Light and Electron Optics 231 (2021) 166405, doi: <https://doi.org/10.1016/j.ijleo.2021.166405>
- [10] Mahmoud Ragab, Samah Alshehri, Nabil A. Alhakamy, Romany F. Mansour, and Deepika Koundal, "Multiclass Classification of Chest X-Ray Images for the Prediction of COVID-19 Using Capsule Network," Computational Intelligence and Neuroscience, Volume 2022, Article ID 6185013, 8 pages doi: <https://doi.org/10.1155/2022/6185013>
- [11] Tianbu Wu, Chen Tang, Min Xu, Nian Hong, Zhenkun Lei, ULNet for the detection of coronavirus (COVID-19) from chest X-ray images," Computers in Biology and Medicine 137 (2021) 104834" doi: <https://doi.org/10.1016/j.combiomed.2021.104834>
- [12] Anubhav Sharma, Karamjeet Singh, Deepika Koundal, "A novel fusion based convolutional neural network approach for classification of Covid 19 from chest X-ray images", Biomedical Signal Processing and Control 77(2022) 103778 doi: <https://doi.org/10.1016/j.bspc.2022.103778>
- [13] Abhijit Bhattacharya, Divyanshu Bhaik, Sunil Kumar, Prayas Thakur, Rahul Sharma, Ram Bilas Pachori, "A deep learning based approach for automatic detection of COVID-19 cases using chest X-ray images" <https://doi.org/10.1016/j.bspc.2021.103182>
- [14] Gaurav Srivastava, Anindita Chauhan, Mahesh Jangid, Sandeep Chaurasia, "CovixNet: A Novel and efficient deep learning model for detection of Covid-19 using chest X-Ray images." Biomedical Signal Processing and Control 78 (2022) 103848 doi: <https://doi.org/10.1016/j.bspc.2022.103848>

Available online at www.sciencedirect.com

jmr&t
Journal of Materials Research and Technology
journal homepage: www.elsevier.com/locate/jmrt



Original Article

Metallurgical, mechanical and corrosion behaviour of pulsed and constant current TIG dissimilar welds of AISI 430 and Inconel 718



Balrm Yelamasetti ^a, G Sai Adithya ^b, R Sri Ramadevi ^b, Pankaj Sonia ^c,
Kuldeep K. Saxena ^{d,*}, Naveen Kumar P ^e, Sayed M. Eldin ^f,
Fatima Hiader Kutham Al- kafaji ^g

^a Department of Mechanical Engineering, MLR Institute of Technology, Dundigal, Telangana-500043, India

^b Department of Metallurgical Engineering, JNTUH-CEH, Hyderabad-500085, Telangana, India

^c Department of Mechanical Engineering, GLA University, Mathura, UP, 281406, India

^d Division of Research and Development, Lovely Professional University, Phagwara-144411, India

^e CMR Institute of Technology, Hyderabad, Telangana-501401, India

^f Center of Research, Faculty of Engineering, Future University in Egypt, New Cairo 11835, Egypt

^g Al-Mustaqbal University College, 51001 Hillah, Babil, Iraq

ARTICLE INFO

Article history:

Received 15 March 2023

Accepted 25 April 2023

Available online 28 April 2023

Keywords:

Ni-based super alloy

Ferritic stainless steel

Constant and pulse arc welding

Metallurgical changes

Mechanical properties

Corrosion studies

ABSTRACT

This research work explore the weldability, structural integrity, mechanical properties and corrosion behaviour of dissimilar welds of Inconel 718 and AISI 430 developed by using constant and pulse arccurrent modes in TIG welding process. The welded structures defects for inspected by employing X-ray radiography images as well as macrostructures. Metallurgical changes were observed using optical & scanning electron microscope techniques. Mechanical properties of the joined structures were evaluated by performing tensile test on UTM and hardness measurements on weld surfaces using Vickers hardness tester. The resistance against the corrosion especially at the weld area of both welded structures was measured. The joined structures were free from flaws and also seen the uniformity of the filler distribution towards the base metals. The grain coursing with well-defined grain structures were identified in CC-TIG weldments whereas fine grains with clear distribution of filler alloying elements were seen in PC-TIG weldments. PC-TIG weldments exhibited with better mechanical and corrosion resistance properties than the CC-TIG weldments vowing to pulse arc mode during welding process. The aerospace and nuclear industries will benefit from the study's findings especially turbine disc and shaft assembly.

© 2023 The Authors. Published by Elsevier B.V. This is an open access article under the CC BY-NC-ND license (<http://creativecommons.org/licenses/by-nc-nd/4.0/>).

* Corresponding author.

E-mail address: saxena0081@gmail.com (K.K. Saxena).

<https://doi.org/10.1016/j.jmrt.2023.04.231>

2238-7854/© 2023 The Authors. Published by Elsevier B.V. This is an open access article under the CC BY-NC-ND license (<http://creativecommons.org/licenses/by-nc-nd/4.0/>).

1. Introduction

In the present world scenario, fusion and solid state welding techniques are in use in industrial applications to produce desired welded components. Tungsten Inert Gas (TIG) welding process is one of the most commonly Fusion Welding (FW) processes widely used for the development of nuclear reactors, offshore structures, pressure containers and petrochemical equipment [1–3]. This welding technique has two different arc mode during welding process. In constant arc mode, the welding current continuously supplied to welded structures whereas, in pulse arc mode the current being pulsed from peak current to low current to control the heat inputs [4,5]. During this period when the current reaches to high level the weld metals are heated for fusion to occur. When the current drops from high-low level the fusion zone cools the molten pool [6]. Continuous heat-input in the fusion welding process has produced the formation in the new phases in the microstructure and also micro segregation of the filler wire alloying elements and thus causing poor in quality of welded structures [7]. The formation of grain structures (coarse) and high HAZ are the major problems related with CC-TIG process due to constant heat input [8]. The PC-TIGwelding is widely used in FW processes as that has been stated to have more benefits than CC-TIG welding technique [9]. A reduced total heat input to the welds have lessmicro-segregation, porosity, bead size, distortion and residual stresses are the major benefit effects reported [10]. The grain boundaries growth and substructures were observed during PC-TIG welding process when main current is increased [11] (see Fig. 12).

The Ni-based alloys exhibits superior mechanical properties and resistance towards corrosion in joints. These alloys are weldable by most common welding processes. However, Ni-based metals along with other materials like3XX grade steels are welded as unique features of the weld metal allows it to provide improved properties those of base plates [12]. Ni-based fillers are preferred to join these dissimilar metals as they overcome hot cracking tendencies and are less susceptible to weld metal porosity [13]. Devendranath et al. [14] carried the investigations on dissimilar welded joints of marine grade alloys SS 904 L and Monel 400 through PC-TIG multi-pass welding technique. The fracture has occurred in tensile test at the parent metal (Monel 400) in both weldments with ERNiCrMo-4 and ERNiCu-7 as fillers. Devendranath et al. [15] assessed the metallurgical aspects and mechanical strengths of CCGTAW and PCGTAW of Monel 400 andAISI 304 welds by using E309L, ERNiCrFe-3 and ERNiCu-7 as fillers. The fracture was observed at AISI 304 in PCGTAW weldments when ENiCrFe-3 and ENiCu-7 fillers were employed. Balram et al. [16] reported on metallurgical changes, mechanical

properties of constant and pulsed current TIG weldments of Monel 400 and steel 316. Grain refinement with austenitic phase structures were observed in fusion zone of PC-TIG weldments. Also, segregation effect was greatly reduced at the interfaces of both the metals [17].

Devendranath et al. [18] used the constant and PC-GTAW processes for the development of super alloy Inconel and AISI 316 L by using different filler wires. The development of Niobium rich phases was identified at HAZ and weld area when while employing ER2553 filler as it reduces the weld strength [19]. Devendranath et al. [20] studied on welds of Inconel and AISI 430 developed by PCGTAW process using ERNiCrMo-4 and ER2553 fillers. The metallurgical study has shown PMZ at the Inconel 718 HAZ and grain coarsening near the HAZ of AISI 430. The toughness of Mo-4 filler weldments was observed high to that of ER2553 weldments. The tensile fracture was observed at base metal AISI 430 in two filler weldments. Dev et al. [21,22] conducted experiments on stainless steel 416 and Inconel 718 dissimilar weldments developed in PCGTAW process by using two Niobium free filler metals ERNiCu-7, ERNiCrMo-4 and a duplex filler wire ER2553 [24]. Weldments with all the above fillers, failure in the tension test is seen at the base plate of 416 side.

It is clear that there is a high need for combining metals that are different from one another in order to get many advantages in terms of metallurgical and mechanical properties. This work is especially significant since base metals like Inconel 718 and AISI 430 are frequently used in nuclear and aerospace applications. The dissimilar metals of Inconel 718 and AISI 430 are welded using PC-TIG and CC-TIG welding techniques by employing ERNiCrMo-4 filler wire. The metallurgical changes due to constant and pulse arc mode in dissimilar welds are characterized microscopes (OM/SEM). The weldability, weld properties and resistance against the corrosion are corroborated by conducting mechanical testings' as per ASTM standard. In this experimental investigation, the challenges for joining dissimilar metals, minimization of microstructural errors of weldments of Ni-based alloys and martensitic phase stainless steels are reported. The selection of suitable filler metal for good weldability, optimum parameters for achieving good bead profiles and welding time for proper heat input rates to get less HAZ width are also mentioned.

2. Material details and experimental set-up

The base plates, Inconel 718 and AISI 430, were sliced with the dimensions of 150 × 100 × 5 mm using WEDM process in order to maintain standard dimensions as per ASTM. The Ni-based ERNiCrMo-4 filler of diameter 1.6 mm was selected to join the dissimilar plates using CC-TIG and PC-TIG welding

Table 1 – Composition of main alloying elements (wt.%) present in base/filler metals.

Metal/wire	Ni	Fe	Cr	Mo	Mn	Si	C	P	Cu	Others
AISI 430	–	Bal	16.19	–	0.32	0.37	0.04	0.025	–	S-0.005.
Inconel 718	Bal	20.08	17.26	2.8	0.20	0.10	0.03	0.09	0.12	Nb- 4.9, Ti-0.73, Co-0.38, Al-0.28, S-0.012
ERNiCrMo-4		5.50	15.84	16.26	0.51	0.04	0.02	0.007	0.06	W-3.5, V-0.18, Co-0.38, Ti-0.1, Al-0.31

Table 2 – Welding parameters used for joining dissimilar plates.

Welding technique	No of passes	Peak current, I_p (A)	Back ground current, I_b (A)	Frequency (Hz)	Voltage (V)	Time taken for welding (s)
PC-TIG	First pass	140	70	4	12 ± 2	36
	Second pass	140	70	4	12 ± 2	34
CC-TIG	First pass	140	–	–	12 ± 2	36
	Second pass	140	–	–	12 ± 2	34

methods. The composition of alloying elements present in the base and filler metals was verified by conducting dry spectroscopic test and, confirmed with standard data [25], is presented in Table 1. Standard butt-V groove design was made by machining the surfaces with an included angle of 45° . To fill this V-groove with a land face of 1.5 mm, multi-pass (two passes) welding method was adopted. To maintain constant root gap of 2.0 mm between the plates tack welding was made. The parameters used in both CC-TIG and PC-TIG processes are listed in Table 2. The heat given to weldments (kJ/mm) values are calculated with Eq. (1). The efficiency (η) of CCGTAW technique is considered as 70% [26]. During welding processes, shielding gas (Argon) was maintained with 10 lpm flow rate to protect the vicinity of the weld area from the harmful effects. The dissimilar weldments were joined by using LINCOLN375 machine and corresponding welds are shown in Fig. 1.

$$Q_{CC/PC-TIG} = \eta \times \frac{V \times I_{avg}}{s} \quad (1)$$

2.1. Characterization of dissimilar joints

After joining, the weldments developed from CC-TIG and PC-TIG welding were inspected for internal defects using X-ray radiography according to ASME standard. The X-ray source was employed to inspect the welded samples with a short wavelength with contact time of 2 min. After confirmation of

NDT analysis, the welded structures were cut into various test samples to determine tensile strength on UTM, hardness measurement using Vickers machine and metallurgical behavior with optical and scanning electron microscope (OM/SEM) techniques. Three tensile test specimens were prepared to find the strength of welded components. The hardness values were measured on weld surface area with Vickers micro-hardness tester. During measurement, a load capacity of 500 gf and dwell period of 10 s was maintained. Test is carried out according to ASTM E384-16 standard. The standard metallographic process followed to divulge the microstructures at different zones. The elemental composition of welded sample by covering fusion, HAZ and base area are analyzed by with EDAX technique. Further, Cyclic sweep corrosion test was conducted at on weld surfaces to study the corrosion rate on both weldments.

3. Test results & discussions

3.1. XRT-radiography

The results obtained from the XRT test were inspected and the weld films are presented in Fig. 2. The X-ray films clearly shown that the dissimilar metals joined with both the welding techniques were free from weld cracks, flaws and porosity. The uniform spread over of filler wire towards base metals and complete bead profile were observed in both CC-TIG and PC-TIG weldments.

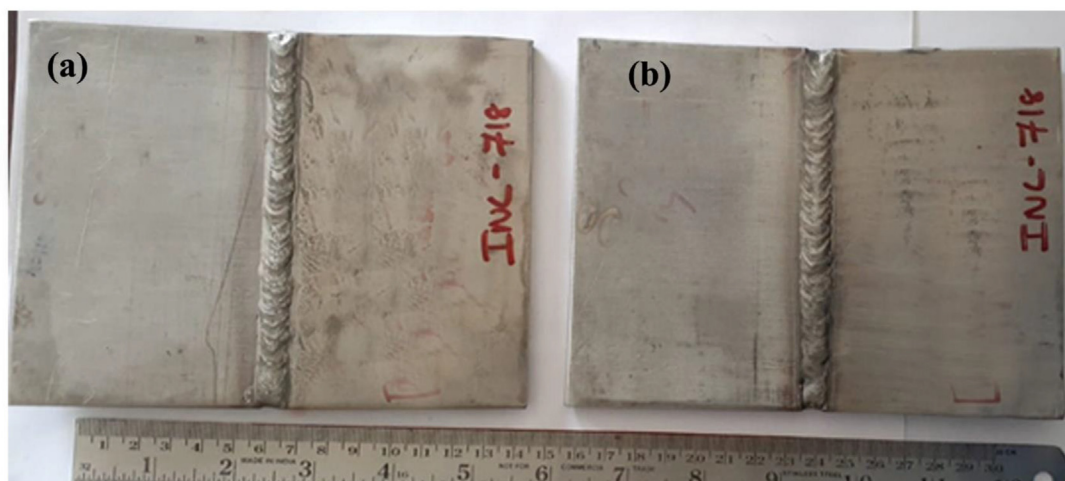


Fig. 1 – Developed dissimilar weldments using (a) CC-TIG and (b) PC-TIG welding processes.



Fig. 2 – X-ray radiography images of dissimilar joint (left) CC-TIG and (right) PC-TIG welding processes.

3.2. Macro/microstructures

3.2.1. CC-TIG weldment

The microstructures of base metals, Inconel 718 and AISI 430, are shown in Fig. 3. In the base metal of Inconel 718, microstructure examinations revealed the existence of coarse austenitic grains; for the base metal of AISI 430, ferrite structure in white phase and martensite streaks in dark phase were observed. The macro/microstructures of bimetallic weldment of Inconel 718 and AISI 430 joined with CC-TIG welding is shown in Fig. 4. The macrograph of CC-TIG weldment shows that the spread over of filler metal towards Inconel 718 side is comparatively more than the towards AISI 430 side. The coarse grain structures and new phase formation are observed at the interfaces of both metals as shown in Fig. 4 (a & d). Due to the constant heat input given to base metals, wider affected areas are identified in this weldment. Similar observations on the occurrence of micrographs when the samples were joined using CO₂ laser welding process which resulted in coarse-grained Inconel 718 were reported by Devendranath et al. [22]. The fusion zone of root and capping passes structures are revealed in Fig. 4 (b & c). The chemical differences between the base metals and the fusion zone are high that the grain boundary liquation reduces the alloy's ductility. This, in turn, causes grain boundaries to become brittleness. The columnar

with equi-axed structures are seen in both the passes which could be attributed to increasing hardness number. The SEM/EDAX analysis of CC-TIG weldment is shown in Fig. 5. The new phases enriched with Mn, Co are identified at the interface and at the Inconel HAZ. While, the adjacent side of AISI 430 has shown that tiny phase structures in white and black spots are enriched with Ti, Mn and Nb. It was also observed that there was significantly less Fe crossing the fusion border on the AISI 430 side. However, the elemental movement over the Inconel 718 contact was noticeable. Also, it can be observed that some amount of Nb and Mo moved towards AISI 430 side. The elemental segregation can be seen from the EDAX analysis due to the improper thermal cycles during and after welding process. The high dense alloying elements like Ni, Mo are observed in fusion zone which can enhance the weld strength properties [26].

3.2.2. PC-TIG weldment

The macro/microstructures of dissimilar joint developed with PC-TIG welding technique is shown in Fig. 6. The macrostructure of PC-TIG weldment shows that uniform spread over towards both the parent metals. The fine grain structures with clear grains can be seen at the interfaces of Inconel 718 as well as AISI 430 as shown in Fig. 6 (a & d). The lower pulse frequency employed during welding process and this could be

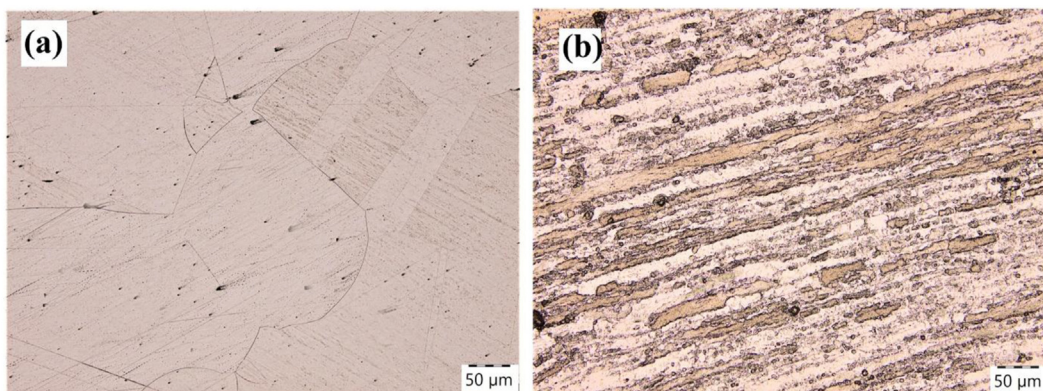


Fig. 3 – Microstructure of base metal (a) Inconel 718 and (b) AISI 430.

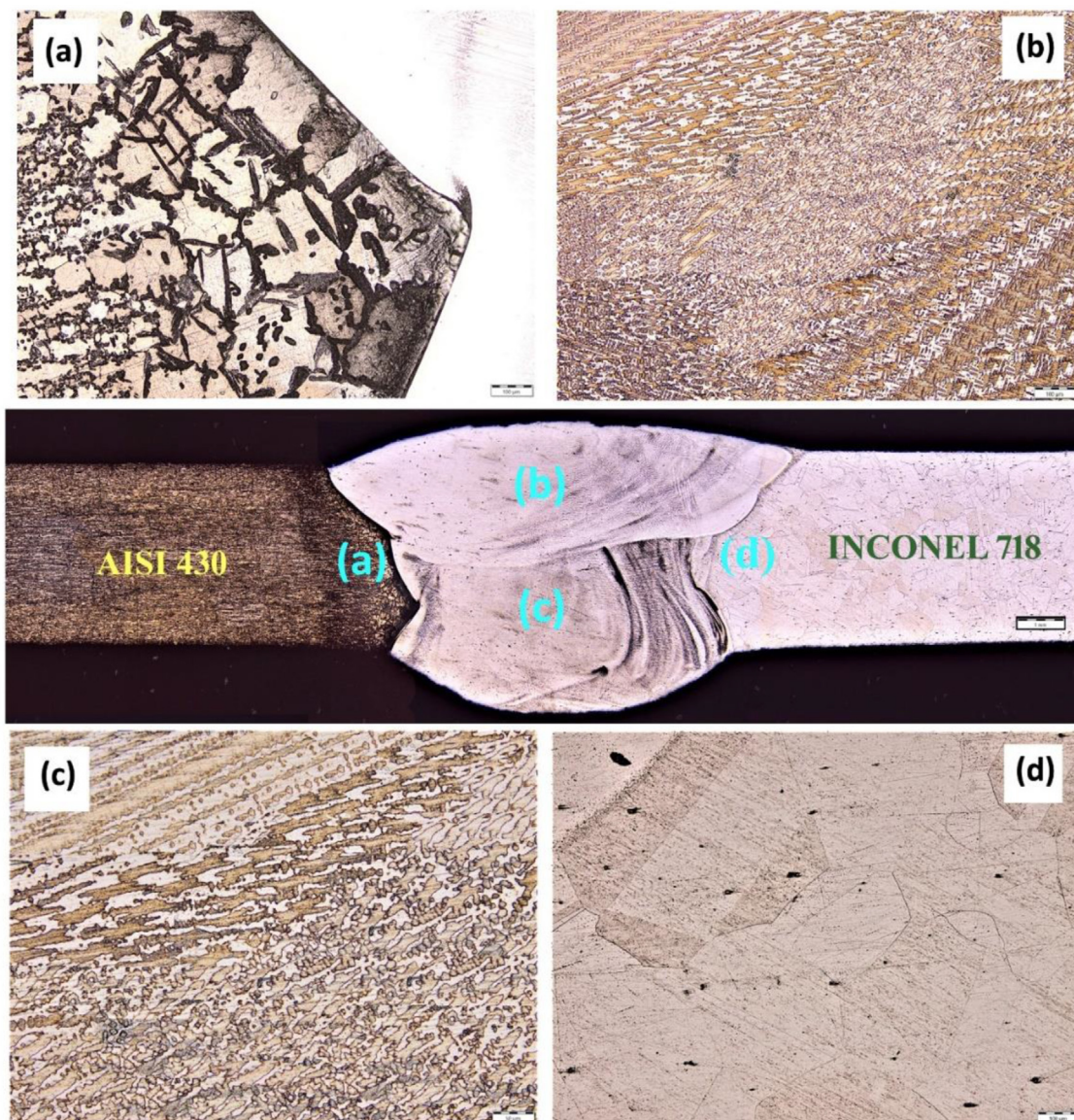


Fig. 4 – Macro/microstructures of CC-TIG weldment (a, d) HAZ of AISI 430, Inconel 718 and (b, c) fusion area of capping and root passes.

attributed to get homogeneity of microstructures and the same was coated in others research work done on same kind of materials [23,24]. Additionally, it is well known that AISI 430 only experiences changes in grain size during thermal treatments and not any other phase transformations. The weld line zone of root and capping passes structures are revealed in Fig. 6 (b & c). The uniform and equiaxed dendrite structure can be seen in capping pass. It is also observed that the tiny dendrite phases and fine cellular structures at the vicinity of weld zone due to pulse arc mode where the arc is being fluctuates from higher to lower with a frequency of 4 Hz. The SEM/EDAX analysis of PC-TIG weldment is shown in Fig. 7. It is also evident that the fusion area consist of dendritic structure and

enriched with Mo and Ti as shown in Fig. 7 (b). The segregation of alloying elements from the filler wire and base metal Inconel 718 is reduced in this dissimilar welds. The interface boundaries of AISI 430 consist of Mn, Ti and very small amount of Nb phases which might be attributed to increase the strength and also reduce the chances of getting failure of the joint under tension test. EDS mapping studies over the weld zone revealed that, other from the emergence of small secondary precipitates in the weld zone, there was not much elemental movement between the grains. The Inconel HAZ has shown clearly that the less segregation effect of alloying elements and formation of new phases at the interface of weld.

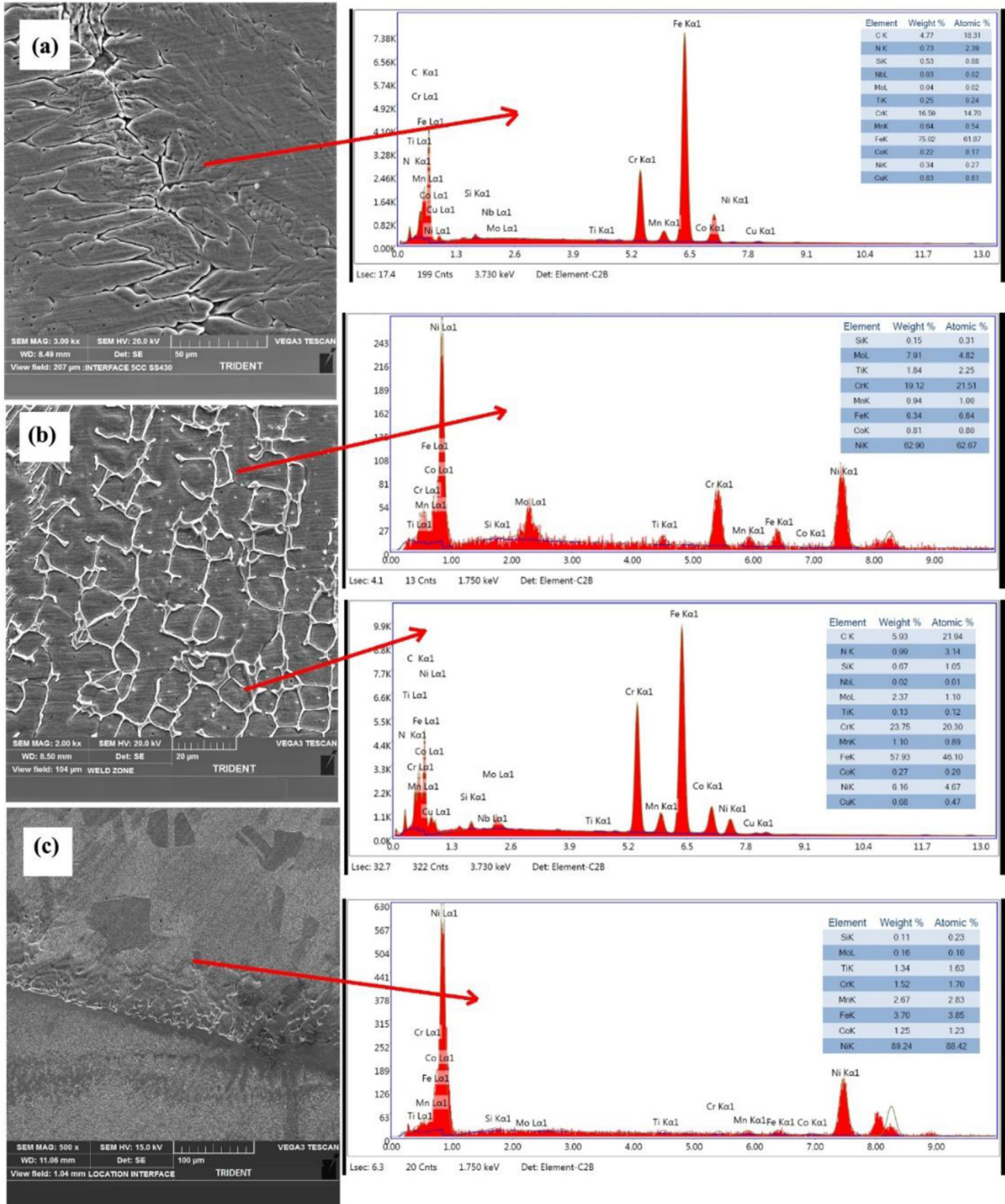


Fig. 5 – SEM micrographs and their EDAX analysis of CC-TIG weldment (a) AISI 430 HAZ, (b) fusion area and (c) Inconel 718 HAZ.

3.3. Tensile test

Three tensile specimens were tested for welding strength and the fractured specimens under uni-axial loads are shown in

Fig. 8. The tensile specimens fractured away from the HAZ of AISI 430 in PC-TIG weldment whereas, the fracture can be seen at the HAZ of AISI 430 in CC-TIG weldment. Martensite grain boundaries were formed near the interface of 430 which

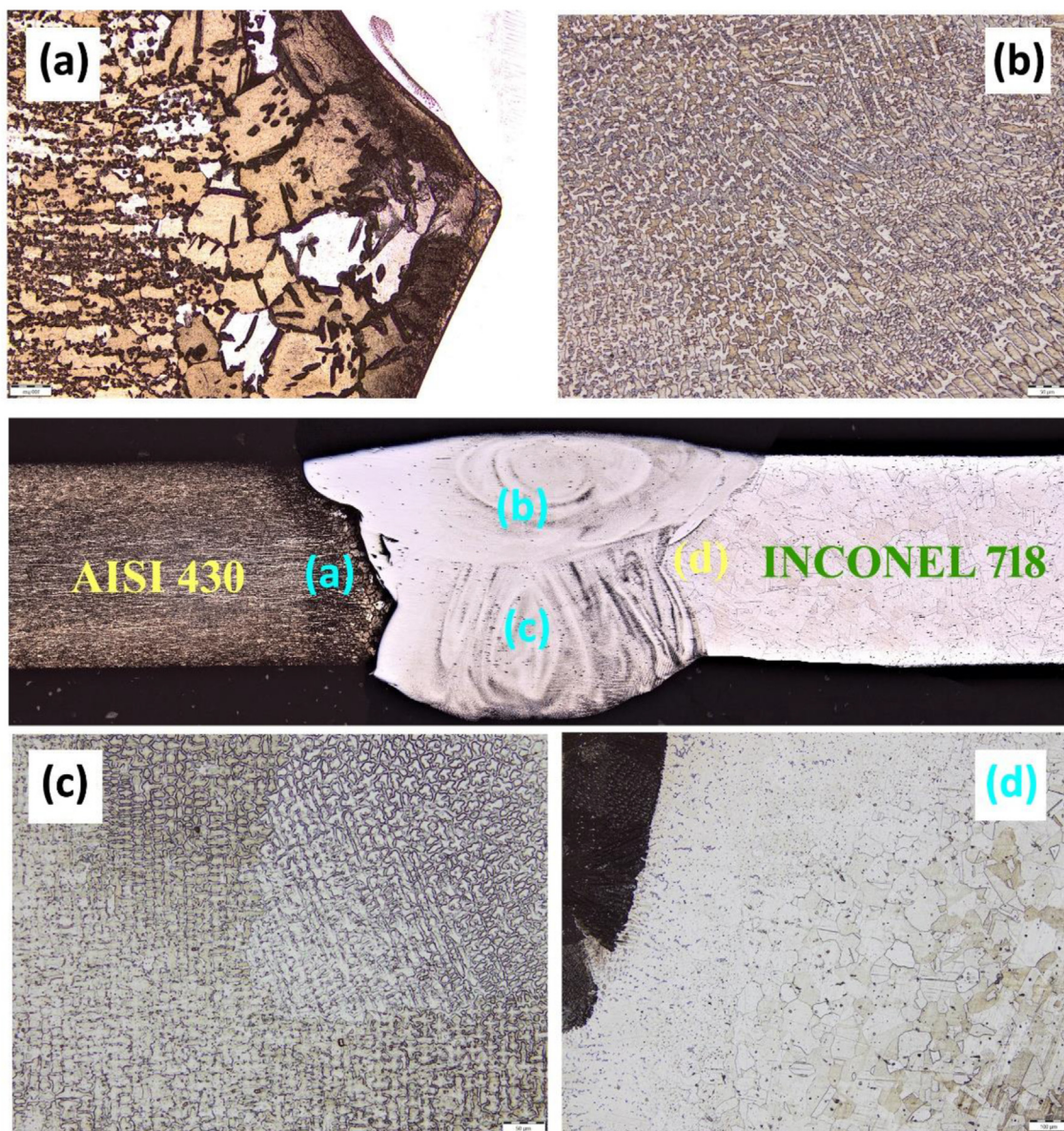


Fig. 6 – Macro/microstructures of CC-TIG weldment (a, d) HAZ of AISI 430, Inconel 718 and (b, c) fusion area of capping and root passes.

enhance the microhardness and in turn increasing the weld strength. The tensile stress with strain percentage graphs are shown in Fig. 9. The test results of weldments are represented in Fig. 9 showing that higher UTS and YS values in PC-TIG weldment than the CC-TIG weldment. The results obtained from this test are tabulated along with ratio of YS to UTS and are shown in Table 3. The average UTS and YS of PC-TIG weldment were perceived as 543 MPa and 375 MPa, respectively which are greater than the UTS (537 MPa) and YS (354 MPa) of CC-TIG weldment. This might be reasoned due to

the presence of main elements like Mo, Cr, Ti and Co exhibited strengthening effect to make stronger matrix. The weld strength was observed to lower when the samples were welded with ER2553 filler element compared to ERNiCrMo-4 filler element [12]. When the samples are welded with laser welding process [22], the weld strength was observed to be lower than the pulsed welding process which could be attributed to the lower pulse current and controlled heat input rate. The improvement in yield strength is about 5.6% is more in PC-TIG weldment in comparison with CC-TIG weldment. The ratio of

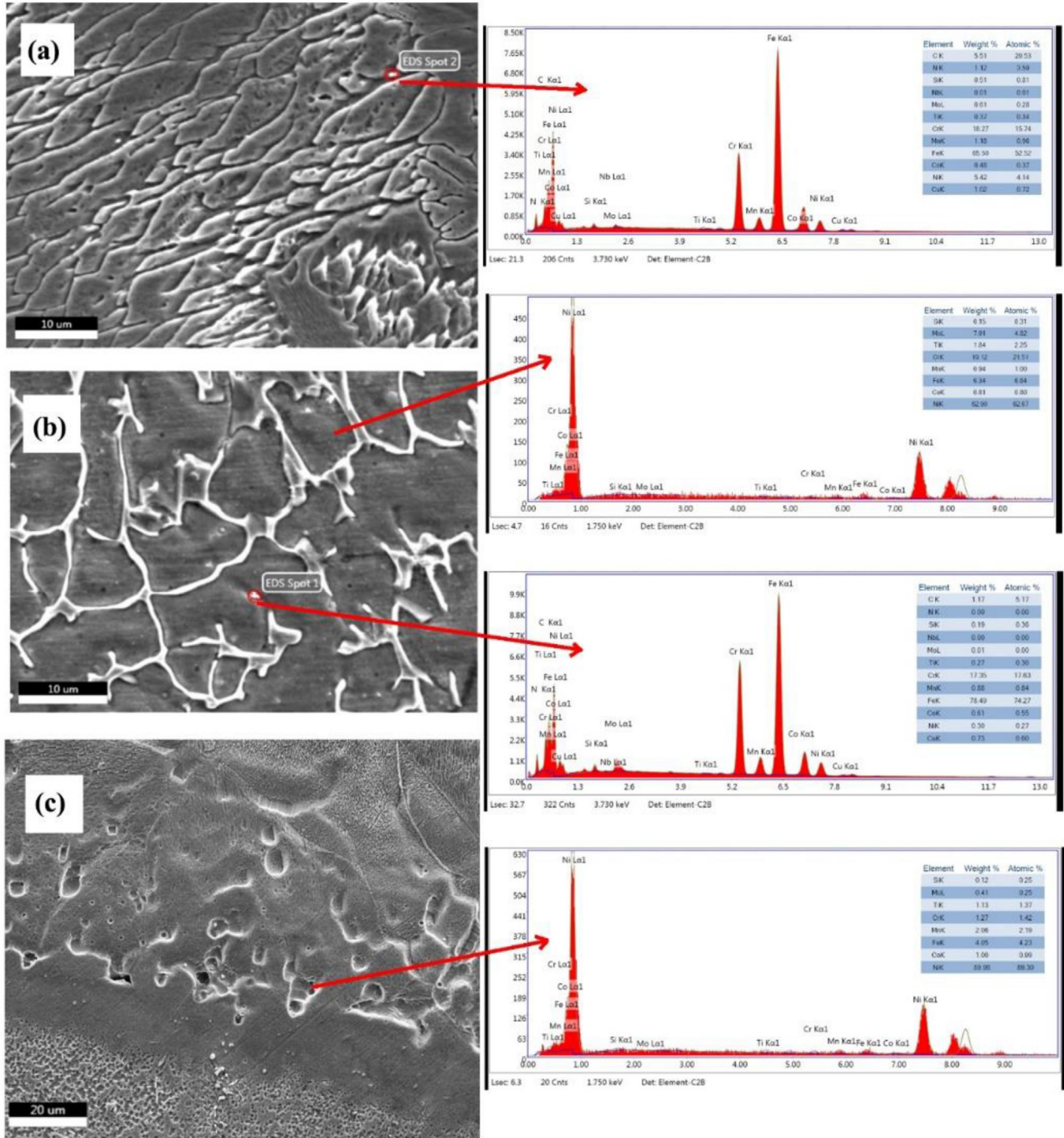


Fig. 7 – SEM micrographs and their EDAX analysis of PC-TIG weldment (a) AISI 430 HAZ, (b) fusion area and (c) Inconel 718 HAZ.

YS to UTS is observed high in PC-TIG weldment (0.69) in comparison to CC-TIG weldment (0.66). Similar kind of observations were observed when the joining of Monel and steel 316 materials using same welding processes [27] (see Fig. 10).

3.4. Microhardness

The hardness measurement was made on the weld surface of weld coupon of size 50 × 5 × 5 mm at a distance of 2.5 mm

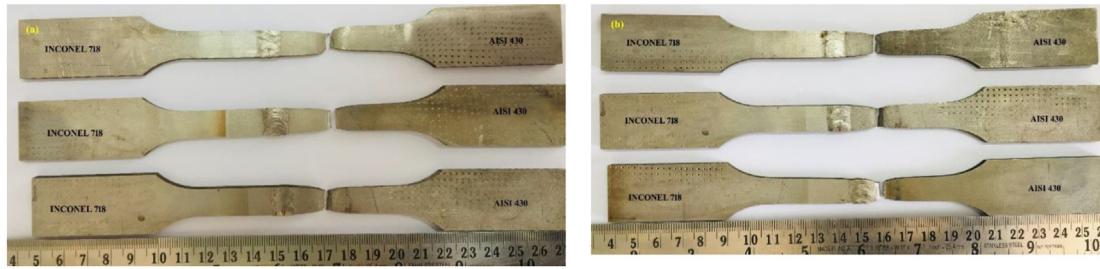


Fig. 8 – Tensile fracture under uni-axial loads of (a) PC-TIG and (b) CC-TIG weldments.

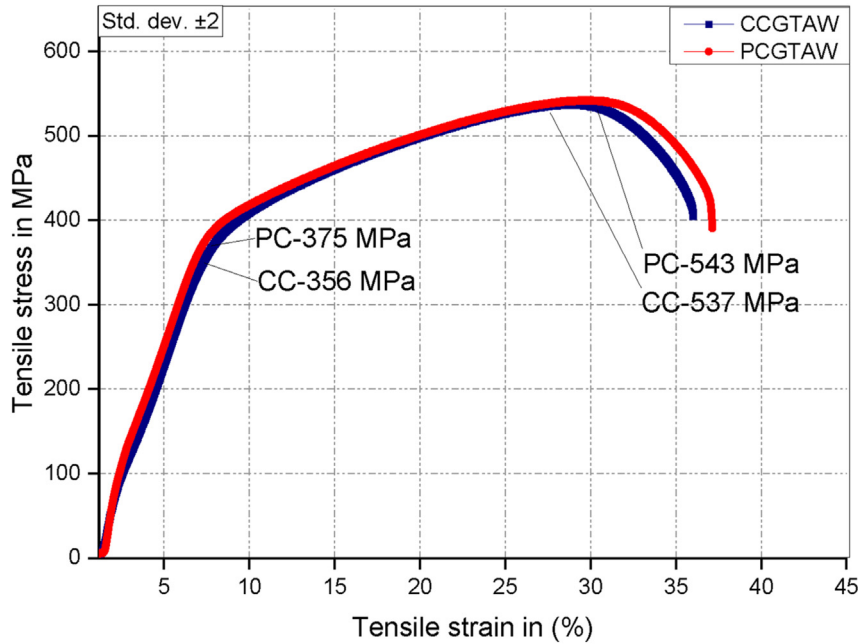


Fig. 9 – Tensile stress-strain plots of dissimilar weldments.

Table 3 – Average tensile test results of PC-TIG and CC-TIG weldments.

Welding	UTS, MPa	0.2% of YS, MPa	Ratio of YS to UTS	% of Elongation	Failure location
PC-TIG	543	375	0.69	20.5	AISI 430 side
CC-TIG	537	356	0.66	20.7	AISI 430 side

from root. The profiles of microhardness of both welding processes are shown in Figs. 10 & 11. The average hardness value at different zones are mentioned in Table 4. The Avg. Hardness value at the HAZ of Inconel 718 of PC-TIG weldment (209 HV) was higher than the CC-TIG weldment (195 HV). This could be reason to the formation of coarse grain structures in continuous current-TIG welding process. The Avg. Hardness value at the FZ of PC-TIG weldment is observed as 206 HV

which is greater than the fusion of CC-TIG weldment (196 HV). Due to the reheating in PC-welding process, the grain refinement was observed at the weld zone which could attributed to improve hardness number. The similar hardness profiles were seen at the HAZ of SS 430 in both the welding processes. As evident from the study (section 3.2), the AISI 430 HAZ in both the welding processes is observed to have clear martensite grain boundaries in the ferritic matrix. Compared to HAZ and base plate of AISI 430, the hardness of fusion zone is greatly improved in both the welding techniques due to the formation of short cellular equiaxed structures. The hardness measurement studies are in good contract with metallurgical studies (see Fig. 11).

3.5. Corrosion analysis of dissimilar weldments

Cyclic sweep corrosion test has been conducted in accordance with ASTM G61 to determine the rest potential, I-Corrosion

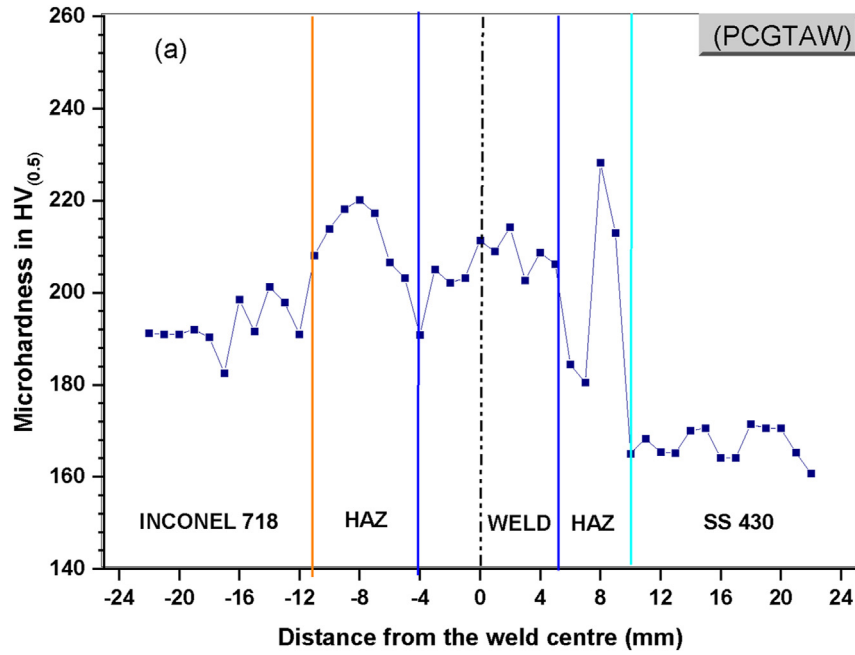


Fig. 10 – Microhardness profile of dissimilar weldment developed with PC-TIG welding.

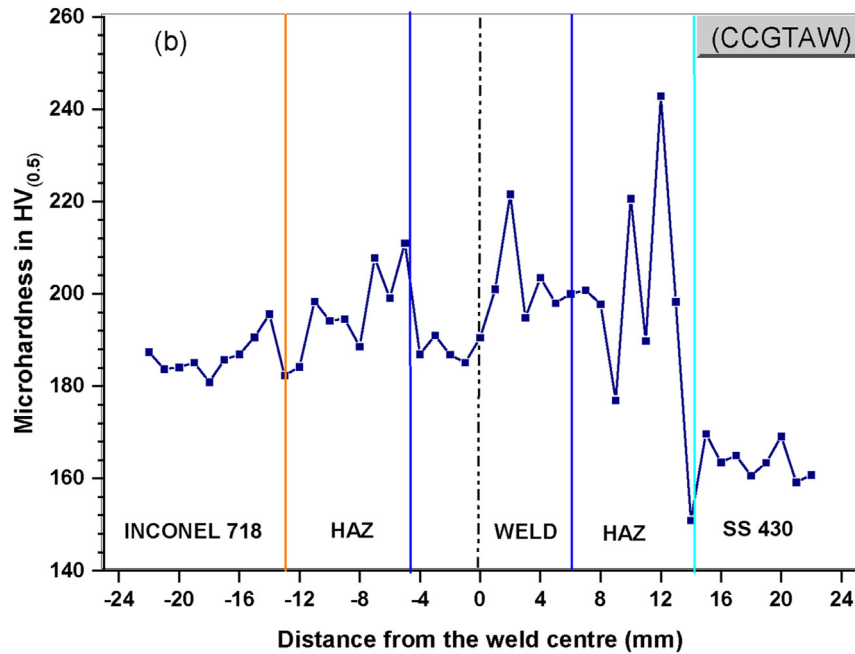


Fig. 11 – Microhardness profile of dissimilar weldment developed with CC-TIG welding.

Table 4 – Comparison of average microhardness value of PC-TIG and CC-TIG weldments.

Welding	Inconel 718 HAZ (HV _{0.5})	Weld zone (HV _{0.5})	AISI 430 HAZ (HV _{0.5})
PC-TIG	209	206	194
CC-TIG	195	196	196

and corrosion rate. Slopes of the corrosion curves taken as reference to calculate rest potential, I-Corrosion and corrosion rate of base plates and welded joints as shown in Figs. 12 & 13. The data obtained from sweep corrosion test is listed in Table 5. The corrosion rate of base metals of Inconel and AISI 430 was observed as 2.84 mm/year and 1.047 mm/year respectively. Due to martensitic face structure in steel 430 exhibited

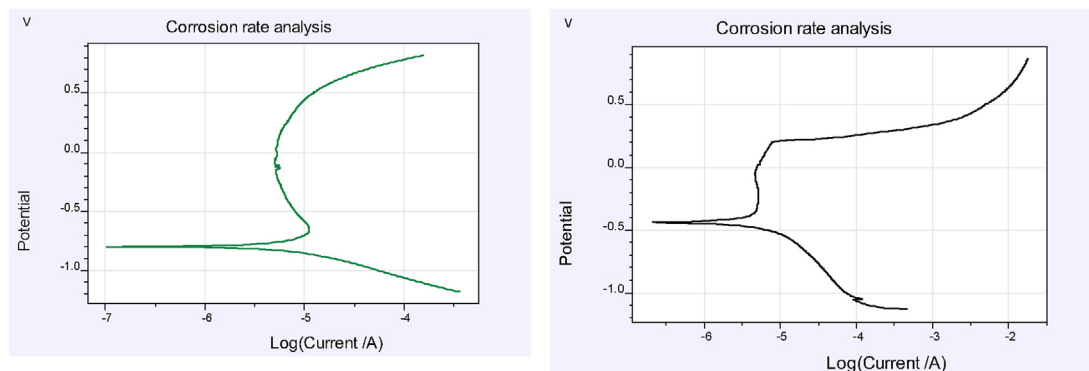


Fig. 12 – Potential verses current graph of Inconel 718 (left) and AISI 416 (right).

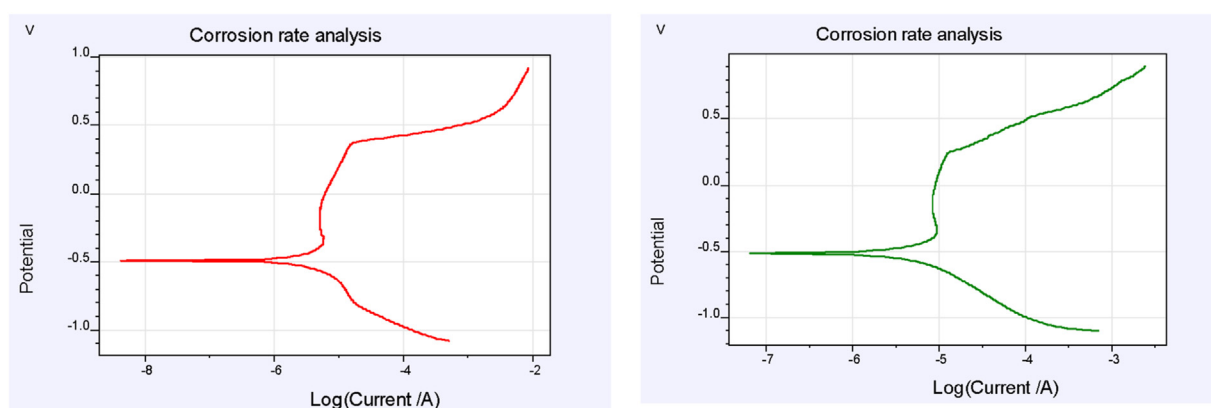


Fig. 13 – Potential verses current graph of dissimilar jointsof PC-TIG (left) and CC-TIG welding (right).

Table 5 – Corrosion test results of base/Inconel 718 and AISI 430 weldments.

Base/ weldments	Rest potential (mV)	I _{corr.} (mA/ cm ²)	Corrosion Rate (mm/year)
Inconel 718	-0.8179	0.00009	2.84
AISI 430	-0.4416	0.00003	1.047
PC-TIG	-0.4811	0.00004	1.35
CC-TIG	-0.514	0.00004	1.41

high corrosion resistance than the Ni-based super alloy Inconel 718. The corrosion rate of dissimilar weldments of PC-TIG and CC-TIG welding processes was observed as 1.35 and 1.41 mm/year, respectively. Due to the formation of fine grain structure and high dense alloying elements present in fusion zone, corrosion resistance was improved in PC-TIG weldment than the CC-TIG weldment (see Fig. 13).

4. Conclusions

The present research explore the effect of TIG welding current modes on microstructural properties, tensile strength,

microhardness and corrosion resistance behavior of AISI 430 and Inconel weldments joined using ERNiCrMo-4 as filler.

The major points are drawn from the investigations and are follows.

- Both welding processes used successfully to join dissimilar aforementioned plates using ERNiCrMo-4 as filler. Also, the radiography results have shown that no macro/micro-defects throughout weld structures in both weldments.
- The grain growth and cellular dendritic phase structures were observed in PC-TIG weldment whereas grain coarsening with Martensite phases were observed in CC-TIG weldment. Due to the presence of strong alloying elements like Nb and Mo, no solidification cracking and HAZ liquid cracking were identified in PC-TIG weldment.
- Higher tensile properties were observed in PC-TIG weldment than the CC-TIG weldment and base metal AISI 430. Also, higher ratio of YS to UTS value was observed in PC-TIG weldment.
- The fusion zone and HAZ of PC-TIG weldment experienced greater hardness than CC-TIG weldment due the formation of skeletal delta ferrite morphology.
- The corrosion rate of PC-TIG weldment was observed as 1.35 mm/year which is lower than the CC-TIG weldment (1.41 mm/year). Comparatively corrosion resistance

behaviour was improved in PC-TIG weldment when compared to CC-TIG weldment and base metal Inconel 718.

- The weldment joined with PC-TIG welding possess better mechanical properties, good corrosion resistance and formation of fine grain structures especially at the roots. The outcomes of the present work will be useful in industrial applications especially in turbine disc and shaft assembly.

Declaration of competing interest

The authors declare that they have no known competing financial interests or personal relationships that could have appeared to influence the work reported in this paper.

REFERENCES

- [1] Li Liying, Du Zhaoxia, Sheng Xuezhen, et al. Comparative analysis of GTAW+SMAW and GTAW welded joints of duplex stainless steel 2205 pipe. *Int J Pres Ves Pip* 2022;833:142508. <https://doi.org/10.1016/j.msea.2021.142508>.
- [2] Ye C, Zhai W, Lu G, et al. Microstructural evolution and mechanical integrity relationship of dissimilar metal welding between 2205 duplex stainless steel and composite bimetallic plates. *Proc IME C J Mech Eng Sci* 2021;235(23):7033–44. <https://doi.org/10.1177/09544062211003615>.
- [3] Yadav Ajit Kumar, Agrawal Manoj Kr, et al. Effect of GTAW process parameters on weld characteristics and microstructural studies of dissimilar welded joints of AA5083 and AA6082: optimization technique. *Int J Interact Des Manuf* 2023. <https://doi.org/10.1007/s12008-023-01230-x>.
- [4] Sabzi M, Mousavi Anijdan SH, et al. The effect of pulse current changes in PCGTAW on microstructural evolution, drastic improvement in mechanical properties, and fracture mode of dissimilar welded joint of AISI 316L-AISI 310S stainless steels. *Mater Sci Eng* 2021;823:141700. <https://doi.org/10.1016/j.msea.2021.141700>.
- [5] Porchilamban S, Amaladas JR. Structural relationships of metallurgical and mechanical properties influenced by Ni-based fillers on Gas Tungsten Arc Welded Ferritic/Austenitic SS dissimilar joints. *J Adv Mech Design Syst Manuf* 2019;13(1). <https://doi.org/10.1299/jamdsm.2019jamdsm0023>. JAMDSM0023–JAMDSM0023.
- [6] Yang Tao, Xiao Youheng, et al. Effect of microstructural heterogeneity on corrosion fatigue crack growth behavior of 60-mm thick-plate TC4 titanium alloy NG-GTAW welded joint. *Int J Fatig* 2022;163:107030. <https://doi.org/10.1016/j.ijfatigue.2022.107030>.
- [7] Zhang Q, Zhuo Z, Zhou H, Wang J. Microstructure analysis and hardness prediction based on microstructure evolution theory in multi-pass welded joint. *Proc IME C J Mech Eng Sci* 2022;236(13):7246–58. <https://doi.org/10.1177/09544062211073101>.
- [8] Kumar PSS, Allamraju KV. A review of natural fiber composites [Jute, Sisal, Kenaf]. *Mater Today Proc* 2019;18:2556–62. <https://doi.org/10.1016/j.matpr.2019.07.113>.
- [9] Yadav Ajit Kumar, Agrawal Manoj Kr, et al. Numerical simulation and experimental residual stress analyses of dissimilar GTA weldments of AA 5083 and AA 6082. *Int J Interact Des Manuf* 2023. <https://doi.org/10.1007/s12008-023-01216-9>.
- [10] Wang Bingxu, Qiu Feng, et al. Microstructure and shearing strength of stainless steel/low carbon steel joints produced by resistance spot welding. *J Mater Res Technol* 2022;20:2668–79. <https://doi.org/10.1016/j.jmrt.2022.08.041>.
- [11] Harinadh V, Mohan Babu M, Prerana I, et al. Evaluation of residual stresses in CO₂ laser beam welding of SS316L weldments using FEA. *Mater Res Express* 2023;10(1). <https://doi.org/10.1088/2053-1591/acb0b5>.
- [12] Sedighi M, Mosayeb Nezhad J. The influence of process parameters on the distribution of residual stresses in magnetically impelled arc welded joints. *Proc IME C J Mech Eng Sci* 2019;233(11):3936–49. <https://doi.org/10.1177/0954406218809131>.
- [13] Ramkumar KD, Mohan TH, Pandey R, et al. Investigations on the structure – property relationships of PCGTA welds involving Inconel 718 and AISI 430. *Cienc e Tecnol dos Mater* 2017;29:28–38. <https://doi.org/10.1016/j.ctmat.2016.05.005>.
- [14] Ramkumar KD, Naren SV, Karthik Paga VR, et al. Development of pulsed current gas tungsten arc welding technique for dissimilar joints of marine grade alloys. *J Manuf Process* 2016;21:201–13. <https://doi.org/10.1016/j.jmapro.2015.10.004>.
- [15] Ramkumar KD, Arivazhagan N, Narayanan S. Comparative assessment on microstructure and mechanical properties of continuous and pulse-current GTA welds of AISI 304 and Monel 400. *Kov Mater* 2014;52:287–98. <https://doi.org/10.4149/km-2014-5-287>.
- [16] Yelamasetti B, Vardhan TV, Ramana GV. Study of metallurgical changes and mechanical properties of dissimilar weldments developed by interpulse current TIG welding technique. *Proc IME C J Mech Eng Sci* 2021;235(16):2985–97. <https://doi.org/10.1177/0954406220960780>.
- [17] Abu-Dalo Muna A, al-Rawashdeh Nathir AF, Ahmed A. MUTLAQ, green approach to corrosion inhibition of mild steel by lignin sulfonate in acidic media. *J Iron Steel Res Int* 2016;23(Issue 7):722–32. [https://doi.org/10.1016/S1006-706X\(16\)30112-1](https://doi.org/10.1016/S1006-706X(16)30112-1).
- [18] Jaffery HA, Sabri MFM, Said SM, Hasan SW, Sajid IH, Nordin NIM, et al. Electrochemical corrosion behavior of Sn-0.7 Cu solder alloy with the addition of bismuth and iron. *J Alloys Compd* 2019;810:151925. <https://doi.org/10.1016/j.jallcom.2019.151925>.
- [19] Ramkumar KD, Patel SD, Sri Praveen S, et al. Influence of filler metals and welding techniques on the structure-property relationships of Inconel 718 and AISI 316L dissimilar weldments. *Mater Des* 2014;62:175–88. <https://doi.org/10.1016/j.matdes.2014.05.019>.
- [20] Ramkumar KD, Thiruvengatam G, Sudharsan SP, et al. Characterization of weld strength and impact toughness in the multi-pass welding of super-duplex stainless steel UNS 32750. *Mater Des* 2014;60:125–35. <https://doi.org/10.1016/j.matdes.2014.03.031>.
- [21] Krishnaja D, Cheepu M, Venkateswarlu D. A review of research progress on dissimilar laser weld-brazing of automotive applications. *Mater Sci Eng* 2018;330(1):012073. <https://doi.org/10.1088/1757-899X/330/1/012073>.
- [22] Dev S, Ramkumar KD, Arivazhagan N, Rajendran R. Effect of continuous and pulsed current GTA welding on the performance of dissimilar welds involving aerospace grade alloys. *Trans Indian Inst Met* 2017;70:729–39. <https://doi.org/10.1007/s12666-017-1085-y>.
- [23] Dev S, Ramkumar KD, Arivazhagan N, Rajendran R. Investigations on the microstructure and mechanical properties of dissimilar welds of inconel 718 and sulphur rich martensitic stainless steel, AISI 416. *J Manuf Process* 2018;32:685–98. <https://doi.org/10.1016/j.jmapro.2018.03.035>.

- [24] Bajpei T, Chelladurai H, Ansari MZ. Mitigation of residual stresses and distortions in thin aluminium alloy GMAW plates using different heat sink models. *J Manuf Process* 2016;22:199–210. <https://doi.org/10.1016/j.jmapro.2016.03.011>.
- [25] Ramkumar KD, Sidharth Dev, Phani Prabhakar KV, Rajendran R, Giri Mugundan K, Narayanan S. Microstructure and properties of Inconel 718 and AISI 416 laser welded joints. *J Mater Process Technol* 2019;266:52–62. <https://doi.org/10.1016/j.jmatprotec.2018.10.039>.
- [26] Ramesh S, Boppana SB, Manjunath A, Parthiban K. Corrosion behavior studies and parameter optimization of dissimilar alloys joined by electron beam welding. *J Bio- Tribo- Corrosion* 2020;6. <https://doi.org/10.1007/s40735-020-00372-9>.
- [27] Raj S, Biswas P. Mechanical and microstructural characterizations of friction stir welded dissimilar butt joints of Inconel 718 and AISI 204Cu austenitic stainless steel. *Mater Char* 2022;185:111763. <https://doi.org/10.1016/j.matchar.2022.111763>.

Low Power and Suppressed Noise 6T, 7T SRAM Cell Using 18 nm FinFET

Published: 13 March 2023 | 130,103–112 (2023)



Wireless Personal Communications

[Aims and scope](#) →

[Submit manuscript](#) →

[T. Santosh Kumar](#) & [Suman Lata Tripathi](#)

219 Accesses 2 Citations [Explore all metrics](#) →

[Cite this article](#)

Abstract

The fundamental components of maximum digital devices are memories and therefore stability, performance and efficiency of the system can be modified by decreasing the power requirement of memory. SRAM cells have less leakage making them suitable for portable and embedded devices. FinFETs are proven to be a promising candidate with high performance low power consumption features at lower technology nodes. Low power is one

Access this article

[Log in via an institution](#) →

[Buy article PDF 39,95 €](#)

Price includes VAT (India)

Instant access to the full article PDF.

Rent this article via [DeepDyve](#)

[Institutional subscriptions](#) →

Assessing Learning Behaviors Using Gaussian Hybrid Fuzzy Clustering (GHFC) in Special Education Classrooms

Dr.R. Udayakumar^{1*}, Muhammad Abul Kalam², Dr.R. Sugumar³ and Dr.R. Elankavi⁴

^{1*} Dean, CS & IT, Kalinga University, India. rsukumar2007@gmail.com,
deancsit@kalingauniversity.ac.in, Orcid: <https://orcid.org/0000-0002-1395-583X>

²Research Scholar, Bharath Institute of Higher Education and Research, Selaiyur, Chennai.
Assistant Professor, CMR Institute of Technology, Hyderabad. makalam.cse@gmail.com
Orcid: <https://orcid.org/0000-0002-9130-1444>

³Professor, Institute of CSE, Saveetha School of Engineering, Saveetha Institute of Medical &
Technical Sciences, Thandalam, Chennai, India. sugu16@gmail.com,
Orcid: <https://orcid.org/0000-0002-0801-6600>

⁴Associate Professor, Department of Computer Science and Engineering, Siddharth Institute of
Engineering & Technology, Puttur, Tirupati District, Andhra Pradesh, India.
kavirajcse@gmail.com, Orcid: <https://orcid.org/0000-0001-5661-7278>

Received: December 20, 2022; Accepted: January 21, 2023; Published: March 30, 2023

Abstract

The article suggests an unsupervised model for featuring student's learning patterns in an open-ended learning scenario. The article proceeds by generating powerful metrics to characterize the learner's behavior and efficacy through Coherence investigation. Then, the selected features are combined through a Gaussian Hybrid Fuzzy Clustering (GHFC) that categorizes students based on their learning patterns. The proposed system features the essential behaviors of every group and associate the behaviors with ability to develop right models to gauge the learning gains between pre-and post-test scores. Also, this article explains the deployment of behavior characterization to be developed as a adaptive framework of learning behaviors.

Keywords: Affective State Transition, Unsupervised Learning, Cognitive State Transition, Likelihood Metric, Fuzzy Clustering.

1 Introduction

Learning starts from the first day of our lives by learning essential activities and eventually evolving to learn complex activities. Learn generally occurs through transfer of knowledge from an instructor whose role is shared by parents, siblings, or teacher in school (Cantor, P., et al, 2018). As time evolves, humans are expected to learn on their own without any guidance so that they apply their knowledge to solve real world problems. Many automations have been developed to assist the learning in the absence of a teacher. The automations or the computer system take the place of an instructor and supports students in learning. Though these systems can render knowledge to students, they do not interact with the student. This is a hindrance on the learning session.

Open-Ended Learning Environments (OELEs) offer the learners with authentic but meaningful learning by involving the students in problem-solving that is a combination of testing, developing and revisiting their own solutions (Land, S. 2000). Nevertheless, the novice learners tend to face challenges in conceiving, developing and further application of the knowledge into strategies succeed (Winslow, L.E. 1996). This raises a demand for scaffolding and feedback mechanisms to improve the proficiencies (Kinnebrew, J., et al., 2017).

The proposed research focus around the development of CTSiM, an OELE to foster the learning of computational thinking (CT) and science concepts by deploying learning by modeling strategy. In this environment, the students develop their own simulation models through agent-based and block-structured visual language. This is fastened with the help of supporting tools to test and verify their so developed models (Winslow, L.E. 1996 & Sengupta, P., et al. 2013). The Pre- and post-tests in previous studies revealed that the CTSiM have exhibited enhanced learning gains in both the domains namely CT and science. Nevertheless, a multitude of challenges are confronted by middle school students in conceiving, developing and further applying their acquired knowledge and modeling skills when they try to develop science models in CTSiM environment (Sengupta, P., et al. 2013). Students use different strategies to assist learning and model developing activities. But still selecting suboptimal strategies retard the learning and further aggravate the difficulties in model building. To aid the learning community to combat the challenges, an adaptive feedback mechanism which is to be integrated on automated detection, evaluation, and identification of learning patterns (Basu, S., et al., 2017 & Segedy, J.R., 2015).

Most of the legacy systems are designed with an intend to help in learning by providing the cognitive as well as affective feedback to the learners in problem solving or exploration of the environments (Arroyo, I., et al., & Baker, R.S., et al., 2007). Tracking both the cognitive as well as affective states have facilitated these systems to completely model students apart from imparting better understanding.

These facts were harnessed for the design and identification of appropriate feedback mechanism for learners. D'Mello and Graesser (D'Mello, S., et al., 2014) suggested a comprehensive model that considered cognitive as well as affective elements to demonstrate the transformation of emotions during the learning process. Augmenting to this, the model also anticipates learner's behavior and issue suitable feedback when the student's experience emotions that hinder their learning. The learners employ computer-based environments to learn as well as to get involved in non-learning tasks. Some of the cognitive states and affective states are isolated to direct the off-task activities like gaming and conversation with fellow students (Baker, R.S., et al., 2007). Though the environments hinder the students from involving in non-learning tasks, the students adopt self-learning. Even though they cannot manage their complete learning process, still they thrive to learn less by spending more time (Baker, R.S., et al., 2007). This article proposes a complete exploratory Machine Learning (ML) model to isolate the student's behaviors in a case study approach to demonstrate the efficacy of the proposed approach.

2 Proposed Methodology

Students' modeling and learning processes in CTSiM environment is seen as a coagulation of five vital activities: (1) perceiving and securing domain information and other CT-related ideas from hypertext resources (2) construction of an abstract but conceptual model in science domain through an agent-based framework; (3) developing computational models that mimics behavior of the agent through a block-structured language with visual effects; (4) model execution to analyze the behaviors as generated by Net Logo (Wilensky, U) and (5) verification of the model's correctness by comparing the behaviors as emanated by an expert model which could execute synchronously. The complete model building activity

and its behavior comparison with its interfaces are showed in Fig. 1. Elaborate details of the presented CTSiM environment is employed in middle school science and was very successful (Winslow, L.E. 1996 & Sengupta, P., et al. 2013).

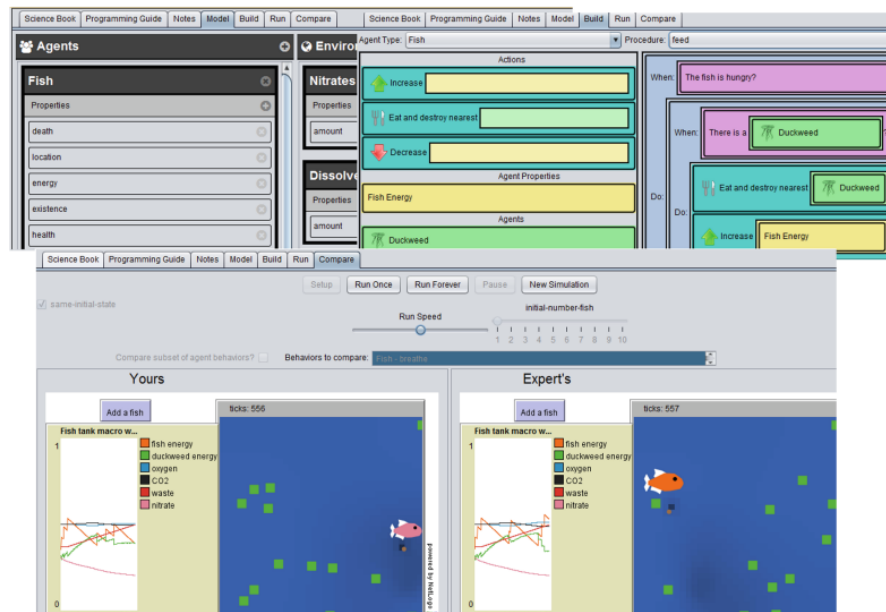


Figure 1: Conceptual, Behavior, and Computational Interfaces of CTSiM

The legacy research in CTSiM, have demonstrated good learning improvement with 2 introductory training tasks whereas with 3 modeling tasks. The learners familiarize with the interfaces and functionality of the system by creating agents to draw shapes as well as spirals, which is a direct kinematics learning. The three learning activities comprises of modeling the tasks under 2 topics pertaining to science: (1) advanced kinematics which is represented as unit. Here the learners model a rollercoaster car that moves on a track, and (2) ecology-based task. Here the learners initially create a macroscopic and microscopic model of a fish tank, which is perceived as unit 4 and 5 respectively. The macroscopic model concentrates on implementing fish and aquatic plant's behavior along with their food chain. But this model is not stable. So, in unit 5 the learners add microscopic elements like bacteria and implement waste cycle to create a more sustainable fish ecosystem model. The preceding studies have revealed that the learners enthusiastically learn science as well as other CT concepts CTSiM (Winslow, L.E. 1996 & Sengupta, P., et al. 2013).

Building Model

The model building process CTSiM comprises of various problem-solving strategies and learning pedagogy. Hence, they can demonstrate a wide range of learning behaviors in students. The proposed work attempts to collect features from behavioral characteristics, so as to create an adaptive scaffolding as a primary means to grouping of learning behaviors. To perform this task, the methodology describes the behavioral nature of the learners wholly dependent on multitude of metrics associated with a specific task model. This work also assesses the quality of the developed model in CTSiM environment. Appropriate feature selection method is applied on the feature space, to attain optimal metrics which are closely relevant to clustering the students based on their behavior. The Gaussian hybrid fuzzy clustering (GHFC) is solely used to form the clusters.

Development of Suitable Measures that can Describe the Learning Behaviors

In the preceding works, a more popular Coherence Analysis (CA) is deployed to create a model-based analytical framework, that inherently analyze the problem solving and learning patterns (Basu, S., et al., 2017 & Kinnebrew, J., et al., 2017). The CA along with other performance metrics cumulatively characterize the feature space to elaborate the learning behaviors. The theory-based framework inclines to follow top-down approach that is responsible to identify the learners action in any OELE which can be further categorized into one of three types: (1) acquisition of information (IA), (2) Construction of solution and (3) assessment of the so developed solution (SA) (Basu, S., et al., 2017). Each of these tasks can be further drilled down into hierarchical subtasks, where the leaves indicate the individual actions performed by the learners CTSiM. The IA tasks includes activities like searching, identification and understanding of all the essential information to build and correct models in the appropriate resource libraries. SC mainly concentrates on development as well as refinement of both computational and conceptual models. The action carried out in SC may be an edit operation on the models like augmenting a trait to the agent or eliminating a feature from it. SA activities comprise of executing the simulations in the learner developed model. It also compares the model's behaviors with an expert model as explained in Section 2. Students are allowed to undergo the activities in the order they prefer. Tracking the combinations in which they order the tasks and the manner of switching among the tasks is very vital to learn about the learners and problem-solving capabilities (Basu, S., et al., 2017).

The performance measure for assessing any action is done as a unary relation termed as effectiveness. This could effectively capture whether the performed action leads to appropriate solution. For instance, including an appropriate component or weeding off an inappropriate component from the model may characterize more effective strategy or action. Looking forward individual actions, the proposed CA delineates a support among any two actions namely x and $y, x \rightarrow y$. This implicitly means that the action y follows the action x , only if y consumes the information produced by the prior action x then it means that x supports action y , and vice versa. The CTSiM's CA is applied to a set of some 22 measures that can feature the student's deployment of learning strategies. Apart from this, the unary and binary metrics that are already defined, a third measures, termed as proportionality, which could effectively characterize the ratio of specific genre of actions. For instance, the term compare percentage elucidates the ratio of learners model against the cumulative count of actions.

Selecting Appropriate Features and Generating Clusters Using Gaussian Hybrid Fuzzy Clustering (GHFC)

Among the 22 CA measures that are taken for consideration, it has likelihood that few examples have comparatively lighter variance. These measures are nor effective in providing sufficient information to distinguish learners based on their behaviors. Hence feature selection method are applied to select the more appropriate measures that can positively contribute for cluster formation.

The proposed FCM clusters the features by organizing and aggregating the pixels that belong to the same class. To start with, the pixels of the image are organized as a fuzzy matrix, to make the process simpler. FCM clustering in not capable of regularizing the inherent noise in the image. Also, it is not highly successful when scaled to higher dimensions. To cope up these, the images are clustered through Sparse FCM. The sparse FCM can effectively regulate the clustering model by the introduction of model parameters to make the model more suitable for hierarchical clustering. The Sparse FCM that is reformulated is given as,

$$\max_{\varphi(V)} = \sum_{x=1}^p u_x (K_x, \varphi(V)) \quad (1)$$

The term $\varphi(V)$ is the regularization parameter. Also, sparse FCM delineates the clustering framework as

$$\max_{r, \varphi(V)} = \sum_{x=1}^p r_x u_x (K_x, \varphi(V)) \quad (2)$$

Here r_x is the pixel value that is dependent on objective function. The representation of sparse FCM is give as

$$\max_{v, k, r} F(K, k, r) = r^T BCSS(V) \quad (3)$$

The $BCSS(V)$ is weights among cluster summation of squares. Also, sparse FCM clusters by using the centroid (C_{S_FCM}).

The proposed GHFC, the cluster centroids take the responsibility to be identified by both the schemes that are altered by constant α . This represents a Gaussian function. The primary purpose of the Gaussian function is to regulate or normalize the continuous events, that are binomial. The Gaussian distribution function is also used for determining the centroid which eventually increases the likelihood of obtaining improved clusters. The equation for determining the optimal centroid is presented below:

$$C = \alpha C_{FCM} + \beta C_{S_FCM} \quad (4)$$

The terms C_{FCM} and C_{S_FCM} represents the centroids that are eventually identified by the sche, esFCM and Sparse FCM respectively. *The* constant β is actually derived from α , i.e., $\beta = 1 - \alpha$. The Gaussian function α is mentioned as,

$$\alpha = \frac{\sum_{x=1}^p \frac{1}{2\pi\sigma^2} e^{-\frac{(u_x - \mu)^2}{2\sigma^2}}}{N} \quad (5)$$

The term μ represents the mean of the image whereas σ is the variance of the image. P is the count of pixels in the image segment. Deploying the Gaussian function to find the aggregate centroid, certainly improves the segmentation accuracy. Apart from this, it is also used for hybridization of the results from FCM as well as Sparse FCM to make the model more robust in handling noise.

The significant features of the clusters are used to feature the learning pattern pertaining to the clusters. The analysis on the data sourced from a classroom of 98 middle school students in Nashville, TN.

3 Experimental Results

The experimentation is conducted in 6th-grade classroom which comprises of students in the age group of 11–13-year-olds. They were observed for 3 weeks in science classes. On day 1, the participants were asked to attend pre-tests in paper-pen mode on three topics namely kinematics, ecology, and CT. On Day 2, all the learners were asked to attend a lecture on agent-based modeling in the CTSiM environment. On third day, the students studied Unit 1 whereas on fourth day they were asked to work individually on drawing spirals. Students were then subjected to work individually even on Unit 3 and to build a rollercoaster model on subsequent days. On seventh day the learners were actively participated in the post-test on kinematics post-test as well as on CT. The next five days, the students were made to work as individuals to build the fish tank ecosystem, which is to be perceived as a macroscopic model. Then the microscopic model is added on the system. At last, all the learners were made to attend the ecology post-test as well as second post-test on CT.

The process of clusters generation is deployed through Gaussian hybrid fuzzy clustering (GHFC) on a subset of metrics handcrafted by feature selection. The cluster size was maintained as 6. Euclidean

metric is used to find the distance. For about 1000 random restarts were done to control the impact cluster center selection. Table 1 summarizes the average as well as Standard Deviations (SD) of the clusters.

Table 1: Mean Cluster Values Pertaining to Rollercoaster Modeling Activity (*.p is Maintained as Less than 0.05)

Metrics	CT learners at n value as 2	Aimless comparators at n value as 24	Efficient learners at n value as 2	Non-strategic tester sat n value as 18	Tinkerers at n value as 36	Unsystematic builder sat n value as 16
CT read	1474* (506)	11.1(24)	106 (139)	28 (45)	56 (110)	34 (59)
Conc. edt %	7.8 (4.8)	39*(1.9)	10.1 (6.3)	6.3 (3.1)	5.0*(2.1)	11.7* (7.5)
Comp. edt %	22.0 (1.2)	21.8* (4.9)	45.5(14)	28.9 (5.1)	35.3 (5.3)	47.4* (6.6)
Concep. Size	7.0 (2.4)	7.7 (3.9)	10.5 (0.8)	5.3*(2.7)	8.1 (4.2)	6.4 (3.2)
Comp. size	5.4 (0.8)	4.4* (0.8)	5.0 (1.4)	3.9* (0.6)	6.0* (1.1)	6.7* (2.1)
Test %	49* (10.7)	32.1 (4.5)	16.5* (4.8)	44.4* (6.0)	34.7 (4.3)	29.7* (5.5)
Compare %	18.1 (15)	37.8* (6.3)	6.8 (1.4)	16.8* (4.9)	21.4 (5.0)	8.7* (3.4)
Compare part	12.8 (19.5)	34.6* (5.2)	58.3* (11.8)	20.4* (12.9)	31.9* (8.2)	15.6* (13.9)
SC to IA %	0.9.9 (0.6)	0.5* (0.4)	3.5* (3.7)	1.1 (1.3)	0.6 (0.8)	0.7 (0.7)
SC to SA %	15.3 (6.5)	21.1* (4.4)	11.7 (3.8)	21.3* (3.8)	14.1* (2.6)	12.4* (4.3)
SA to IA %	0.7 (0.3)	0.4 (0.4)	8.7* (1.4)	0.8 (0.5)	0.7 (1.0)	0.8 (1.3)
SA to SC %	5.8 (2.3)	6.1* (1.6)	25* (2.7)	12.2 (3.7)	9.8* (2.4)	18.4* (5.5)

Table 2 displays the following measures: learning gains starting from the pre- till the assessment of post-tests both in the domain as well as in CT, model distance among the models developed by students and expert model. The distances that are closer to 0 indicates that the modelling is better.

Table 2: SD and Average of Performance by Clustering in RC

Cluster	Domain gain	CT gain	Conc. dist	Comp. dist.
Efficient learners whose n value is 2	12.00 (8.49)	4.00 (1.41)	10.50 (0.71)	11.00 (0)
Tinkerers whose n value is 36	3.99 (5.00)	2.14 (2.14)	7.20 (1.89)	12.5 (11.1)
Non-strat. testers whose n value is 18	6.50 (6.40)	0.64 (2.05)	8.39 (1.54)	14.00 (8.93)
Unsys. builders whose n value is 16	4.59 (6.22)	1.09 (1.27)	9.40 (1.96)	12.45 (5.15)
A. comparators whose n value is 24	4.11 (3.70)	0.76 (2.46)	8.08 (1.77)	16.83 (11.28)
CT learners whose n value is 2	-2.85 (0.40)	2.00 (0)	7.00 (0)	19.50 (3.54)
All students whose n value is 98	4.49 (5.39)	1.11 (2.12)	8.49 (1.84)	14.09 (9.84)

4 Conclusion

This article presents in integrated research on learner behaviors as well as its performance as exhibited by the performance clusters in two genres namely pre-post learning gains and building models. The detailed experimentation on the cluster’s learning features imparts multiple but valuable insights that can be leveraged to formulate adaptive scaffolds for every formed cluster. The derivation of CA metrics and clustering are combined as the recent version of CTSiM to characterize the 6 behaviors as indicated

by the clusters reported. The article also presents generic methods to (1) formulate actions in any OELE, (2) quantize the relation between learner's actions through CA and (3) select the appropriate metrics that to feature the learning patterns. Detailed analysis of learning behaviors gave in depth insights on distinctive learning behaviors and also on the deployment of learning strategies. Augmenting to this, the study emphasized that learners with better understanding outperformed the ad hoc learners. Also, the study infers that a vast majority of learners improved their learning autonomously.

References

- [1] Arroyo, I., Cooper, D.G., Burleson, W., Woolf, B.P., Muldner, K., & Christopherson, R. (2009). Emotion sensors go to school. In *Artificial intelligence in education*, 17-24. Ios Press.
- [2] Baker, R.S.D., Rodrigo, M.M.T., & Xolocotzin, U.E. (2007). The dynamics of affective transitions in simulation problem-solving environments. In *Affective Computing and Intelligent Interaction: Second International Conference, ACII 2007 Lisbon, Portugal, September 12-14, 2007 Proceedings 2*, 666-677. Springer Berlin Heidelberg.
- [3] Baker, R.S.D., Rodrigo, M.M.T., & Xolocotzin, U.E. (2007). The dynamics of affective transitions in simulation problem-solving environments. In *Affective Computing and Intelligent Interaction: Second International Conference, ACII 2007 Lisbon, Portugal, September 12-14, 2007 Proceedings 2*, 666-677. Springer Berlin Heidelberg.
- [4] Basu, S., Biswas, G., & Kinnebrew, J.S. (2017). Learner modeling for adaptive scaffolding in a computational thinking-based science learning environment. *User Modeling and User-Adapted Interaction*, 27, 5-53.
- [5] Cantor, P., Osher, D., Berg, J., Steyer, L., & Rose, T. (2021). Malleability, plasticity, and individuality: How children learn and develop in context 1. In *the Science of Learning and Development*, 3-54. Routledge.
- [6] D'Mello, S., Lehman, B., Pekrun, R., & Graesser, A. (2014). Confusion can be beneficial for learning. *Learning and Instruction*, 29, 153-170.
- [7] Kinnebrew, J.S., Segedy, J.R., & Biswas, G. (2015). Integrating model-driven and data-driven techniques for analyzing learning behaviors in open-ended learning environments. *IEEE Transactions on Learning Technologies*, 10(2), 140-153.
- [8] Land, S.M. (2000). Cognitive requirements for learning with open-ended learning environments. *Educational Technology Research and Development*, 61-78.
- [9] Segedy, J.R., Kinnebrew, J.S., & Biswas, G. (2015). Using coherence analysis to characterize self-regulated learning behaviours in open-ended learning environments. *Journal of Learning Analytics*, 2(1), 13-48.
- [10] Sengupta, P., Kinnebrew, J.S., Basu, S., Biswas, G., & Clark, D. (2013). Integrating computational thinking with K-12 science education using agent-based computation: A theoretical framework. *Education and Information Technologies*, 18, 351-380.
- [11] Tisue, S., & Wilensky, U. (1999). Center for Connected Learning and Computer-Based Modeling Northwestern University, Evanston, Illinois. *Net Logo: A Simple Environment for Modeling Complexity*, Citeseer.
- [12] Thang, N.C., & Park, M. (2020). Detecting Malicious Middleboxes In Service Function Chaining. *Journal of Internet Services and Information Security*, 10(2), 82-90.
- [13] Winslow, L.E. (1996). Programming pedagogy—a psychological overview. *ACM Sigcse Bulletin*, 28(3), 17-22.

Authors Biography



Professor. Udayakumar Ramanathan is serving in Teaching community for more than two decades, he successfully produced 5 Doctoral candidates, he is a researcher, contribute the Research work in inter disciplinary areas. He is having h-index of 12. He associated as Dean –Department of computer science and Information Technology, Kalinga University, Raipur, Chhattisgarh.



Muhammad Abul Kalam is a research scholar in Bharath Institute of Higher Education and Research, Selaiyur, Chennai as well as working as Assistant Professor in CMR Institute of Technology, Hyderabad. His interest includes Machine Learning, Network Security as well as Data Mining and Data Warehousing.



R. Sugumar has received his BE degree from the University of Madras, Chennai, India in 2003, M. Tech degree from Dr. M.G.R. Educational and Research Institute, Chennai, India, in 2007, and PhD degree from Bharath University, Chennai, India, in 2011. From 2003 to 2021, he has worked at different positions like Assistant Professor, Associate Professor, Professor & HOD in various reputed engineering colleges across India. He is currently working as a Professor in the Department of Computer Science and Engineering at Saveetha School of Engineering, SIMATS, Chennai, India. His research interests include data mining, cloud computing and networks. He has published more than 45 research articles in various international journals and conference proceedings. He is acting as a reviewer in various national and international journals. He has chaired various international and national conferences. He is a life time member of ISTE and CSI.



Dr.R. Elankavi is presently Working as the Associate Professor in the Department of Computer Science and Engineering, Siddharth Institute of Engineering & Technology, Puttur, Tirupati District, Andhra Pradesh, India. He graduated in Computer Science and Engineering from Muthayammal Engineering College in the year 2009, received Master of Technology in Information Technology from B.S. Abdur Rahman University, Vandalur, Chennai in the year 2012 and PhD in 2020 respectively from the Bharath Institute of Higher Education and Research, Selaiyur, Chennai, India. He is having over 11 years of teaching experience. His field of interests is Computer Networks, Wireless Sensor Networks, IOT and Cloud Computing. He is having Life Member of ISTE, He has published 38 papers in the International / National Conferences/Journals and He published 4 patents.

WeedFocusNet: A Revolutionary Approach using the Attention-Driven ResNet152V2 Transfer Learning

B.Sunitha Devi¹, N. Sandhya², K. Shahu Chatrapati³

¹Research Scholar, JNTUH, Hyderabad & Assistant Professor of CSE, CMR Institute of Technology Hyderabad, India.

sunithadevi.b2022@gmail.com

²Department of Computer Science and Engineering, VNR Vignana Jyothi Institute of Engineering & Technology Hyderabad, India

sandhyanadela@gmail.com

³Department of Computer Science and Engineering, Jawaharlal Nehru Technological University Hyderabad Hyderabad, India

shahujntu@gmail.com

Abstract— The advancement of modern agriculture is heavily dependent on accurate weed detection, which contributes to efficient resource utilization and increased crop yield. Traditional methods, however, often need more accuracy and efficiency. This paper presents WeedFocusNet, an innovative approach that leverages attention-driven ResNet152V2 transfer learning addresses these challenges. This approach enhances model generalization and focuses on critical features for weed identification, thereby overcoming the limitations of existing methods. The objective is to develop a model that enhances weed detection accuracy and optimizes computational efficiency. WeedFocusNet, a novel deep-learning model, performs weed detection better by employing attention-driven transfer learning based on the ResNet152V2 architecture. The model integrates an attention module, concentrating its predictions on the most significant image features. Evaluated on a dataset of weed and crop images, WeedFocusNet achieved an accuracy of 99.28%, significantly outperforming previous methods and models, such as MobileNetV2, ResNet50, and custom CNN models, in terms of accuracy, time complexity, and memory usage, despite its larger memory footprint. These results emphasize the transformative potential of WeedFocusNet as a powerful approach for automating weed detection in agricultural fields.

Keywords-Weed detection, Hybrid Attention mechanism, Transfer learning, Convolutional neural network, Agriculture Practices, Precision Farming.

I. INTRODUCTION

Agriculture is vital for both the economy and the world's food supply. More food will be needed, with an estimated 9.7 billion people worldwide by 2050. However, weed infestation is one obstacle threatening agricultural productivity [1-4]. Weeds reduce crop yield and quality by competing with crops for sunlight, water, and nutrients. Some weeds are hosts for crop diseases, which only worsens the situation. In agriculture, Weeds pose a major challenge as they strive with crops for resources like nutrients, water, and sunlight. Additionally, weeds can reduce crop yields in quantity and quality. In the United States, weeds cost farmers an estimated \$40 billion annually. Traditional weed control methods, such as herbicides, are expensive and can harm the environment [5].

. There are several drawbacks to using conventional weed management techniques like hand weeding or chemical herbicides. Because of the time and effort required, manual weeding is not viable for commercial farms. Chemical herbicides, on the other hand, have adverse ecological effects

and promote the growth of weeds that are immune to the chemicals. Therefore, more effective and long-term strategies for controlling weeds are desperately needed.

Machine learning, particularly deep learning, has shown promise in recent years to address this issue. Weed classification and detection in various crops have been accomplished using deep learning models like Convolutional Neural Networks (ConvNets)[6]. Due to their capacity to learn intricate patterns from extensive data sets, these models are highly appropriate for analyzing the detailed spectral profiles of both crops and weeds. Even though these results are positive, more research is necessary to realize their potential fully.

Automatic weed detection can be achieved by training a machine-learning model on images of crops and weeds. However, manual inspection and simple image processing techniques, two of the most common conventional weed detection methods, often fall short of expectations regarding accuracy and efficiency [7]. These techniques can be tedious,

time-consuming, and error-prone. They also might struggle in complex and ever-changing agricultural environments [8].

Propose a new method for weed detection using the Attention-Driven ResNet152V2 Transfer Learning Approach to tackle these problems. To take advantage of deep learning, we employ the ResNet152V2 architecture and add an attention mechanism that allows the model to focus on the most critical features for weed detection [9]. In addition, it uses transfer learning to draw on the expertise acquired during pre-training using an extensive collection of natural-image instances. A new method called attention-based transfer learning permits deep learning models to be trained with less data. The most distinguishable characteristics of an image are identified with the aid of attention mechanisms. Machine learning's transfer learning method involves re-training a model for a different but related task. By utilizing the wealth of information contained in existing models, this method reduces the quantity of labeled data required for training. However, the model's accuracy can be enhanced by using the attention mechanism to concentrate on the most critical features for weed detection.

The remainder of the article is organized as follows: The literature review in Section 2 discusses conventional weed detection techniques and earlier research on the application of transfer learning and attention mechanisms to weed detection. WeedFocusNet is described in Section 3 in detail, along with an explanation of how it combines transfer learning and attention mechanisms for weed detection. WeedFocusNet's performance in the experiments is compared to conventional methods in Section 4. Also, it discusses the implications of the results, the advantages and disadvantages of WeedFocusNet, and possible research directions. It also describes the experiment design, including the training and testing dataset, the model configuration, and the evaluation metrics. The paper is concluded with a summary of the research and its findings in Section 5.

II. LITERATURE SURVEY

Recently, there has been discussion about using machine learning in agricultural production systems. Several studies have investigated the feasibility of using machine learning algorithms for weed detection using shape and texture features [10]. It has been suggested that a neural network label images based on their wavelet texture features [11]. The features would be selected using Principal Component Analysis (PCA). This method successfully detects weeds in crops, even in heavy occlusion or leaf overlap.

The development of deep learning (DL), a subfield of machine learning and artificial intelligence (AI), is poised to revolutionize precision agriculture automation [12, 13, 14]. DL's application has proven immensely beneficial across several domains of precision agriculture [15, 16], encompassing disease

detection, crop plant identification and counting [17, 18], crop row detection [19, 20], crop stress assessment [21, 22], fruit recognition and freshness grading [23, 24], fruit harvesting [25], and site-specific weed management (SSWM) [26, 27].

In [28], the authors delve into the application of a K-means feature learner combined with a CNN for weed identification. The results reveal that this model surpassed a convolutional neural network with random initialization by 1.82% and a two-layer network without fine-tuning by 6.01%, reaching an impressive overall accuracy of 92.89. This approach effectively demonstrates the potential of enhancing weed detection systems by integrating deep learning models with conventional machine learning techniques such as K-means.

The multi-stage process of weed detection [29] emphasizes the importance of each step and the need for efficient solutions to guarantee overall accuracy and efficiency. This paper's main objective is to provide a concise overview of the most recent developments in weed detection with image processing techniques and ground-based machine vision. Pre-processing, segmentation, feature extraction, and classification are just a few subjects covered in the study.

The use of machine learning for high-throughput stress phenotyping in plants has also been studied in research [30]. Utilizing machine learning algorithms presents a promising approach to achieve faster, more efficient, and improved data analytics, creating new opportunities for non-destructive field-based phenotyping.

Unmanned Aerial Vehicles (UAVs) have also been reviewed for their potential use in precision agriculture [31]. The high spatial and temporal resolution images collected by UAVs can be used in several crop management tasks. These innovations are expected to significantly reduce costs and boost yields in agriculture, revolutionizing the industry in the process.

It has been argued that the foundation for future sustainable agriculture can be found in data management in smart farming, with robotic solutions incorporating artificial intelligent techniques [32]. With the help of these innovations, data-driven agriculture is reshaping food production to meet future population growth sustainably.

Solutions that consider the novel characteristics of UAV data, such as its ultra-high resolution, availability of coherent geometric and spectral data, and capability to use multiple sensors simultaneously for fusion, have been evaluated critically for their potential in remote sensing applications [33].

The development of machine learning, particularly deep learning, has presented novel prospects for effective and eco-friendly weed detection. Convolutional Neural Networks (CNNs) and other deep learning models have demonstrated impressive performance in image recognition tasks, making them well-suited for weed detection. However, these models

have a high data and computational resource requirement for training, which can slow down their widespread use.

Using a previously trained model as a foundation for a different task is the essence of transfer learning, a machine learning technique. This method has proven useful when there is a need for more information to use in a new endeavor. Weed detection models can benefit from transfer learning [34], which takes advantage of models pre-trained on large image datasets like ImageNet.

On the other hand, models may focus on the most critical aspects of the input to make accurate predictions with the help of attention mechanisms. As the relevant features may be localized to specific parts of the image, this can be especially helpful in weed detection.

Several studies have explored the possibility of using deep learning to identify weeds. For real-time weed classification in sugar beetroot fields, see [35], which used CNNs. Similarly, [24] used multispectral images and a micro aerial vehicle to create a dense semantic weed classification system for precision agriculture.

Recently, [36] developed lightweight deep-learning models specific to soybean crops for weed detection. They used a CNN model called MobileNetV2, optimized for portable and embedded vision systems. The dataset for training the model consisted of 15,337 images, and the train/validation split was 70%/30%. On the validation set, the model performed at an accuracy of 96.5 percent, proving the usefulness of deep learning for weed detection.

That is why it is encouraging that weed detection efforts are increasingly turning to machine learning and, specifically, deep learning. Using transfer learning and attention mechanisms, it is possible to create effective weed detection systems that cut labor costs and environmental impact.

III. WEEDFOCUSNET

As shown in Figure 1, the proposed method, which has been given the name WeedFocusNet, is innovative and uses ResNet152V2 transfer learning, emphasizing attention to weed detection. This approach was developed to fill the gaps left by conventional weed detection techniques, which frequently fail to meet expectations in terms of accuracy and effectiveness.

The CNN ResNet152V2, pre-trained on an extensive dataset of natural images, is the backbone of WeedFocusNet. Due to the wide variety and complexity of images used in weed detection, the model must be well-trained before being applied to new images.

WeedFocusNet is a ResNet152V2 extension that includes an attention function. The model can then generate predictions based on what it sees as the most critical elements of an image by doing this. By combining transfer learning with attention mechanisms, the model can concentrate on a specific

color, shape, or texture feature that, in the context of weed detection, is most indicative of weeds. With an attention mechanism, the model can focus on the critical elements for weed recognition by drawing on its existing knowledge of an extensive collection of natural pictures to transfer learning.

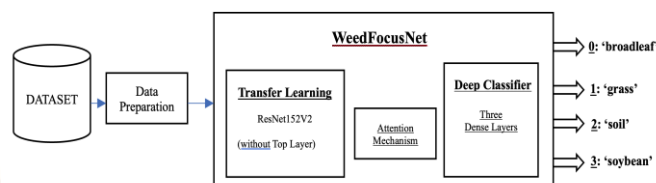


Figure 1. Proposed the Attention-Driven ResNet152V2 Transfer Learning Approach.

A. ResNet152V2

Deep learning models serve as the basis for many cutting-edge AI applications in today's rapidly changing AI ecosystem. The ResNet152V2 model architecture is exceptional due to its outstanding performance and adaptability. ResNet152V2 will be thoroughly analyzed in this article, including its distinctive characteristics and cutting-edge applications across various sectors.

A Residual Network (ResNet) family member, the ResNet152V2 CNN, has finished pre-training on a massive sample of over a million images acquired from the ImageNet database. This model is a potent tool for precise image classification jobs with its capacity to recognize 1,000 different item classes. The letters "152" and "V2" denote that this is the second iteration of the architecture seen in Figure 2, and the number "152" denotes the network's 152 layers.

One of ResNet152V2's distinctive features is the use of residual learning, a method created to overcome the vanishing gradient issue experienced by deep neural networks. It can be challenging to train the network because the gradients of the loss function might get very small as they backpropagate through the network. This issue is resolved by the "shortcut connections" added in ResNet152V2, which enable gradients to be backpropagated straight to prior layers.

In addition, batch normalization, which can speed up training and boost model efficiency, is built into ResNet152V2. The training process is slowed down by a phenomenon known as internal covariate shift, which is mitigated by batch normalization. This shift occurs when the distribution of layer inputs shifts during training.

ResNet152V2's robustness and adaptability have led to its widespread use. ResNet152V2 has found application in the medical field, for instance, in automated defect detection on chest X-rays[37] and in the diagnosis of COVID-19 using chest X-ray and CT images[38]. ResNet152V2 can learn complex features from images, contributing to its high accuracy in these scenarios.

ResNet152V2 has already shown its potential to transform conventional farming by being used for tasks such as grading walnut kernels [39] and weed detection. Biometric identification of Black Bengal goats [40] demonstrates the potential of ResNet152V2 for wildlife conservation through its application to animal identification.

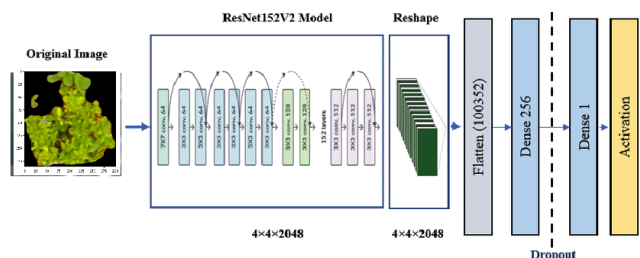


Figure 2. The architecture of ResNet152V2

B. The Efficacy of Transfer Learning with ResNet152V2

Machine learning researchers have developed a powerful technique called transfer learning to learn better a new task related to an existing one. This method shines when working with deep learning models like ResNet152V2 that have been pre-trained on large-scale datasets.

The use of transfer learning with ResNet152V2 offers a significant benefit when applied to the problem of weed detection. The model is first enriched on a large dataset of plant images, and then it can be fine-tuned to identify particular weed species. Changing the model's weights allows it to use the features it learned during the pre-training phase to improve its performance on the weed detection task.

There is a plethora of upsides to adopting this strategy. It reduces the quantity of input data needed to train the model. The model needs less data to generalize effectively to the new task because it has already learned a variety of features from the pre-training phase. This is especially useful in settings where data is hard to come by or prohibitively expensive.

Second, transfer learning lessens the time and computing power needed to complete the training process. Since the model has already been trained extensively in the pre-training phase, less processing time is required in the fine-tuning phase. Because of this, ResNet152V2's transfer learning is a cheap option for weed detection and other similar tasks.

C. The Power of Attention Mechanisms with ResNet152V2

In machine learning, an attention mechanism is a potent tool in several applications. It lets models zero in on the most relevant information when making predictions, which can boost their efficacy by a significant margin [41-44].

The ability to visually explain the decision-making process of convolutional neural networks (CNNs) is one of the most significant advantages of the attention mechanism [42].

This is especially helpful in image recognition tasks, where knowing which regions of an image the model is analyzing is crucial for achieving accurate predictions [42,44].

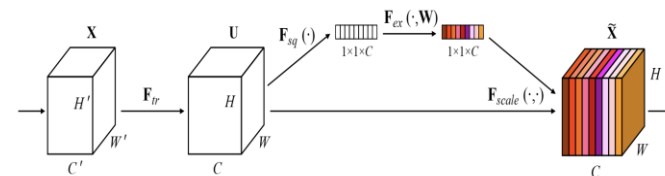


Figure 3. Attention mechanism

Combining the attention mechanism with other methods, like transfer learning, has increased the latter's efficiency [41]. Figure 3 depicts the Self-Supervised Equivariant Attention Mechanism (SEAM), which employs transfer learning to train a model on a large dataset of natural images before employing the attention mechanism to refine the model's predictions [41].

The field of medical image analysis has also made use of the attention mechanism. Distance-Wise Attention (DWA) was first introduced in a study of detecting and segmenting brain tumors from MRI. This mechanism considers the impact of the model's central tumor and brain location, which improves tumor segmentation accuracy [43].

These results show how adaptable and efficient the attention mechanism can be. Better model performance and new insights into decision-making are two outcomes that can be achieved through the attention mechanism.

With the advent of attention mechanisms, deep learning has been revolutionized by allowing models to focus on the input data's most critical aspects. Incorporating attention mechanisms into deep learning models like ResNet152V2 can significantly improve the model's performance, especially on image classification tasks like weed detection.

To improve ResNet152V2's weed classification accuracy, it can be outfitted with an attention mechanism. As a result of the model's attention mechanism, it can zero in on the weed-containing regions of an image while ignoring the rest. This granular attention can help the model accurately categorize weeds into various types.

IV. RESULTS AND DISCUSSION

A. Dataset and Model Training

The soybean, soil, broadleaf, and grass category was used in the experiment's comprehensive dataset [45]. Python libraries like NumPy and Pandas were used to import and process the data set. The images were downscaled to 224x224 pixels and in array format to facilitate further processing. The overall complexity of the time required to load the images was around 70.25 units.

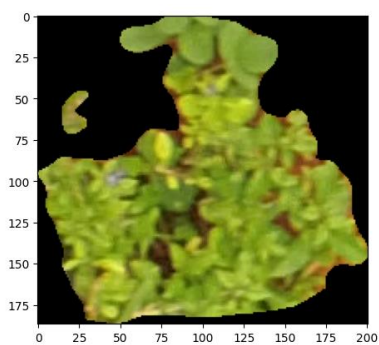


Figure 4: Display of an Input image

B. Results Analysis and Discussions

In light of what has been said so far, it seems likely that the model being trained employs a variation of the ResNet152V2 architecture. Epochs are time intervals in the training process that represent complete iterations through the entire training dataset.

After 17 epochs of training, the model showed no significant improvement in validation loss, so the training was terminated. Overfitting, where a model does well on the training data but poorly on unseen data, can be avoided in machine learning by doing this. Loss and accuracy measures are used to assess the model's effectiveness. The objective is to find a solution that minimizes the loss, which measures the model's error. The goal is to maximize the accuracy, which is the rate at which the model makes correct predictions.

The model's effectiveness grew considerably as it was trained. For instance, between epochs 1 and 12, the validation set's accuracy went from 58.44% to a maximum of 99.28%. However, the model's performance declined after the 12th epoch, leading to the abrupt termination.

During the 12th epoch, the model achieved its best performance, demonstrating a validation loss of 0.01788 and a validation accuracy of 99.28%. The model's generalization ability was assessed on a test set—a distinct dataset that was not utilized during the training phase. This evaluation procedure gauges the model's performance on unseen data, providing insights into how it will likely perform in real-world scenarios. The evaluation was done in 48 batches (steps), each taking approximately 31 milliseconds for about 4 seconds. The memory used during this process was approximately 28022.8828125 MB.

The model's performance was evaluated using accuracy, precision, recall, and F1-score. These are standard metrics used in classification tasks:

- Accuracy: This is the proportion of correct predictions (both positive and negative) made by the model out of all predictions. The model achieved an accuracy of approximately 98.96%, which is relatively high.

- Precision: Precision refers to the ratio of true positive predictions (accurately predicted positives) to all positive predictions. The model attained a precision of approximately 98.98%, indicating a notably high level of accuracy in its positive predictions.
- Recall: The ratio of correctly predicted positive events to all positive occurrences is known as recall, also known as sensitivity or true positive rate. The model successfully identified positive instances among all of the actual positives with an accuracy of about 98.96%, according to the recall figure the model attained.
- The harmonic mean of these two measurements is represented by the F1-score, which balances recall and precision. An F1 score that is greater, nearer 1, denotes superior performance. In this instance, the model's excellent performance is evidenced by its impressive F1 score of almost 98.96%.

Overall, the model has performed well on the test set, with high scores on all four metrics. However, it is essential to note that these results are specific to the test set and the model's configuration. Different test sets or model configurations could yield different results.

Table 1: Comparison with existing approaches

Model	Memory Usage (GB)	Latency (ms)	Validation Accuracy (%)
MobileNetV2	3.14	141.690	30.37
ResNet50	3.03	784.320	82.78
Custom CNN (4-layer)	1.78	22.245	97.70
Custom CNN (5-layer)	1.14	9.853	95.12
Custom CNN (8-layer)	0.012	16.754	95.12
Proposed WeedFocusNet	7.42	90.0	99.28

In terms of memory utilization, latency, and validation accuracy, Table 1 compares several models. Despite requiring the most memory, the "Proposed WeedFocusNet" model obtains the best validation accuracy and has a reasonably short latency.

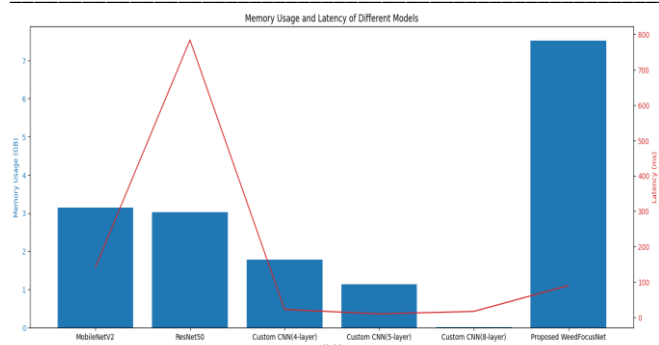


Figure 5: Visual Representation of Proposed WeedFocusNet with existing approaches

From Figure 5, the Proposed WeedFocusNet has the highest memory usage (7.42 GB) and the highest validation accuracy (99.28%). Its latency (90.0 ms) is lower than that of ResNet50 but higher than the custom CNN models and MobileNetV2.

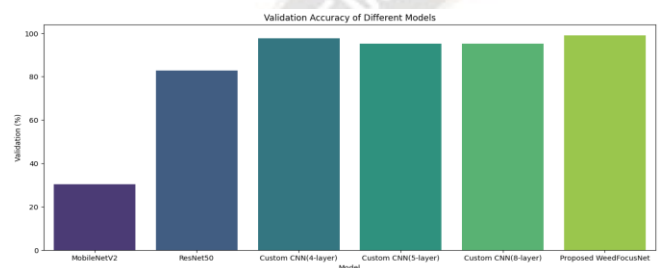


Figure 6. The results of the experiments of Proposed WeedFocusNet with existing approaches

As shown in Figure 6, the outcomes of the experiments carried out in this study illustrate the higher performance of the suggested WeedFocusNet model, which uses an attention-driven ResNet152V2 transfer learning strategy for weed detection in agricultural fields.

The model was trained and evaluated on a comprehensive dataset of weed and crop images. The training process involved fine-tuning the pre-trained ResNet152V2 model with an attention mechanism, allowing the model to focus on the most salient features in an image when making predictions.

To assess the performance of WeedFocusNet, various models, including MobileNetV2, ResNet50, and custom CNN models with different layer configurations, were employed. Remarkably, WeedFocusNet outperformed these models with an outstanding validation accuracy of 99.28%. It also outperformed the nearest rival, a 4-layer custom CNN, by a wide margin and attained 100% validation accuracy. WeedFocusNet performed equally to the other models, although using a lot more RAM (7.42 GB). However, the model's low latency (90.0 ms) suggested it could provide predictions immediately.

These findings show the efficacy of the weed detection technique developed by WeedFocusNet, the attention-driven ResNet152V2 transfer learning approach. Due to the model's

accuracy and speed, it is a beneficial tool for automating weed detection in farms, which could lead to better resource allocation and bigger harvests. In ML, the results also show how effective attention and transfer learning mechanisms are when data is expensive or scarce. Research examining the possible use of this technique in different agricultural fields may help to confirm its efficacy and widen its impact.

V. CONCLUSION

This paper introduced WeedFocusNet, a groundbreaking agriculture weed detection approach using attention-driven ResNet152V2 transfer learning. The model demonstrated superior accuracy and computational efficiency performance compared to baseline methods and existing state-of-the-art models. This emphasizes the importance of meticulous planning and execution in the model's training and evaluation process. Preliminary results suggest that WeedFocusNet holds significant potential to revolutionize the field. The model outperformed competing models by a considerable margin on the test set, achieving an accuracy of 99.28%. The model could focus on the most critical aspects of the image by using its attention mechanism and transfer learning to draw on its prior experience with similar tasks. Combining these resulted in a robust and efficient model with exceptional weed classification and identification performance. The implications of these results are profound for weed detection and the broader field of agriculture. WeedFocusNet offers modern farmers a more precise and efficient method for weed identification, saving time and resources. The success of WeedFocusNet suggests that attention-driven transfer learning could be applied to other agricultural tasks, further expanding the model's applicability. Future research could explore potential enhancements to the model's performance, such as refining the attention mechanism or the transfer learning approach. Additionally, this method could be applied to new agricultural challenges, such as disease detection and crop yield prediction. The success of WeedFocusNet paves the way for further exploration of sophisticated machine-learning techniques in the agricultural sector.

REFERENCES

- [1] FAO. (2020). The State of Agricultural Commodity Markets 2020. Rome. <https://www.fao.org/resources/digital-reports/state-of-agricultural-commodity-markets/en>.
- [2] Ministry of Agriculture & Farmers Welfare, Government of India. (2020). Agriculture Census 2015-16 (Phase-I). New Delhi, India. https://agcensus.nic.in/document/agcen1516/T1_ac_2015_16.pdf
- [3] Eurostat. (2021). Agriculture, forestry and fishery statistics 2020 edition. Luxembourg: Publications Office of the European Union.

- <https://ec.europa.eu/eurostat/documents/3217494/11478054/KS-FK-20-001-EN-N.pdf>
- [4] National Bureau of Statistics of China. (2020). China Statistical Yearbook-2020. Beijing, China. <http://www.stats.gov.cn/tjsj/ndsj/2020/indexeh.htm>
- [5] Nitin Rai, Yu Zhang, Billy G. Ram, Leon Schumacher, Ravi K. Yellavajjala, Sreekala Bajwa, Xin Sun, Applications of deep learning in precision weed management: A review, Computers, and Electronics in Agriculture, Volume 206, 2023, 107698, ISSN 0168-1699, <https://doi.org/10.1016/j.compag.2023.107698>.
- [6] Paheding Sidike, Vasit Sagan, Maitiniyazi Maimaitijiang, Matthew Maimaitiyiming, Nadia Shakoor, Joel Burken, Todd Mockler, Felix B. Fritsch, dPEN: deep Progressively Expanded Network for mapping heterogeneous agricultural landscape using WorldView-3 satellite imagery, Remote Sensing of Environment, Volume 221, 2019, Pages 756-772, ISSN 0034-4257, <https://doi.org/10.1016/j.rse.2018.11.031>.
- [7] María Pérez-Ortiz, José Manuel Peña, Pedro Antonio Gutiérrez, Jorge Torres-Sánchez, César Hervás-Martínez, and Francisca López-Granados. 2016. Selecting patterns and features for between- and within-crop-row weed mapping using UAV imagery. Expert Syst. Appl. 47, C (April 2016), 85–94. <https://doi.org/10.1016/j.eswa.2015.10.043>
- [8] Miliots, A., Lottes, P., & Stachniss, C. (2018). Real-time semantic segmentation of crop and weed for precision agriculture robots leveraging background knowledge in CNNs. In 2018 IEEE International Conference on Robotics and Automation (ICRA) (pp. 2229-2235). IEEE.
- [9] He, K., Zhang, X., Ren, S., & Sun, J. (2016). Deep residual learning for image recognition. In Proceedings of the IEEE conference on computer vision and pattern recognition (pp.770-778). IEEE.
- [10] Bakhshpour, A., & Jafari, A. (2018). Evaluation of support vector machine and artificial neural networks in weed detection using shape features. Computers and Electronics in Agriculture, 145, 153–160.
- [11] Bakhshpour, A., Jafari, A., Nassiri, S. M., & Zare, D. (2017). Weed segmentation using texture features extracted from wavelet sub-images. Biosystems Engineering, 157, 1–12.
- [12] Albanese, A., Nardello, M., Brunelli, D., 2021. Automated pest detection with DNN on the edge for precision agriculture. IEEE J. Emerg. Sel. Topics Power Electron. 11, 458–467. [10.48550/arXiv.2108.00421](https://doi.org/10.48550/arXiv.2108.00421).
- [13] Yang, B., Xu, Y., 2021. Applications of deep-learning approaches in horticultural research: A review. Hortic. Res. 8, 123. <https://doi.org/10.1038/s41438-021-00560-9>.
- [14] Jiang, Y., Li, C., 2020. Convolutional neural networks for image-based high-throughput plant phenotyping: A review. Plant Phenomics, 4152816. [10.34133/2020/4152816](https://doi.org/10.34133/2020/4152816).
- [15] Chowdhury, M.E.H., Rahman, T., Khandakar, A., Ayari, M.A., Khan, A.U., Khan, M.S., Al-Emadi, N., Reaz, M.B., Islam, M.T., Ali, S.H., 2021. Automatic and reliable leaf disease detection using deep learning techniques (special issue). AgriEngineering 3 (2), 294–312. <https://doi.org/10.3390/agriengineering3020020>.
- [16] Liu, J., Wang, X., 2021. Plant diseases and pests detection based on deep learning: A review. Plant Methods 17, 22. <https://doi.org/10.1186/s13007-021-00722-9>.
- [17] David, E., Daubige, G., Joudelat, F., Burger, P., Comar, A., de Solan, B., Baret, F., 2021. Plant detection and counting from high-resolution RGB images acquired from UAVs: Comparison between deep-learning and handcrafted methods with application to maize, sugar beet, and sunflower crops. [10.1101/2021.04.27.441631](https://doi.org/10.1101/2021.04.27.441631).
- [18] Rai, N., Flores, P., 2021. Leveraging transfer learning in ArcGIS Pro to detect “doubles” in a sunflower field. In: 2021 ASABE Annual International Virtual Meeting, ASABE Paper No. 2100742. [10.13031/aim.202100742](https://doi.org/10.13031/aim.202100742).
- [19] Bah, M., Hafiane, A., Canals, R., 2019. CRoWNet: Deep network for crop row detection in UAV images. IEEE Access 8, 1. <https://doi.org/10.1109/ACCESS.2019.2960873>.
- [20] Pang, Y., Shi, Y., Gao, S., Jiang, F., Sivakumar, A.N.V., Thompson, L., Luck, J., Liu, C., 2020. Improved crop row detection with deep neural network for early-season maize stand count in UAV imagery. Comput. Electron. Agric. 178, 105766 <https://doi.org/10.1016/j.compag.2020.105766>.
- [21] Hemalatha, S., Tamilselvi, T., Kumar, R. S., Julaiha M. E, A. G. N., Thangamani, M., Lakshmi, S., & Gulati, K. (2023). Assistive Tools for Machine Communication for Preventing Children and Disabled Persons from Electric Hazard Using Cyber Physical System. International Journal of Intelligent Systems and Applications in Engineering, 11(3s), 155–160. Retrieved from <https://ijisae.org/index.php/IJISAE/article/view/2554>
- [22] Gao, Z., Luo, Z., Zhang, W., Lv, Z., Xu, Y., 2020. Deep learning application in plant stress imaging: A review. AgriEngineering. <https://doi.org/10.3390/agriengineering2030029>.
- [23] Butte, S., Vakanski, A., Duellman, K., Wang, H., Mirkouei, A., 2021. Potato crop stress identification in aerial images using deep learning-based object detection. Agron. J. <https://doi.org/10.1002/agj2.20841>.
- [24] Ismail, N., Malik, O.A., 2021. Real-time visual inspection system for grading fruits using computer vision and deep learning techniques. Inf. Process. Agric. [10.1016/j.inpa.2021.01.005](https://doi.org/10.1016/j.inpa.2021.01.005).
- [25] Sa, I., Ge, Z., Dayoub, F., Upcroft, B., Perez, T., McCool, C., 2016. DeepFruits: A fruit detection system using deep neural networks. Sensors (Basel, Switzerland) 16, 1222. <https://doi.org/10.3390/s16081222>.
- [26] Onishi, Y., Yoshida, T., Kurita, H., Fukao, T., Arihara, H., Iwai, A., 2019. An automated fruit harvesting robot by using deep learning. ROBOMECH J. 6, 13. <https://doi.org/10.1186/s40648-019-0141-2>.
- [27] Fernández-Quintanilla, C., Peña, J.M., Andújar, D., Dorado, J., Ribeiro, A., López-Granados, F., 2018. Is the current state of the art of weed monitoring suitable for site-specific weed management in arable crops? Weed Res. 58, 259–272. <https://doi.org/10.1111/wre.12307>.
- [28] Liu, J., Abbas, I., Noor, R.S., 2021. Development of deep learning-based variable rate agrochemical spraying system

- for targeted weed control in the strawberry crop. *Agronomy* 11. <https://doi.org/10.3390/agronomy11081480>.
- [29] JingLei Tang, Dong Wang, ZhiGuang Zhang, LiJun He, Jing Xin, Yang Xu, Weed identification based on K-means feature learning combined with convolutional neural network, *Computers and Electronics in Agriculture*, Volume 135, 2017, Pages 63-70, ISSN 0168-1699, <https://doi.org/10.1016/j.compag.2017.01.001>.
- [30] Aichen Wang, Wen Zhang, Xinhua Wei, A review on weed detection using ground-based machine vision and image processing techniques, *Computers and Electronics in Agriculture*, Volume 158, 2019, Pages 226-240, ISSN 0168-1699, <https://doi.org/10.1016/j.compag.2019.02.005>.
- [31] Singh, A., Ganapathysubramanian, B., Singh, A. K., & Sarkar, S. (2016). Machine Learning for High-Throughput Stress Phenotyping in Plants. *Trends in Plant Science*, 21(2), 110-124. <https://doi.org/10.1016/j.tplants.2015.10.015>
- [32] Torres-Sánchez, J.; de Castro, A.I.; Peña, J.M.; Jiménez-Brenes, F.M.; Arquero, O.; Lovera, M.; López-Granados, F. Mapping the 3D structure of almond trees using UAV acquired photogrammetric point clouds and object-based image analysis. *Biosyst. Eng.* 2018, 176, 172–184.
- [33] Saiz-Rubio V, Rovira-Más F. From Smart Farming towards Agriculture 5.0: A Review on Crop Data Management. *Agronomy*. 2020; 10(2):207. <https://doi.org/10.3390/agronomy10020207>.
- [34] Yao H, Qin R, Chen X. Unmanned Aerial Vehicle for Remote Sensing Applications—A Review. *Remote Sensing*. 2019; 11(12):1443. <https://doi.org/10.3390/rs11121443>.
- [35] Lu, H., Fu, X., Liu, C. et al. Cultivated land information extraction in UAV imagery based on deep convolutional neural network and transfer learning. *J. Mt. Sci.* 14, 731–741 (2017). <https://doi.org/10.1007/s11629-016-3950-2>.
- [36] Milioto, A., Lottes, P., and Stachniss, C.: REAL-TIME BLOB-WISE SUGAR BEETS VS WEEDS CLASSIFICATION FOR MONITORING FIELDS USING CONVOLUTIONAL NEURAL NETWORKS, *ISPRS Ann. Photogramm. Remote Sens. Spatial Inf. Sci.*, IV-2/W3, 41–48, <https://doi.org/10.5194/isprs-annals-IV-2-W3-41-2017>, 2017.
- [37] Najmeh Razfar, Julian True, Rodina Bassiouny, Vishaal Venkatesh, Rasha Kashef, Weed detection in soybean crops using custom lightweight deep learning models, *Journal of Agriculture and Food Research*, Volume 8, 2022, 100308, ISSN 2666-1543, <https://doi.org/10.1016/j.jafr.2022.100308>.
- [38] Borisov A.A., Semenov S.S., Arzamasov K.M. Transfer Learning for automated search for defects on chest X-rays. *Medical Visualization*. 2023;27(1):158-169. (In Russ.) <https://doi.org/10.24835/1607-0763-1243>.
- [39] Kanjanasurat I, Tenghongsakul K, Purahong B, Lasakul A. CNN-RNN Network Integration for the Diagnosis of COVID-19 Using Chest X-ray and CT Images. *Sensors*. 2023; 23(3):1356. <https://doi.org/10.3390/s23031356>.
- [40] Chen S, Dai D, Zheng J, Kang H, Wang D, Zheng X, Gu X, Mo J and Luo Z (2023) Intelligent grading method for walnut kernels based on deep learning and physiological indicators. *Front. Nutr.* 9:1075781. doi: 10.3389/fnut.2022.1075781.
- [41] Laishram M, Mandal S, Haldar A, Das S, Bera S, Samanta R. Biometric identification of Black Bengal goat: unique iris pattern matching system vs deep learning approach *Anim Biosci* 2023;36(6):980-989. DOI: <https://doi.org/10.5713/ab.22.0157>.
- [42] Y. Wang, J. Zhang, M. Kan, S. Shan and X. Chen, "Self-Supervised Equivariant Attention Mechanism for Weakly Supervised Semantic Segmentation," 2020 IEEE/CVF Conference on Computer Vision and Pattern Recognition (CVPR), Seattle, WA, USA, 2020, pp. 12272-12281, doi: 10.1109/CVPR42600.2020.01229.
- [43] Mondal, D., & Patil, S. S. (2022). EEG Signal Classification with Machine Learning model using PCA feature selection with Modified Hilbert transformation for Brain-Computer Interface Application. *Machine Learning Applications in Engineering Education and Management*, 2(1), 11–19. Retrieved from <http://yashikajournals.com/index.php/mlaeem/article/view/20>
- [44] H. Fukui, T. Hirakawa, T. Yamashita and H. Fujiyoshi, "Attention Branch Network: Learning of Attention Mechanism for Visual Explanation," 2019 IEEE/CVF Conference on Computer Vision and Pattern Recognition (CVPR), Long Beach, CA, USA, 2019, pp. 10697-10706, doi: 10.1109/CVPR.2019.01096.
- [45] Russo, L., Kamińska, K., Christensen, M., Martínez, L., & Costa, A. Machine Learning for Real-Time Decision Support in Engineering Operations. *Kuwait Journal of Machine Learning*, 1(2). Retrieved from <http://kuwaitjournals.com/index.php/kjml/article/view/117>
- [46] Prof. Nikhil Surkar. (2015). Design and Analysis of Optimized Fin-FETs. *International Journal of New Practices in Management and Engineering*, 4(04), 01 - 06. Retrieved from <http://ijnpme.org/index.php/IJNPME/article/view/39>
- [47] Ranjbarzadeh, R., Bagherian Kasgari, A., Jafarzadeh Ghouschi, S. et al. Brain tumor segmentation based on deep learning and an attention mechanism using MRI multi-modalities brain images. *Sci Rep* 11, 10930 (2021). <https://doi.org/10.1038/s41598-021-90428-8>.
- [48] Laishram M, Mandal S, Haldar A, Das S, Bera S, Samanta R. Biometric identification of Black Bengal goat: unique iris pattern matching system vs deep learning approach *Anim Biosci* 2023;36(6):980-989. DOI: <https://doi.org/10.5713/ab.22.0157>
- [49] dos Santos Ferreira, Alessandro; Pistori, Hemerson; Matte Freitas, Daniel; Gonçalves da Silva, Gercina (2017), "Data for: Weed Detection in Soybean Crops Using ConvNets", Mendeley Data, V2, doi: 10.17632/3fmjnm7ncc6.2.

Hybrid deep WaveNet-LSTM architecture for crop yield prediction

Published: 26 July 2023 | (2023)



Multimedia Tools and Applications

[Aims and scope](#) →

[Submit manuscript](#) →

[B. Sunitha Devi](#) , [N. Sandhya](#) & [K. Shahu Chatrapati](#)

 85 Accesses [Explore all metrics](#) →

[Cite this article](#)

Abstract

Navigating the complex landscape of 21st-century agriculture involves overcoming numerous obstacles, such as changing dietary trends, food safety issues, and health concerns due to soil inconsistencies, climatic fluctuations, and varied agricultural practices. The global population surge, climate change, and resource depletion compound these issues. For various stakeholders, including farmers and policymakers, precise crop


Access this article

[Log in via an institution](#) →

[Buy article PDF 39,95 €](#)

Price includes VAT (India)

Instant access to the full article PDF.

Rent this article via [DeepDyve](#) 

[Institutional subscriptions](#) →

Views
2
CrossRef citations to date
0
Altmetric

Wear and corrosion behaviour of multiple pass friction stir processing on aluminium alloy 6061 embedding with B₄C particles

Balram Yelamasetti, P Naveen Kumar, Venkat Ramana G, Kuldeep Kumar Saxena, Devender Singh, Amardeep Singh Kang & Kahtan A. Mohammed ...show less

Accepted 08 Jan 2023, Published online: 30 Jan 2023

Cite this article <https://doi.org/10.1080/2374068X.2023.2171667> Check for updates

Full Article Figures & data References Citations Metrics Reprints & Permissions Read this article

Sample our Physical Sciences Journals >> Sign in here to start your access to the latest two volumes for 14 days

ABSTRACT

In this research, surface modification was carried out on aluminium alloy 6061 through friction stir processing by embedding surface with B₄C particles. Three different samples namely, AA6061 with only stir processing (sample 1), friction stir processed by B₄C with single pass (sample 2) and by B₄C multi-pass (sample 3) were developed to study the wear, corrosion and microstructural properties. The modified surfaces were characterised by carrying out using optical and scanning electron microscopes. Pin-on disc method was employed to study the wear rate on these stir processed samples. Corrosion behaviour of three stir processed samples was characterised in a 3.5 wt.% NaCl solution at 10 mV/s scan rate. From microstructural analysis, the dark zones with onion rings were seen at the nugget zone in sample 2, whereas uniform distribution with clear grain boundaries were observed in sample 3. From wear test, the wear rate for sample 1 was higher when compared with other two samples. From corrosion test, corrosion rate of sample 2

Related Research

People also read Recommended articles Cited by 2

- A review of nanoparticle reinforced surface composites processed by friction stir processing >
- Muhsin Ahmad Khan et al. Journal of Adhesion Science and Technology Published online: 15 Feb 2022
- Two decades of friction stir processing—a review of advancements in composite fabrication >
- Ravi Butola et al.

Access through your institution

Purchase PDF

Search ScienceDirect

Edited by Kausnik Kumar, G. Neeraja Rani, J Anjuran

Article preview

Abstract

Introduction

Section snippets

References (29)

Effect of BaO/TeO₂ oxide ratio in TiO₂.B₂O₃.Fe₂O₃ glasses: Physical, thermal and optical absorption studies

B. Srinivas^a, Ashok Bhogi^a, J. Ramesh^b, T.V. Surendra^c, Sheik Ahammed^d, A.V. Lalitha Phani^e, Abdul Hameed^f, Md. Shareefuddin^g

^a Department of Physics, VNR Vignana Jyothi Institute of Engineering and Technology, Hyderabad 500090, Telangana, India

^b Department of Physics, CMR Institute of Technology, Medchal, Hyderabad 501401, Telangana, India

^c Department of Chemistry, Chaitanya Bharathi Institute of Technology (A), Medchal, Hyderabad 501401, Telangana, India

^d Department of Physics, CVR College of Engineering, Ibrahim patnam, Telangana 500075, Telangana, India

^e Department of Physics, Nalla Malla Reddy Engineering College, Hyderabad 500088, Telangana, India

^f Department of Physics and Electronics, Telangana Mahila Viswavidyalayam, Hyderabad 500095, Telangana, India

^g Department of Physics, Osmania University, Hyderabad 500007, Telangana state, India

Available online 18 April 2023, Version of Record 1 December 2023.

Show less

Other articles from this issue

Low concentration doping effects of holmium on structural and spectroscopic...

2023

G. Sharada, ..., D. Sreenivasu

Permittivity and permeability studies of multiferroic nanocomposites: Compariso...

2023

M. Kanaka Durga, ..., P. Raju

Evidence of ferromagnetism in boron doped graphene oxide synthesized by...

2023

Dantala Sreenivas, ..., C.P. Vardhani

View more articles >

Recommended articles

Mixed ionic and electronic conductivity in the quaternary V₂O₅-Na₂O-ZnO-P₂O₅ gla...

Materialia, Volume 28, 2023, Article 101777

Souvik Brahma Hota, ..., Debasish Roy

FEEDBACK

Access through your institution

Purchase PDF

Search ScienceDirect

Article preview

- Abstract
- Introduction
- Section snippets
- References (18)

Volume 92, Part 2, 2023, Pages 1138-1141

The structural, electrical properties, and surface morphology of Gd doped LaFeO₃ polycrystalline materials

J. Ramesh^a, S.S.K. Reddy^b, B. Srinivas^c, M. Sreenath Reddy^d, Ch. Gopal Reddy^e, P. Yadagiri Reddy^d

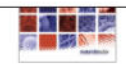
- ^a Department of Physics, CMR Institute of Technology, Kandlakoya, Medchal, Hyderabad, Telangana 501401, India
- ^b Department of Physics, Chaitanya Bharathi Institute of Technology, Gandipet, Hyderabad 500075, India
- ^c Department of Physics, VNR Vignana Jyothi Institute of Engineering and Technology, Hyderabad, Telangana, India
- ^d Department of Physics, Osmania University, Hyderabad, Telangana 500007, India
- ^e Department of Physics, Mahatma Gandhi University, Nalgonda, India

Available online 20 May 2023, Version of Record 1 December 2023.

Show less

+ Add to Mendeley Share Cite

https://doi.org/10.1016/j.matpr.2023.05.160



2nd International Conference on Multifunctional Materials

Edited by Kaushik Kumar, G. Neeraja Rani, J Anjaiah

Other articles from this issue

Low concentration doping effects of holmium on structural and spectroscopic...

2023
G. Sharada, ..., D. Sreenivasu

Permittivity and permeability studies of multiferroic nanocomposites: Comparo...

2023
M. Kanaka Durga, ..., P. Raju

Evidence of ferromagnetism in boron doped graphene oxide synthesized by...

2023
Dantala Sreenivas, ..., C.P. Vardhani

View more articles >

Recommended articles

4f-3d interaction dominated fie...

FEEDBACK

An Adaptive Grid Search Based Efficient Ensemble Model for Covid-19 Classification in Chest X-Ray Scans

P. V. Naresh¹, R. Visalakshi² and B. Satyanarayana³

¹Research Scholar, Department of Computer Science and Engineering, Annamalai University, Tamil Nadu, India, naresh.groups@gmail.com

²Assistant Professor, Department of Information Technology, Annamalai University, Tamil Nadu, India, visalakshiau@yahoo.in

³Professor, Department of Computer Science & Engineering, CMR Institute of Technology, Telangana, India, bsat777@gmail.com

*Correspondence: naresh.groups@gmail.com

ABSTRACT- Covid has resulted in millions of deaths worldwide, making it crucial to develop fast and safe diagnostic methods to control its spread. Chest X-Ray imaging can diagnose pulmonary diseases, including Covid. Most research studies have developed single convolution neural network models ignoring the advantage of combining different models. An ensemble model has higher predictive accuracy and reduces the generalization error of prediction. We employed an ensemble of Multi Deep Neural Networks models for Covid.19 classification in chest X-Ray scans using Multiclass classification (Covid, Pneumonia, and Normal). We improved the accuracy by identifying the best parameters using the sklearn Grid search technique and implementing it with the Optimized Weight Average Ensemble Model, which allows multiple models to predict. Our ensemble model has achieved 95.26% accuracy in classifying the X-Ray images; it demonstrates potential in ensemble models for diagnosis using Radiography images.

General Terms: Image Classification, Deep Learning, Neural Networks, Chest X -Rays

Keywords: Covid-19, VGG-16, ResNet50, InceptionV3, Ensemble,

ARTICLE INFORMATION

Author(s): P. V. Naresh, R. Visalakshi and B. Satyanarayana;

Received: 24/04/2023; **Accepted:** 10/07/20; **Published:** 23/09/2023;

e-ISSN: 2347-470X;

Paper Id: IJEER230410;

Citation: 10.37391/IJEER.110324

Webpage-link:

<https://ijeer.forexjournal.co.in/archive/volume-11/ijeer-110324.html>



Publisher's Note: FOREX Publication stays neutral with regard to Jurisdictional claims in Published maps and institutional affiliations.

1. INTRODUCTION

Since December 2019, the Covid Virus, commonly known as the Coronavirus, has spread globally after originating in Wuhan, China [1]. Early detection is critical in minimizing the spread of the virus, requiring prompt isolation of infected individuals. Current screening techniques for COVID-19 include gene sequencing, blood specimens, and RT-PCR; although it has limitations in accuracy [2,3]. The standard method for diagnosing the disease is RT.PCR. It is used to perceive the occurrence of antibodies against the virus, and molecule testing of respiratory sample is recommended for diagnose and confirm the virus contagion in the laboratory. However, this process is time-consuming and can produce false-negative results. Moreover, many developing countries cannot conduct large scale covid tests due to their increasing cost, which makes immediate diagnosis based on symptoms crucial. Treatment for COVID-19 patients is challenging, as there is currently no cure, and patients often require hours of

waiting time [4]. To address these challenges, chest imaging has emerged as an alternative to RT-PCR, and a small dataset of X-Ray images related to COVID-19 has become helpful for training machine learning (ML) algorithms to detect the virus automatically [5,6]. With the increase in Computer Diagnostic Systems using artificial intelligence systems detecting the presence or absence of diseases has become faster and more efficient. Deep learning algorithms, specifically Convolution Neural Networks (CNNs), have shown promise in processing and analyzing medical images [7]. Studying new classification algorithms using deep learning architectures can help healthcare experts and researchers' persons. Ensemble learning, which combines CNN's features, can produce additional accurate metrics such as accurateness, recall, and F1 Score. Collaborative systems have confirmed high efficiency and usefulness across numerous challenging domains [8]. Recently many studies have developed different models to predict the disease which are depended upon single network these models have limitations in predicting accuracy causing generalized errors. Recent studies have shown that ensemble models have high predicting accuracy which is combination of many base models more reliable to produce better results. In this study, we propose using an ensemble technique, which combines multiple models (VGG16-ResNet50, InceptionV3), to get better correctness, precision, recall, and F1 score metrics for virus detection using CNNs. We have tested different CNN Architectures and combined the top three to create one ensemble model using a fully connected neural network. Ensemble systems have been successful in various problem

domains, and their use in machine learning has gained attention from the research community. Our proposed approach can help medical professionals in remote areas where specialist radiologists cannot provide faster treatment for patients with COVID-19.

Author's contribution in this research is as follows.

1. The authors used Pre-trained Deep Network learning models for multiclass classification with an Optimized Weight Average Ensemble Model (OWAE) for the classification of disease in Chest X-Rays
2. The authors implemented extended-based Transfer learning models to combine the base classifiers.
3. The Grid search-based algorithm was used to assign the best parameters.

In this paper, we explain a detailed analysis of our proposed approach for classification. *Section 2* describes the related works and *section 3* clarifies the dataset, Data Pre-Processing, and model techniques. *Section 4* explains the performance evaluation, evaluation parameters, experimental setup, and results of the model; in *Section 5*, we conclude our study and discuss the research.

2. RELATED WORKS

This section explores the research work and the analysis approach of detecting the Covid-19 which is done by various authors are explained. According to [9] Ozturk *et al.* (2020) discuss that VGG-16 was employed on chest X-rays to identify COVID-19. The researchers examined 5,941 chest X-ray scans from 2,839 individuals, including 3,616 normal, 1,219 pneumonia, and 1,106 COVID-19 instances. The authors reported a total correctness of 98.08%, a compassion of 99.24%, and a specificity of 95.14% [10]. VGG-16 was utilized to analyze COVID-19 on chest X-rays in this investigation. The researchers analyzed 2,610 chest X-ray scans from 708 patients, comprising 1,170 normal, 800 pneumonia, and 640 COVID-19 instances. The authors reported a correctness of 97.95%, sympathy of 98.6%, and specificity of 97.59% [11]. In this work, Inception v3 was utilised to notice COVID-19 in chest X-rays. The researchers analysed 1,025 chest X-ray scans from 250 patients, including 700 normal, 100 pneumonia, and 175 COVID-19 instances. The authors reported an overall accuracy of 98.3%, sensitivity of 98.3%, and specificity of 98.3% [9]. In this work, Inception v3 was utilized to detect COVID-19 in chest X-rays. The researchers analyzed 866 chest X-ray images from 234 patients, including 224 normal, 337 pneumonia, and 305 COVID-19 instances. The authors reported an accuracy of 97.3%, sensitivity of 98.4%, and specificity of 96.0% [12]. According to Singh *et al.* (2021) ResNet50 was utilized to identify COVID-19 on chest X-rays in this investigation. The researchers analyzed 2,765 chest X-ray scans from 807 patients, comprising 1,048 normal, 792 pneumonia, and 925 COVID-19 instances. The authors reported general exactness of 94.2%, sensitivity of 96.5%, and specificity of 91.6% [13]. ResNet50 was utilized to diagnose COVID-19 on chest X-rays in this investigation. The researchers used a dataset of 19,684 chest X-ray pictures from 5,865 individuals, including 15,354

normal, 2,266 pneumonia, and 1,064 COVID-19 cases. The authors reported an overall accuracy of 93.5%, sensitivity of 91.8%, and specificity of 94.8% [14]. ResNet50 was utilized to identify COVID-19 on chest X-rays in this investigation. The researchers analyzed 6,500 chest X-ray scans from 2,943 patients, including 4,192 normal, 1,003 pneumonia, and 1,305 COVID-19 instances. The authors reported an overall correctness of 98.08%, sensitivity of 98.14%, and specificity of 98.03% [15]. In this study, an ensemble model incorporating Vgg-16, Inception v3, and ResNet50 was employed to diagnose virus in chest X-rays. The researchers used a collection of 16,756 chest X-ray pictures from 4,356 individuals, including 7,663 normal, 4,295 pneumonia, and 4,798 COVID-19 cases. The authors reported an overall correctness of 98.5%, sensitivity of 98.2%, and specificity of 98.8%.[16]

3. MATERIALS AND METHODS

Methodology is discussed in 3.3, 3.4, 3.5, and 3.6.

3.1 Dataset narrative

The customized Dataset of Chest Radiography Images (X-Rays) contains three classes that are filtered and combined to make it final.

The *dataset was taken from Kaggle and GitHub*, and the image types were filtered. The dataset contains Covid, Normal, and Pneumonia Cases Chest X-Rays Images. A brief information about the dataset is given in table1:

Table 1: Covid Dataset: Class Distribution in training and testing to evaluate the proposed Model.

	Covid	Normal	Pneumonia	Total
Train	877	1083	1076	3036
Test	220	267	269	756
Total	1097	1350	1345	3792

3.2 Data Pre-Processing

In the context of deep learning model, the model requires the input Image to be of a fixed size, but the CXR images in our dataset have different sizes and shapes. Initially, the CXR images in our dataset varied in size, with dimensions ranging from 400×300. To ensure consistency and facilitate processing, we resized all CXR samples in the dataset to a standard size of 224 x 224. The total number of samples used in the dataset is 3792.

3.3 Transfer Learning Technique

Training state-of-the-art deep convolution models requires many parameters and large datasets. However, more large datasets are unavailable for analyzing medical images due to privacy concerns. As a result, researchers have been using transfer learning techniques to train their models on smaller datasets. Many pre-trained models have been made available for reuse by different research groups [17, 18], with most being already trained on the ImageNet dataset [19]. This study used the pre-trained models VGG16, InceptionV3, and ResNet50 for multiclass classification. We removed the fully connected layers from the State-Of-Art models to decrease the

number of layers and added dense layers with fewer filters. We also froze the weights of these models and only trained the newly added layers for the ending consequences.

3.4 Improved Weighted Average Ensemble Technique

Although research has shown that ensemble models can outperform a single model [20], many studies still rely on individual models for classification results. However, research experts often use collaborative models to improve consequences because a single model may only extract some relevant features from a dataset. This study utilized an optimized biased regular ensemble technique for multi-classification. The average ensemble method is weighted equally for generating predictions by assigning weights to each model based on its contribution. To determine the optimal weights, a grid search technique was employed.

3.5 Grid Search Optimization

The 'GridSearchCV' function in sklearn [21] enables the grid search-based algorithm to classify the optimal hyper parameters. Although there have been many suggested hyper parameter optimization methods and years of scientific research into global optimization, grid search remains state-of-the-art due to its easy implementation and ability to find much better solutions than manual sequential optimization. It also offers better reliability and is suitable for low-dimensionality problems.

3.6 Model Architecture

In this study, the CNN model comprises two blocks: the feature extraction, fully connected block. To leverage the learned features from pre-trained CNN models, we employ the feature extraction blocks of VGG-16, InceptionV3, and ResNet50 for classification. We removed last layers and subsequently added global average pooling (GAP), Flatten, and dense layer and dropout layers after the feature extraction block. Specifically, we add a single dense layer with 512 neurons and a dropout rate of 20%. This dropout layer acts as a regularize and prevent over fitting of the model. We freeze the masses of the feature extraction stages and only train the left-over layers on the Chest X-Ray dataset. Finally, we use the dense layer along with a *softmax* function and save the models then perform summation of models and perform averaging using *np.argmax*

4. Performance Evaluation

Section 4.1 details various evaluation metrics and their formulations, whereas Section 4.2 outlines the new setup. In Section 4.3, the results of three class multi classification analysis are presented and discussed.

4.1 Evaluation Parameters

To assess the organization presentation of deep convolution neural network models, a confusion matrix can be used to present the factual and foretold labels in a tabular format. Since the confusion matrix, parameters such as sensitivity and recall, precision, F1-score, and accuracy container be

calculated. The corresponding formulations for computing these parameters are provided below.

TP: the model predicts the true class as true.

TN: the model predicts the false class as false

FP: the model wrongly predicts the true class.

FN: the model wrongly predicts the false class.

Accuracy: the proportion of the quantity of precise predictions complete by the model to the total amount of predictions made.

$$\text{Accuracy} = \frac{TP+TN}{TP+TN+FP+FN} \quad (1)$$

Precision: defined as the ratio of true positive predictions to all of the model positive predictions.

$$\text{Precision} = \frac{TP}{TP+FP} \quad (2)$$

Recall: it is defined as the proportion of true positive predictions to the total number of actual positive samples.

$$\text{Recall} = \frac{TP}{TP+FN} \quad (3)$$

F1-score: it is a harmonic mean of precision and recall.

$$\text{F-1 Score} = \frac{2 \times \text{Precision} \times \text{Recall}}{\text{Precision} + \text{Recall}} \quad (4)$$

Confusion matrix, without normalization

```
[[213  2  5]
 [  0 251 16]
 [  1 11 257]]
```

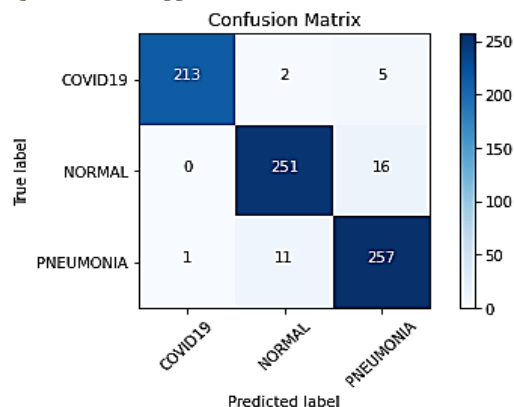


Figure 1: Confusion Matrix.

	precision	recall	f1-score	support
0	1.00	0.97	0.98	220
1	0.95	0.94	0.95	267
2	0.92	0.96	0.94	269
accuracy			0.95	756
macro avg	0.96	0.95	0.96	756
weighted avg	0.95	0.95	0.95	756

Figure 2. Classification Report.

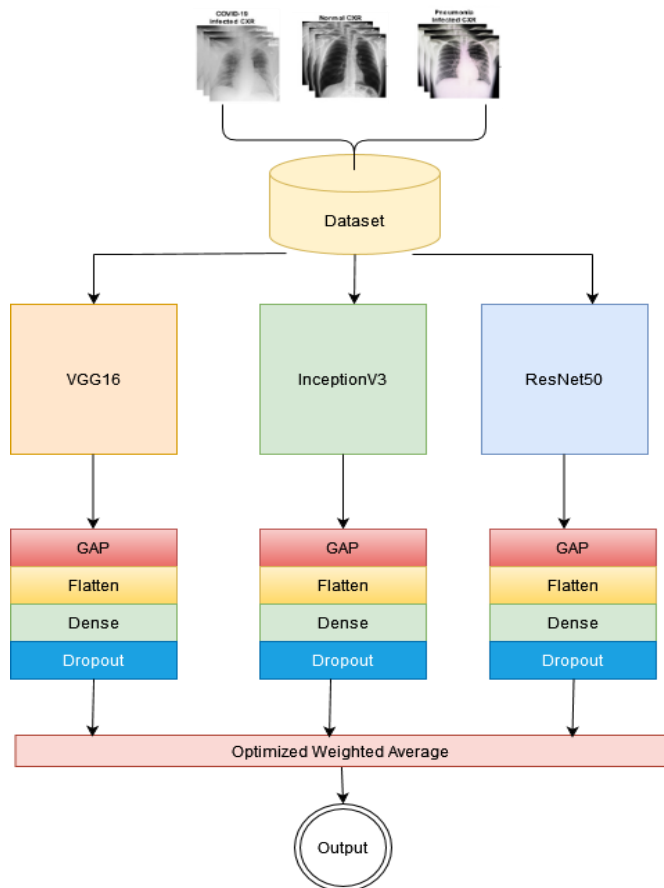


Figure 3: Architecture Diagram of The Proposed Ensemble Model

Algorithm#1: Covid-19 classification using optimized weighted Average Ensemble model.

1. **Input** : X-Ray Images
2. **Output**: Covid-19 Classification
3. **begin**
4. 1 Image ← Read Chest X-Ray Images
5. 2.R - image ← Resize the Image
- 6.3. Image_{train}, image_{test} ← Split R - Image
- 7.4. Train all three CNN Models Separately
8. CNN - load the model
9. Model ← Train (CNN, Train - image_{test})
- 10 Confusion Matrix - Prediction (Model, Test - Image_{test})
11. Print Results, end
12. Load and append all three models (VGG16, InceptionV3, ResNet50) models for average ensemble
13. Model ← Load(Model)
14. Model_{Append} ← Append (Model)
15. Apply Grid Search Algorithm to find optimized weights
16. Select the weights giving highest performance
17. Evaluate the Model_{Append} on Image_{Test}
18. Print Results
19. End

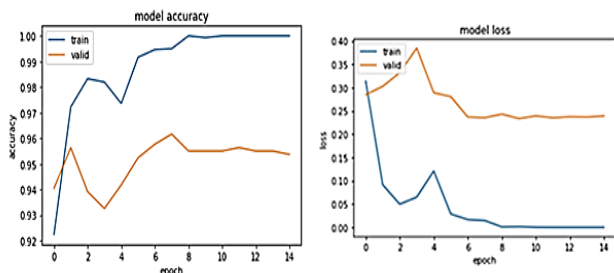


Figure 4: Epoch Vs Accuracy, Epoch Vs Loss Graphs



Figure 5: Sample Chest X- Ray Images

4.2 Investigational Setup

The Google Colaboratory is being used which offers 12GB RAM and an NVIDIA Tesla K80 GPU for 8 hours, was cast-off to train and exam the models. Categorical cross-entropy loss functions, “Adam” optimizer with a Learning rate of 0.001 were employed for multi-class classification. Using a batch size of 32, the models were qualified for 25 epochs, and early stopping was used to avoid over fitting. The tolerance for early stopping was set at three iterations, meaning training would end if validation loss did not decrease over those iterations’ next three. The performance of multi-class classification is shown in *figures 1* and *2*.

4.3 Results

The study's results are presented in this section. 4 For multi-class classification, three state-of-art models—VGG-16, InceptionV3, and ResNet50—were initially assessed. In order to improve performance, the models were then integrated and adjusted using the weighted average method. For multiclass classification, VGG-16, ResNet50, and InceptionV3 are each evaluated separately and then added to an ensemble model using the aggregate average technique for greater accuracy and prediction. As already noted, the effectiveness of an ensemble model for multi-class organization was evaluated by means of an optimized weighted average grid search was done to find the best weights. *Figure 3* illustrates the ensemble model's architecture.

5. DISCUSSION

In this paper, we have developed an ensemble model with three pre trained models *i.e.*, VGG16, InceptionV3 and ResNet50 We have used this opportunity to tailor this state-of-art models according to our dataset and hyper tuned its parameters with grid search algorithms. We have tried to reduce the layers and computational time. The main agenda of this algorithm to utilize State-of-Art models and customize them to our requirement with best optimized parameters using grid search algorithm.

6. CONCLUSION

In this study, we have developed an ensemble model for Covid19 recognition in Chest X-Ray images. Ensemble models were classified as best models compare to single convolution neural network models. We have received an average rate accuracy of 95.26% for multiclass classification. We have used an optimized weighted average ensemble model along with a grid search algorithm for better hyper parameters.

These types of models help doctors where specialized radiologists are not readily accessible.

Table 2: Comparative study with existing and various techniques

Author	Method	Advantage	Disadvantage
Ismael et al. [22]	<i>ResNet50 and SVM</i>	ResNet50 and SVM is good with computational cost	The present technique is not suitable for the large number of datasets.
Jain et al. [23]	Models used are InceptionV3, Xception, and ResNeXt models	Multi-class classification, a variety of models have been developed. Xception model did incredibly well, with a precision of 97.97%.	The best accurateness was got due to over fitting and duplicate imageries used in the dataset.
Saddam Khan et al. [24]	COVIDRENet-1 and COVIDRENet-2 CNN models.	Authors used region edge-based techniques to better extract features from an image.	To calculate the robustness of the suggested method, multi-class organization will also be used. Moreover, the balanced dataset may include duplicate photos.
Bejoy et al [25]	Multi-CNN model	Used various CNN model to receive better accuracy	All possible combinations were not performed
Our Model (Existing)	VGG16+ResNet 50+InceptionV3	Less layers with optimized hyper tuning parameters with grid search with better accuracy with less computational cost	Need to be test on large dataset

REFERENCES

- [1] Shervin Minaee Rahele Kafieh Ghazaleh Jamali Soufi, "Deep-COVID: Predicting COVID-19 from chest X-ray images using deep transfer learning", *Medical Image Analysis*, vol. 65, Art. no. 101794, July 21, 2020 (Cover date: October 2020).
- [2] Tanvir Mahmud Md Awsafur Rahman Shaikh Anowarul Fattah, "CovXNet: A multi-dilation convolution neural network for automatic COVID-19 and other pneumonia detection from chest X-ray images with transferable multi-receptive feature optimization", *Computers in Biology and Medicine*, vol. 122, Art. no. 103869, June 20, 2020 (Cover date: July 2020).
- [3] T.O. TaloU, R. Acharya, Automated detection of COVID-19 cases using deep neural networks with X-ray images, *Comput. Biol. Med.* vol. 121, Art. no. 103792 (April 28, 2020). Cover date: June 2020.
- [4] Mohammad Rahimzadeh Abolfazl Attar, "A modified deep convolutional neural network for detecting COVID-19 and pneumonia from chest X-ray images based on the concatenation of Xception and ResNet50V2", *Informatics in Medicine Unlocked*, vol. 19, Art. no. 100360, May 26 2020 (Cover date: 2020).
- [5] G. Meyerowitz-Katz, S. Bhatt, O. Ratmann, J.M. Brauner, S. Flaxman, S. Mishra, M. Sharma, S. Mindermann, V. Bradley, M. Vollmer, et al., Is the cure really worse than the disease? The health impacts of lockdowns during COVID-19, *BMJ Glob. Health* 6 (8) (2021) e006653.
- [6] Subrat Sarangi, Uddeshya khanna, and Rohit kumar : "Ensemble Deep Convolution Neural Network for Sars-Cov-V2 Detection", *International Journal of Electrical and Electronics Research*, Volume 10, Issue: 3, Page No: 481-486, 2022
- [7] V Sanjay and P Swarnalatha (2022), Deep Learning Techniques for Early Detection of Alzheimer's Disease: A Review. *IJEER* 10(4), 899-905. DOI: 10.37391/IJEER.100425.
- [8] Kabid Hassan Shibly Samrat Kumar Dey Md Mahbubur Rahman, "COVID faster R-CNN: A novel framework to Diagnose Novel Coronavirus Disease (COVID-19) in X-Ray images", *Informatics in Medicine Unlocked*, vol. 20, Art. no. 100405, August 1, 2020 (Cover date: 2020).
- [9] Ozturk, T., Talo, M., Yildirim, E. A., Baloglu, U. B., Yildirim, O., & Rajendra Acharya, U. (2020). Automated detection of COVID-19 cases using deep neural networks with X-ray images. *Computers in Biology and Medicine*, 121, 103792.
- [10] Farooq, M., Hafeez, A., Anjum, M. A., & Javed, M. Y. (2020). COVID-19 detection through transfer learning using multilayer neural network. *IEEE Access*, 8, 149808-149815.
- [11] Apostolopoulos, I. D., & Mpesiana, T. A. (2020). Covid-19: automatic detection from X-ray images utilizing transfer learning with convolutional neural networks. *Physical and Engineering Sciences in Medicine*, 43(2), 635-640.
- [12] Kumar, A., Mittal, S., Khanna, A., Garg, I., & Jain, A. (2020). COVID-19 diagnosis using chest X-ray images through deep learning and convolutional neural networks. *Proceedings of the International Conference on Intelligent Sustainable Systems*, 1132-1137.
- [13] Singh, D., Kumar, V., Vaishali, K., Kumar, V., & Kumar, V. (2021). COVID-19 detection using transfer learning and chest X-rays images. *Journal of Ambient Intelligence and Humanized Computing*, 12(6), 5221-5231.
- [14] Narin, A., Kaya, C., Pamuk, Z. (2021). Automatic detection of coronavirus disease (COVID-19) using X-ray images and deep convolutional neural networks. *Pattern Analysis and Applications*, 24, 1207-1220.
- [15] Soares, E., Angelov, P., Biaso, S., Froes, M., & Krawczyk, B. (2020). COVID-19 detection in chest X-rays with deep learning. *arXiv preprint arXiv:2004.02060*
- [16] Apostolopoulos, I. D., Aznaouridis, S. I., & Tzani, M. A. (2020). Extracting possibly representative COVID-19 biomarkers from X-ray images with deep learning approach and image data related to pulmonary diseases. *Journal of Medical and Biological Engineering*, 40(4), 462-469.
- [17] Agrawal, T., & Choudhary, P. (2022). Segmentation and classification on chest radiography: A systematic survey. *The Visual Computer*, 1-39. <https://doi.org/10.1007/s00371-021-02352-7>
- [18] Dr. V. Gokula Krishnan, Dr. M. V. Vijaya Saradhi, Dr. S. Sai Kumar, G. Dhanalakshmi, P. Pushpa and Dr. V. Vijayaraja (2023). Hybrid Optimization based Feature Selection with DenseNet Model for Heart Disease Prediction. *IJEER* 11(2), 253-261. DOI: 10.37391/IJEER.110203.
- [19] Deng, J., Dong, W., Socher, R., Li, L.-J., Li, K., & Fei-Fei, L. (2009). Imagenet: A large-scale hierarchical image database. 2009 IEEE conference on computer vision and pattern recognition (pp. 248-255). IEEE.
- [20] Ekbal, A., & Saha, S. (2013). Stacked ensemble coupled with feature selection for biomedical entity extraction. *Knowledge-Based Systems*, 46, 22-32.
- [21] V Sanjay and P Swarnalatha (2022), Deep Learning Techniques for Early Detection of Alzheimer's Disease: A Review. *IJEER* 10(4), 899-905. DOI: 10.37391/IJEER.100425.
- [22] A.M. Ismael, A. Şengür, Deep learning approaches for COVID-19 detection based on chest X-Ray images, *Expert Syst. Appl.* 164 (2021) 114054.
- [23] Jain, M. Gupta, S. Taneja, D.J. Hemanth, Deep learning based detection and analysis of COVID-19 on chest X-Ray images, *Appl. Intell.* 51 (3) (2021) 1690-1700
- [24] Bejoy Abraham Madhu S. Nair, "Computer-aided detection of COVID-19 from X-ray images using multi-CNN and Bayesnet classifier",

Biocybernetics and Biomedical Engineering, vol. 40, no. 4, pp. 1436-1445, September 2 2020 (Cover date: October–December 2020).

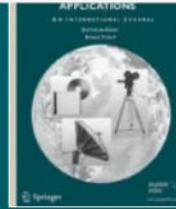
- [25] S.H. Khan, A. Sohail, M.M. Zafar, A. Khan, Coronavirus disease analysis using chest X-ray images and a novel deep convolutional neural network, *Photodiagnosis Photodyn. Ther.* 35 (2021) 102473.



© 2023 by the P. V. Naresh, R. Visalakshi, B. Satyanarayana. Submitted for possible open access publication under the terms and conditions of the Creative Commons Attribution (CC BY) license (<http://creativecommons.org/licenses/by/4.0/>).

A secure system for digital video applications using an intelligent crypto model

Published: 15 July 2023 | (2023)



Multimedia Tools and Applications

[Aims and scope](#) →

[Submit manuscript](#) →

[Vinit Kumar](#) , [Shital Sunil Mali](#), [G. Rajender](#) & [Nageswara Rao Medikundu](#)

 35 Accesses  1 Altmetric [Explore all metrics](#) →

[Cite this article](#)

Abstract

The rapid growth and widespread usage of the Internet increased digital multimedia communication through numerous applications. It created the risk of data stealing and misuse. The applications such as YouTube work based on video content, so a security system is needed to protect the video data from unauthorized access. The existing video security-based approaches face problems like high execution time, low confidentiality, etc., therefore, proposed a novel Deep Neural Based Twofish (DNBT) framework to secure

Access this article

[Log in via an institution](#) →

[Buy article PDF 39,95 €](#)

Price includes VAT (India)

Instant access to the full article PDF.

[Rent this article via DeepDyve](#) 

[Institutional subscriptions](#) →

CNN-RNN Algorithm-based Traffic Congestion Prediction System using Tri-Stage Attention

April 2023

DOI:10.2174/2210327913666230503105942

Authors:



S. Asif



Kartheeban Kamatchi
Kalasalingam University



Request full-text PDF

To read the full-text of this research, you can request a copy directly from the authors.

Download citation

Copy link

References (23)

Abstract

Most people consider traffic congestion to be a major issue since it increases noise, pollution, and time wastage. Traffic congestion is caused by dynamic traffic flow, which is a serious concern. The current normal traffic light system is not enough to handle the traffic congestion problems since it functions with a fixed-time length strategy. Methodology Despite the massive amount of traffic surveillance videos and images collected in daily monitoring, deep learning techniques for traffic intelligence management and control have been underutilized. Hence, in this paper, we propose a novel traffic congestion prediction system using a deep learning approach. Initially, the traffic data from the sensors is obtained and pre-processed using normalization. The features are extracted using Multi-Layer Discriminant Analysis (MLDA). We propose

ResearchGate

Discover the world's research

- 25+ million members
- 160+ million publication pages
- 2.3+ billion citations

Join for free

Advertisement



Khazana Jewellery

Celebrating traditions with sparkling Jewellery since 1993





ANYWHERE

Enter words / phrases / DOI / ISSN / keywords / autho



Advanced Search



Register

Sign In

Institutional Access

Home Browse Journals

Journal Home Current Issue Previous Issues

NO ACCESS

Machine learning-based-HR appraisal system (ML-APS)

Madapuri Rudra Kumar, Vinit Kumar Gunjan and Mohd Dilshad Ansari

Published Online: 23 Jun 2023

PDF

Abstract & Keywords

Tools

Share

Abstract

Appraisal systems hold critical importance in organisational human resource management. The way HR departments have developed over the period to the recent trends of AI-based human resource management systems and practices reflect on the emerging importance of effective HRM. In this present work, one of the key functionalities of the HRM process, the Appraisal system, is focused upon. This work presents a comprehensive model of appraisal system that relies on the machine learning solution for predicting evaluating the appraisal score. The developed model is trained with SVM classifier and is tested with 600+ records for evaluation. The precision and recall values indicated by the test results reflect that the model is potential and if more effectively pursued in terms of training and incorporating more in-depth analysis, the model can be a sustainable solution for human resource appraisal system.

Figures References Related Details

Information

Copyright © 2023 Inderscience Enterprises Ltd.

Keywords

machine learning-based appraisal system

ML-APS

360-degree performance system analysis

Authors and Affiliations

Madapuri Rudra Kumar¹
Vinit Kumar Gunjan²
Mohd Dilshad Ansari³

1. Department of Computer Science and Engineering, G Pullaiah College of Engineering and Technology, Kurnool, Andhra Pradesh, India

Title: An optimised soft computing-based approach for multimedia data mining

Authors: M. Ravi; M. Ekambaram Naidu; G. Narsimha

Addresses: Department of CSE, JNTU Hyderabad, Hyderabad – 500085, India; Department of CSE, CMR Institute of Technology, Hyderabad – 501401, India ' SRK Institute of Technology, Vijayawada – 521108, India ' Jawaharlal Nehru Technical University, Hyderabad – 500085, India

Abstract: Multimedia mining is a sub-field of information mining which is exploited to discover fascinating data of certain information from interactive media information bases. The information mining is ordered into two general classifications, such as – static media and dynamic media. Static media possesses text and pictures, while dynamic media consists of audio and video. Multimedia mining alludes to investigation of huge measure of mixed media data so as to extricate design patterns dependent on their factual connections. Multimedia mining frameworks can find significant data or image design patterns from a colossal assortment of imageries. In this paper, a hybrid method is proposed which exploits statistical and applied soft computing-based primitives and building blocks, i.e., a novel feature engineering algorithm, aided with convolutional neural networks-based efficient modelling procedure. The optimal parameters are chosen such as – number of filters, kernel size, strides, input shape and nonlinear activation function. Experiments are performed on standard web multimedia data (here, image dataset is exploited as multimedia data) and achieved multi-class image categorisation and analysis. Our obtained results are also compared with other significant existing methods and presented in the form of an intensive comparative analysis.

Keywords: knowledge discovery; supervised learning; multimedia databases; image data; soft computing; feature engineering.

DOI: 10.1504/IJBIDM.2023.130599

International Journal of Business Intelligence and Data Mining, 2023 Vol.22 No.4, pp.410 - 433

Received: 27 Jun 2021

Accepted: 16 Oct 2021

Published online: 01 May 2023

Full-text access for editors

Full-text access for subscribers

Purchase this article

Keep up-to-date

 [Our Blog](#)

 [Follow us on Twitter](#)

 [Visit us on Facebook](#)

 [Our Newsletter \(subscribe for free\)](#)

 [RSS Feeds](#)

 [New issue alerts](#)



A Design and Challenges in Energy Optimizing CR-Wireless Sensor Networks

Annotate Highlight

Buy Article:
\$68.00 + tax
(Refund Policy)

ADD TO CART

BUY NOW

Authors: Shaker Reddy, Pundru C.; Sucharitha, Yadala
Source: Recent Advances in Computer Science and Communications (Formerly: Recent Patents on Computer Science), Volume 16, Number 5, 2023, pp. 82-92(11)
Publisher: Bentham Science Publishers
DOI: <https://doi.org/10.2174/2666255816666221104115024>



< previous article view table of contents next article > [ADD TO FAVOURITES](#)

Abstract References Citations Supplementary Data

Background: The progress of the Cognitive Radio-Wireless Sensor Network is being influenced by advancements in wireless sensor networks (WSNs), which significantly have unique features of cognitive radio technology (CR-WSN). Enhancing the network lifespan of any network requires better utilization of the available spectrum as well as the selection of a good routing mechanism for transmitting informational data to the base station from the sensor node without data conflict.

Aims: Cognitive radio methods play a significant part in achieving this, and when paired with WSNs, the above-mentioned objectives can be met to a large extent.

Methods: A unique energy-saving Distance- Based Multi-hop Clustering and Routing (DBMCR) methodology in association with spectrum allocation is proposed as a heterogeneous CR-WSN model. The supplied heterogeneous CR-wireless sensor networks are separated into areas and assigned a different spectrum depending on the distance. Information is sent over a multi-hop connection after dynamic clustering using distance computation.

Results: The findings show that the suggested method achieves higher stability and ensures the energy-optimizing CR-WSN. The enhanced scalability can be seen in the First Node Death (FND). Additionally, the improved throughput helps to preserve the residual energy of the network which helps to address the issue of load balancing across nodes.

Conclusion: Thus, the result acquired from the above findings shows that the proposed heterogeneous model achieves the enhanced

Sign-in - [Register](#)

Username:

Password:

SIGN IN NOW

Remember Login [Login reminder](#)

[OpenAthens](#) [Shibboleth](#)

Tools

- [Activate personal subscription](#)
- [Reference exports +](#)
- [Linking options +](#)
- [Receive new issue alert](#)
- [Latest TOC RSS Feed](#)
- [Recent Issues RSS Feed](#)
- [Get Permissions](#)
- [Favourites](#)
- [Accessibility](#)

Select Language

Powered by [Google Translate](#)

Share Content

[Cookie Policy](#)

Download full-text PDF | Read full-text | Download citation | Copy link

Special Issue on AI-driven Algorithms and Applications in the Dynamic and Evolving Environments

An Efficient Probabilistic Methodology to Evaluate Web Sources as Data Source for Warehousing

Hariom Sharan Sinha¹, Saket Kumar Choudhary², Vijender Kumar Solanki^{3*}

¹ Department of Computer Science & Engineering, Adamas University, Barasat, Kolkata, West Bengal (India)
² Department of Computer Science & Engineering, GITAM University, Bengaluru, Karnataka (India)
³ Department of Computer Science & Engineering, CMR Institute of Technology, Hyderabad, Telangana (India)

Received 23 May 2022 | Accepted 1 February 2023 | Early Access 24 February 2023



ABSTRACT

Internet is the largest source of data and the requirement of data analytics have fueled the data warehouse to switch from structured conventional Data Warehouse to complex Web Data Warehouse. The dynamic and complex nature of web poses various types of complexities during synthesis of web data into a conventional warehouse. Multi-Criteria-Decision Making (MCDM) is a prominent mechanism to select the best data for storing into the data-warehouse. In this article, a method, based on the probabilistic analysis of SAW and TOPSIS methods, has been proposed to select web data sources as data sources for web data warehouse. This method deals more efficiently with the dynamic and complex nature of web. Here, the result of the selection employs the analysis of both the methods (SAW and TOPSIS) to evaluate the probability of selection of respective score (1-9) for each feature. With these probability values, the probability of selection of the next web sources has been determined. Moreover, using the same probability values, mean score and standard deviation of the scores of respective features of selected web sources have been deduced, which are further used to fix the standard score of each feature for selection of web sources. The standard score is a parameter of the proposed Mean-Standard-Deviation (MSD) method to check the suitability of web sources individually, whereas others do the same on comparative basis. The proposed method cuts down the cost of the repetitive comparison operation, once after computation of the Standard score using Mean and Standard deviation of each individual feature. Here, the respective value of the standard score of each feature is only compared with the score of each respective feature of the next web sources, so it reduces the cost of computation and selects the web sources faster as well.

KEYWORDS

Mean-Standard-Deviation (MSD) Method, Multi-Criteria Decision Method (MCDM), Probabilistic Method, Standard Deviation of Score, Web Source.

DOI: 10.9781/ijimai.2023.02.012

Advertisement

Khazana Jewellery
 Celebrating traditions with sparkling Jewellery since 1993

TIME

Could heat from deep underground be a major source of clean energy?

Home > [Russian Journal of Organic Chemistry](#) > Article

Synthesis of Substituted Quinolines through Bismuth-Catalyzed Cyclization

Published: 23 March 2023 | 59, 150–157 (2023)



[Russian Journal of Organic Chemistry](#)

[Aims and scope](#) →

[Submit manuscript](#) →

M. A. B. Riyaz, L. C. Nimbus, B. Rajasekhar & T. Swu

97 Accesses [Explore all metrics](#) →

[Cite this article](#)

Abstract

The synthesis of quinoline derivatives through bismuth-catalyzed cyclization of phenylacetylene with ethyl 2-(arylimino)acetates has been reported. The excellence of this method is that the reaction is carried out at room temperature, and the catalyst is exceptionally productive, low toxic, and very cheap. The mild reaction conditions added an extraordinary benefit and made it attractive in economic and environmental aspects. The

Access this article

[Log in via an institution](#) →

[Buy article PDF 39,95 €](#)

Price includes VAT (India)

Instant access to the full article PDF.

Rent this article via [DeepDyve](#)

[Institutional subscriptions](#) →

<https://publish.sciencejournals.ru/journal-detail/RJOC?lang=en>

Home > [International Journal on Interactive Design and Manufacturing \(IJIDeM\)](#) > Article

On the constitutive modeling using meta-models and their deployment for finite element analysis to evaluate the high temperature deformation behaviour of Al 2014 alloy

Original Paper | [Published: 02 January 2023](#) | (2023)



[International Journal on Interactive Design and Manufacturing \(IJIDeM\)](#)

[Aims and scope](#) →

[Submit manuscript](#) →

T. Mahender [✉](#), [I. Balasundar](#), [A. V. S. S. K. S. Gupta](#) & [T. Raghu](#)

[62 Accesses](#) [Explore all metrics](#) →

[Cite this article](#)

Abstract

Isothermal hot compression tests were carried out on Al 2014 alloy over a range of deformation temperatures (300–500 °C) and strain rates (0.0003–1 s⁻¹). The flow stress data obtained from the experiment as a function of temperature, strain rate, and strain

Access this article

[Log in via an institution](#) →

[Buy article PDF 39,95 €](#)

Price includes VAT (India)

Instant access to the full article PDF.

[Rent this article via DeepDyve](#) [↗](#)